

Characterization and investigation of DNA replication helicase defect as a consequence of aneuploidy

Dissertation zur Erlangung des Doktorgrades der Fakultät für Biologie
der Ludwig-Maximilians-Universität München



vorgelegt von

Mario Davide Maria Avarello

M.Sc. Molecular Biology and Genetics

aus

Pavia, Italy

Jahr

2021

Eidesstattliche Erklärung

Hiermit erkläre ich an Eides statt, dass ich die vorliegende Dissertation selbstständig und ohne unerlaubte Hilfe angefertigt habe. Ich habe weder anderweitig versucht eine Dissertation einzureichen oder eine Doktorprüfung durchzuführen, noch habe ich diese Dissertation oder Teile derselben einer anderen Prüfungskommission vorgelegt.

München, den 16/03/2022

Mario Davide Maria Avarello

(Unterschrift)

Tag der Einreichung: 18/06/2021

Datum der mündlichen Prüfung: 01/12/2021

Erster Gutachter: Prof. Dr. Angelika Böttger

Zweiter Gutachter: Prof. Dr. Heinrich Leonhardt

1. Table of Contents

EIDESSTAATLICHE ERKLÄRUNG	2
2. ABBREVIATIONS.....	6
3. SUMMARY	10
3.1. ZUSAMMENFASSUNG	14
4. AIM OF THE THESIS	20
5. INTRODUCTION.....	21
5.1. ANEUPLOIDY.....	21
5.2. CAUSES OF ANEUPLOIDY	24
5.3. MODEL SYSTEMS.....	25
5.4. CONSEQUENCES OF ANEUPLOIDY	28
5.4.1. GENE DOSAGE IMBALANCE	29
5.4.2. Deregulation of biological processes.....	31
5.4.3. Protein homeostasis is impaired in aneuploid cells.....	32
5.4.4. Metabolic alterations due to chromosome gain	34
5.4.5. Aneuploidy negatively affects cell proliferation.....	35
5.4.6. Aneuploidy leads to increased genomic instability	36
5.5. CAUSES OF GENOMIC INSTABILITY IN ANEUPLOID CELLS.....	36
5.5.1. DNA replication as a source of DNA damage	37
5.5.2. Cell cycle and checkpoint defects lead to GIN.....	40
6. RESULTS.....	44
6.1. GENERATION OF CONSTITUTIVE ANEUPLOID CELLS	44
6.2. Prolonged cell cycle in aneuploid cells is due to extended G1	45
6.3. Licensing of origins of replication is defective in aneuploid cells.....	47
6.4. MCM2-7 helicase levels in cells released from mitosis.....	51
6.5. MASS SPECTROMETRY ANALYSIS OF THE NUCLEOPLASMIC AND CHROMATIN-BOUND FRACTIONS CONFIRMS MCM2-7 HELICASE DOWNREGULATION	53
6.6. STABILITY OF THE MCM2-7 HELICASE DURING THE CELL CYCLE IN ANEUPLOID CELLS	58
6.7. IMPAIRED MCM2-7 LOADING IS NOT DUE TO THE DECREASED EXPRESSION OF ITS SUBUNITS	62
6.8. LOWER LEVELS OF MCM2 DO NOT AFFECT THE CELL CYCLE	64
6.9. ENDOGENOUS OVEREXPRESSION OF MCM7 DOES NOT RESCUE THE CELL CYCLE DEFECTS OF ANEUPLOID CELLS.....	65
6.10. DEFECTIVE CHECKPOINT FACTORS AND CONSEQUENT IMPAIRMENT OF MCM2-7 HELICASE REGULATION MAY BE RESPONSIBLE FOR THE EXTENDED G1 IN ANEUPLOID CELLS	67
6.11. Deregulation of MCM2-7 helicase phosphorylation in aneuploid cells	73
6.12. GENERATION OF MCM2 AND MCM7 MUTANTS ACCORDING TO THE MS RESULTS	76
7. DISCUSSION	79
7.1. CELL CYCLE DELAY AT THE G1 TO S PHASE TRANSITION IS NOT SOLELY DUE TO REDUCED DNA BINDING OF THE MCM2-7 HELICASE	79
7.2. IMPAIRMENTS OF CDK2/CYCLIN E AFFECT THE CELL CYCLE.....	82

7.3.	DEREGULATION OF CDK2 AFFECTS THE CELL CYCLE THROUGH DEFECTIVE PHOSPHORYLATION OF MCM2-7 HELICASE.....	84
7.4.	THE ROLE OF ANEUPLOIDY IN PROMOTING GENOMIC INSTABILITY	86
7.5.	ANEUPLOIDY, GIN AND TUMORIGENESIS	90
8.	MATERIAL AND METHODS	92
8.1.	MATERIALS	92
8.1.1.	CHEMICALS:	92
8.1.2.	BUFFERS AND SOLUTIONS	93
8.1.3.	ANTIBODIES.....	93
8.1.4.	CELL LINES.....	96
8.1.5.	TECHNICAL EQUIPMENT	97
8.1.6.	SOFTWARE.....	98
8.2.	METHODS	98
8.2.1.	CELL CULTURE	98
8.2.2.	MICROSCOPY	99
8.2.3.	CELL SYNCHRONIZATION BY GROWTH FACTORS DEPRIVATION.....	99
8.2.4.	CELL SYNCHRONIZATION IN MITOSIS.....	99
8.2.5.	TRANSFECTION	100
8.2.6.	CHROMOSOME TRANSFER	101
8.2.7.	CELL CYCLE ANALYSIS BY FLOW CYTOMETRY	103
8.2.8.	ISOLATION OF RNA, CDNA SYNTHESIS AND QRT-PCR	103
8.2.9.	CELL LYSIS	104
8.2.10.	SDS PAGE.....	105
8.2.11.	TOWBIN AND BJERRUM SCHAFFER-NIELSEN BUFFER (SEMI-DRY TRANSFER).....	105
8.2.12.	CELLS FRACTIONATION BY THERMO KIT.....	105
8.2.13.	CELLS FRACTIONATION BY CSK	105
8.2.14.	CELL FRACTIONATION FOR MASS SPECTROMETRY	107
8.2.15.	IMMUNOBLOTTING AND QUANTIFICATION OF BAND INTENSITIES	107
8.3.	BACTERIA WORK FLOW	108
8.3.1.	CULTURE MEDIUM AND ANTIBIOTICS.....	108
8.3.2.	HEAT SHOCK TRANSFORMATION AND GLYCEROL-STOCKS	108
8.3.3.	PREPARATION OF PLASMID DNA	109
8.4.	MOLECULAR BIOLOGICAL METHODS	109
8.4.1.	QUICKCHANGE MUTAGENESIS	110
8.4.2.	DNA EXTRACTION FROM AGAROSE GELS.....	111
8.4.3.	DIGESTION AND LIGATION OF PLASMID DNA	112
8.4.4.	DNA SEQUENCING.....	112
8.5.	PROTEOMICS	112
8.5.1.	DATA PRE-PROCESSING	112

9.	SUPPLEMENTARY	114
10.	REFERENCES.....	123
11.	CURRICULUM VITAE	136
	MARIO DAVIDE MARIA AVARELLO.....	136

2. Abbreviations

17-AAG	17-N-allylamino-17-demethoxygeldanamycin
53BP1	p53 binding protein 1
A	Adenosine
AICAR	5-Aminoimidazole-4-carboxamide ribonucleotide
APC/C	anaphase-promoting complex / cyclosome
APS	Ammonium persulfate
ARP	aneuploidy response pattern
ATM	ataxia telangiectasia mutated
ATP	Adenosine Tri-Phosphate
ATR	ATM- and RAD3-related
BER	base excision repair
Bp	base pairs
BS	bloom's syndrome
CDK	cyclin-dependent kinase
cDNA	complementary DNA
CENP-E	centromere-associated protein
EDDK	Dbf4-dependent protein kinase)
CIN	chromosomal instability
CNA	copy number aberration
DAPI	4',6-diamidino-2-phenylindole
DDR	DNA damage response
DDR	DNA damage response
DMEM	Dubelcco's Modified Eagle Medium
DMSO	Dimethyl sulfoxide
DNA	deoxyribonucleic acid
DNA	Deoxyribonucleic acid

dNTP	deoxynucleotide triphosphates
DS	down's syndrome
dNTP	Deoxyribonucleotide
DSB	double strand break
DTT	Dithiothreitol
ECL	enhanced chemiluminescence
EDTA	Ethylendiamintetraacetat
EdU	5-ethynyl-2'-deoxyuridine
ESR	environmental stress response
FA	fanconi anemia
FBS	Foetal bovine serum
GFP	Green fluorescent protein
GG-NER	global genome nucleotide excision repair
GIN	genomic instability
HEPES	4-(2-hydroxyethyl)-1-piperazineethanesulfonic acid
HR	homologous recombination
HRP	Horseradish peroxidase
HSF1	Heat shock factor 1
HSP90	heat shock protein 90
HU	Hydroxyurea
HU	Hydroxyurea
ICL	interstrand cross-link
iPSC	inducible pluripotent stem cells
KAR1	karyogamy gene 1
kDA	Kilo Dalton
LFQ	Label-free quantification
MCM	Minichromosome maintenance protein

MEF	Mouse Embryonic Fibroblasts
MMBIR	microhomology-mediated break-induced replication
MMR	mismatch repair
mRNA	Messenger RNA
MVA	mosaic variegated aneuploidy
NBS1	Nibrin
NEB	New England Biolabs
NER	nucleotide excision repair
PAGE	Polyacrylamide Gel electrophoresis
PBS	Phosphate-buffered saline
PCR	Polymerase chain reaction
PI	Propidium iodide
PN	Proteostasis network
qRT-PCR	quantitative real-time PCR
RNA	Ribonucleic acid
RNA	Ribonucleic acid
RNA Pol II	RNA polymerase II
ROS	Reactive oxygen species
RPA1	Replication Protein A1, 70kDa
RPE-1	Retinal pigment epithelium cells
RT	Room Temperature
SAC	Spindle assembly checkpoint
SDS	Sodium dodecyl sulfate
siRNA	small interfering RNA
SNP	Single nucleotide polymorphism
STY	Phospho (<i>STY</i>)Sites
TBS	Tris-buffered saline

TEMED	Tetramethylethylenediamine
TKNEO	thymidine kinase with neomycin
Tris	Tris- (hydroxymethyl)-aminomethane
Ubp6	Ubiquitin carboxyl-terminal hydrolase 6
UPR	Unfolded protein response
v-Src	Proto-oncogene tyrosine-protein kinase Src
w/v	weight per volume
XIST	X-inactive specific transcript
XRCC1	X-ray repair cross-complementing protein1
YAC	Yeast artificial chromosome

3. Summary

Most eukaryotes cells are diploid and contain two complete sets of chromosomes. This state is usually defined as euploidy. However, cells can sometimes contain an unbalanced number of chromosomes, known as aneuploidy. Changes of chromosomes, either numerical with different chromosome numbers, or structural, with copy number changes of large parts of chromosomes or their arms, are characteristics for aneuploid states. These conditions are in most cases very harmful for human cells. Aneuploidy is linked to several diseases such as trisomies of chromosome 21, 18 and 13 (Down, Edwards and Patau syndromes, respectively). Additionally, aneuploidy is found in about 70% of solid tumors, as well as in leukemias, lymphomas, neurological defects and some other pathologies (Donnelly, 2015) .

The molecular causes of aneuploidy have been investigated for a long time. Numerical aneuploidy is caused by the missegregation of homologous chromosomes during metaphase, which occurs for example due to defects in the mitotic spindle functions, in the sister chromatids cohesion or due to a compromised spindle assembly checkpoint function (Davidsson, 2014). In contrast, structural aneuploidy may arise as a consequence of erroneous DNA replication and repair processes. Additionally, aneuploidy in cancer is often associated with chromosomal and genomic instability, poor prognosis and elevated resistance to chemotherapeutic drugs.

Analysis of aneuploidy is difficult because no model has been available that could be used to compare directly isogenic diploid and aneuploid cells. For our investigations, we created stable cell lines where an additional copy of a single chromosome was introduced. We used two different cell lines. HCT116 comes from the colon of a male patient affected by colorectal cancer. This cell line is nearly diploid with mutation in Ras gene (HCT 116 (ATCC CCL-247). RPE1 is a near diploid human cell line of female origin. The hTERT-immortalized retinal pigment epithelial cell line, hTERT RPE-1, was derived by transfecting the RPE-340 cell line with the pGRN145 hTERT-expressing plasmid, and then stable clones were selected in medium supplemented with hygromycin B (hTERT RPE-1 (ATCC CRL-4000). By transfer of individual chromosomes, it was able to make cells closely mimicking the aneuploid state that are isogenic with parental cell lines (Stingele, 2012).

This chromosome gain has a strong effect on the cells. As they carry extra chromosome, the gene copy number variation affects various cellular processes. It was observed that the expression of additional genes increases and affects various cellular pathways (Donnelly,

2014). One of the features caused by numeric chromosome variation is altered genome stability.

This is documented by the chromosomal rearrangements such as chromosomal translocations, deletions or inversion that may occur on different chromosomes . This is probably a consequence of genotoxic stress that can be documented by increased levels of DNA damage.

Another evidence of the cellular alteration due to aneuploidy is a slow rate proliferation. Cells show a delay in the cell cycle, and actually they seem to stay longer in G1 and S phase compared to diploid cells. Further, as a result of aneuploidy, cells suffer from proteotoxic stress, probably due to increased expression of superfluous proteins (Oromendia, 2014).

Analyses of mRNA and protein levels in different aneuploid cells revealed significant deregulation of multiple pathways. It was observed upregulations of factors involved in pathways related to endoplasmic reticulum (ER), Golgi apparatus, lysosomes and vacuoles, membrane metabolism and the MHC protein complex and antigen processing (Durrbaum, 2014).

In contrast, strong downregulation was observed for proteins that have a function in DNA replication and repair and in RNA metabolism. Thus, addition of even a single chromosome has strong effects on human cells. We found particularly interesting the strong downregulation of pathways related to DNA replication. Impairment of DNA machineries could explain the genetic instability phenotype in aneuploid cells.

The proteins that are particularly downregulated in response to replication are involved in the origin of replication sites recognition, maintenance of the ssDNA and proteins that form the core of the replication fork. We found that all six subunits of a multimeric complex named MCM helicase are downregulated in response to aneuploidy. MCM complex has a typical helicase structure: all the subunits join each other to form a circle shape with a hole in the middle where DNA passes through. This helicase belongs to superfamily 6 helicase, and each subunit has an AAA+ domain; actually, the ATPase motif is in conjunction with the species conserved motif Walker A and Walker B. Each Walker A motif of one subunit works together with the Walker B motif of its neighbor to create functional ATPase; in this way the helicase unwinds the helix (Bell, 2013).

Within the complex, each subunit has its individual role: MCM 4-6-7 have a helicase activity, as they are able to unwind dsDNA in the 5'-3' direction. MCM2 is involved in a complex loading on to the chromatin and in interplay with histones, favoring their deposition on chromatin. Subunits MCM2 and MCM5 function as a gate: by hydrolyzing ATP they can

switch between open and close state to mediate loading of the entire complex. MCM3 functions as a surveillance factor for the complex integrity and MCM7 interacts with DNA damage checkpoint. All these proteins are produced in the cytoplasm and are imported into nuclei. Another protein, CDT1, joins MCMs and together they are translocated to the nucleus. CDT1 links MCM2-7 with the other pre-RC proteins onto DNA filament; specifically, it binds MCM6 by its C-terminal domain and ORC6 by the N-terminal domain (Bell, 2013; Li, 2019).

The MCM helicase is a part of a large complex named pre-Replicative Complex (pre-RC). It has an important role in recognition of specific sites on DNA, from where the replication will start, known as origins of replication. The pre-RC consist of origin recognition complex (ORC1-6) and cell division cycle 6 (Cdc6) proteins. The ORCs are able to bind DNA at replication origin sites, while Cdc6 serves to locate properly ORCs and also helps to bind MCMs in an ATP dependent manner. Firstly, ORC1 binds the sites of replication origin and this then serves as a nucleation point for the rest of ORCs. When the ORC platform is built, then Cdc6 and MCMs-CDT1 are loaded on DNA in these sites. All the subunits use energy derived from ATP hydrolysis in order to bind each other, which allows the formation of this large multimeric complex (Fernandez-Cid, 2013).

MCM helicase is loaded onto DNA fiber using the ORCs-Cdc6 platform. Once the entire complex is loaded, cyclin-dependent kinase (Cdc7) and Dbf4-dependent kinase (DDK) phosphorylates MCMs. Then the complex is joined by other proteins: Cdc45 and GINS, forming the Cdc45-GINS-MCMs complex (CMG). The main function of this complex machinery within the pre-RC in the cells is the correct and timely start of replication.

All the necessary proteins are produced and activated in specific cell cycle phases. MCM2-7 proteins are produced at the end of mitosis, but they are loaded on chromatin during the G1 phase and their levels peak during the transition from late G1 to early S phase. The ORCs are usually present throughout the entire cell cycle: ORC1 is produced in the M-G1 and it stays chromatin-bound till G1/S boundary when it is ubiquitinated and degraded. The other ORCs bind DNA after ORC1, but in late G1 early S phase they are dissociated from it (Kara, 2015). Thus, DNA replication is tightly controlled by many different mechanisms and different type of proteins, and each is regulated in a precise spatio-temporal manner.

There is a reason for these synchronously regulated activities as it ensures that cells use each origin of replication only once per cell cycle. In eukaryotes, DNA replication starts simultaneously from many replication origins to assure that the whole longer chromosome

will be duplicated in appropriate time. Interestingly, eukaryotic cells have frequently more origins of replication loaded with pre-RC than is required for DNA duplication, so called “dormant origins” (Das, 2014). All these huge numbers of sites have a specific function: they can be initiated when forks stall on the DNA filaments, thus preventing that replication process delays too much in case of DNA damage. During DNA replication, whole replicative machinery can slow down and even stop in response to endogenous or exogenous factors such as oxidative stress, DNA damage or low levels of DNA synthesis precursors. However, genome integrity is compromised when replication is delayed for a long time, as the large complexes at the replication forks cannot be maintained for an extensive period of time. As a result, cells could contain many errors such as dsDNA and chromosome rearrangements.

The “dormant origins” are able to impede these errors: upon replicative fork stops, the alternative origins could be activated, and replication continues from these alternative sites. In this way, DNA replication may be finished without a delay and DNA will be replicated mostly without errors or rearrangements. Therefore, correct levels of MCM proteins are essential of genomic stability.

Many studies in mouse models and in cell lines have shown that low and unbalanced MCMs levels render cells cancer prone: different type of cancer or diseases may occur due to under- or overexpression of one or most specific MCMs subunit.

We observed that MCMs levels as well as levels of other pre-RC factors are downregulated in aneuploid cells. Further, the MCM subunits are also mis-regulated by defect of CDK2/cyclin E. Indeed, these checkpoint factors are downregulated and their accumulation within nuclei is delayed.

Thus, insufficient amount of MCM2-7, and the deregulation of its phosphor-sites, lead to the insufficient licensing of replication origins and insufficient replication in case of replication stress. This may cause DNA damage, DNA under-replication and, subsequently, genomic instability. Indeed, we observed that aneuploid cells show elevated DNA damage, accumulation of *de novo* structural rearrangements and altered replication dynamics.

Additionally, increasing the levels of MCM helicases rescues some of the defects. Thus, the low levels of MCM helicase might be responsible for the DNA damage observed in aneuploid cells. However, the causes of the downregulation of MCM helicase and other replicative proteins are not known.

Defects in protein folding machinery impair replication as consequence of aneuploidy. Others and we showed that the function of chaperone heat-shock protein 90 (HSP90), the major folding protein, is downregulated in aneuploid cells.

Additionally, downregulation of the transcriptional factor promoting HSP gene transcription, named heat-shock factor 1 (HSF1), has been also observed. HSP90 or HSF1 downregulation may cause cellular proteotoxic stress. We hypothesize that the proteotoxic stress and the HSF1 and HSP90 downregulation observed in aneuploid cells may lead to downregulation of the MCMs levels.

As a consequence, proteotoxic stress may impair pre-RC activity by MCMs downregulation either in mRNA or protein levels, or both (Sharma, 2012).

3.1. Zusammenfassung

Die meisten Eukaryontenzellen sind diploid und enthalten zwei vollständige Chromosomensätze. Dieser Zustand wird gewöhnlich als Euploidie bezeichnet. Allerdings können Zellen manchmal eine unausgewogene Anzahl von Chromosomen enthalten, was als Aneuploidie bezeichnet wird. Charakteristisch für aneuploide Zustände sind Veränderungen der Chromosomen, entweder numerisch mit unterschiedlichen Chromosomenzahlen oder strukturell mit Veränderungen der Kopienzahl großer Teile der Chromosomen oder ihrer Arme. Diese Zustände sind in den meisten Fällen sehr schädlich für menschliche Zellen. Aneuploidie wird mit mehreren Krankheiten in Verbindung gebracht, wie z. B. Trisomien der Chromosomen 21, 18 und 13 (Down-, Edwards- bzw. Patau-Syndrom). Darüber hinaus wird Aneuploidie bei etwa 70 % der soliden Tumore sowie bei Leukämien, Lymphomen, neurologischen Defekten und einigen anderen Pathologien gefunden (Donnelly, 2015).

Die molekularen Ursachen der Aneuploidie werden schon seit langem untersucht. Numerische Aneuploidie wird durch die Fehlsortierung homologer Chromosomen während der Metaphase verursacht, die beispielsweise durch Defekte in den Funktionen der mitotischen Spindel, im Zusammenhalt der Schwesterchromatiden oder durch eine beeinträchtigte Funktion des Spindelassamblierungs-Checkpoints entsteht (Davidsson, 2014). Im Gegensatz dazu kann strukturelle Aneuploidie als Folge von fehlerhaften DNA-Replikations- und Reparaturprozessen entstehen. Darüber hinaus wird Aneuploidie bei Krebs häufig mit chromosomaler und genomischer Instabilität, schlechter Prognose und erhöhter Resistenz gegenüber Chemotherapeutika in Verbindung gebracht.

Die Analyse der Aneuploidie ist schwierig, da bisher kein Modell zur Verfügung stand, mit dem isogene diploide und aneuploide Zellen direkt verglichen werden konnten. Für unsere

Untersuchungen haben wir stabile Zelllinien hergestellt, in die eine zusätzliche Kopie eines einzelnen Chromosoms eingeführt wurde. Wir haben zwei verschiedene Zelllinien verwendet. HCT116 stammt aus dem Dickdarm eines männlichen Patienten, der an Darmkrebs erkrankt ist. Diese Zelllinie ist nahezu diploid mit einer Mutation im Ras-Gen (HCT 116 (ATCC CCL-247)). RPE1 ist eine fast diploide menschliche Zelllinie weiblichen Ursprungs. Die hTERT-immortalisierte retinale Pigmentepithelzelllinie, hTERT RPE-1, wurde durch Transfektion der RPE-340-Zelllinie mit dem pGRN145 hTERT-exprimierenden Plasmid gewonnen, und anschließend wurden stabile Klone in einem mit Hygromycin B ergänzten Medium selektiert (hTERT RPE-1 (ATCC CRL-4000)). Durch den Transfer einzelner Chromosomen konnten Zellen erzeugt werden, die dem aneuploiden Zustand sehr nahe kommen und mit den elterlichen Zelllinien isogen sind (Stingele, 2012).

Dieser Chromosomenzuwachs hat eine starke Wirkung auf die Zellen. Da sie ein zusätzliches Chromosom tragen, wirkt sich die Variation der Genkopienzahl auf verschiedene zelluläre Prozesse aus. Es wurde beobachtet, dass die Expression zusätzlicher Gene zunimmt und verschiedene zelluläre Wege beeinflusst (Donnelly, 2014). Eines der Merkmale, die durch numerische Chromosomenvariationen verursacht werden, ist eine veränderte Genomstabilität.

Dies wird durch chromosomale Umlagerungen wie chromosomale Translokationen, Deletionen oder Inversionen dokumentiert, die auf verschiedenen Chromosomen auftreten können. Dies ist wahrscheinlich eine Folge des genotoxischen Stresses, der sich durch erhöhte DNA-Schäden nachweisen lässt.

Ein weiteres Anzeichen für eine zelluläre Veränderung aufgrund von Aneuploidie ist eine langsame Proliferation. Die Zellen zeigen eine Verzögerung im Zellzyklus und scheinen im Vergleich zu diploiden Zellen länger in der G1- und S-Phase zu verweilen. Außerdem leiden die Zellen infolge der Aneuploidie unter proteotoxischem Stress, der wahrscheinlich auf eine erhöhte Expression überflüssiger Proteine zurückzuführen ist (Oromendia, 2014).

Analysen der mRNA- und Proteinspiegel in verschiedenen aneuploiden Zellen ergaben eine signifikante Deregulierung mehrerer Signalwege. Es wurde eine Hochregulierung von Faktoren beobachtet, die an Wegen beteiligt sind, die mit dem endoplasmatischen Retikulum (ER), dem Golgi-Apparat, den Lysosomen und Vakuolen, dem Membranstoffwechsel sowie dem MHC-Proteinkomplex und der Antigenverarbeitung zusammenhängen (Durrbaum, 2014).

Im Gegensatz dazu wurde bei Proteinen, die eine Funktion bei der DNA-Replikation und -Reparatur sowie beim RNA-Stoffwechsel haben, eine starke Herabregulierung beobachtet.

Somit hat die Hinzufügung auch nur eines einzigen Chromosoms starke Auswirkungen auf menschliche Zellen. Besonders interessant fanden wir die starke Herunterregulierung von Signalwegen, die mit der DNA-Replikation zusammenhängen. Die Beeinträchtigung der DNA-Maschinerie könnte den Phänotyp der genetischen Instabilität in aneuploiden Zellen erklären.

Die Proteine, die als Reaktion auf die Replikation besonders herunterreguliert werden, sind an der Erkennung des Replikationsursprungs, der Aufrechterhaltung der ssDNA und an Proteinen beteiligt, die den Kern der Replikationsgabel bilden. Wir fanden heraus, dass alle sechs Untereinheiten eines multimeren Komplexes namens MCM-Helikase als Reaktion auf Aneuploidie herunterreguliert werden. Der MCM-Komplex hat eine typische Helikase-Struktur: Alle Untereinheiten verbinden sich zu einer Kreisform mit einem Loch in der Mitte, durch das die DNA läuft. Diese Helikase gehört zur Superfamilie 6 der Helikasen, und jede Untereinheit hat eine AAA⁺-Domäne; das ATPase-Motiv ist eigentlich mit den erhaltenen Walker-A- und Walker-B-Motiven verwandt. Jedes Walker-A-Motiv einer Untereinheit kooperiert mit dem Walker-B-Motiv der Nachbareinheit, um eine funktionelle ATPase zu bilden; auf diese Weise wickelt die Helikase die Helix ab.

Innerhalb des Komplexes hat jede Untereinheit ihre eigene Rolle: MCM 4-6-7 haben Helikase-Aktivität und sind in der Lage, dsDNA in 5'-3'-Richtung abzuwickeln. MCM2 ist an der Beladung des Komplexes auf Chromatin und an der Interaktion mit Histonen beteiligt, wodurch deren Ablagerung auf Chromatin begünstigt wird. Die Untereinheiten MCM2 und MCM5 fungieren als Tore: Durch die Hydrolyse von ATP können sie zwischen dem offenen und dem geschlossenen Zustand wechseln und so die Beladung des gesamten Komplexes vermitteln. MCM3 fungiert als Überwachungsfaktor für die Integrität des Komplexes und MCM7 interagiert mit dem DNA-Schadenskontrollpunkt. Alle diese Proteine werden im Zytoplasma produziert und in die Zellkerne importiert. Ein weiteres Protein, CDT1, verbindet die MCMs und gemeinsam werden sie in den Zellkern verlagert. CDT1 bindet MCM2-7 an die anderen Prä-RC-Proteine auf dem DNA-Filament; insbesondere bindet es MCM6 über seine C-terminale Domäne und ORC6 über seine N-terminale Domäne.

Die MCM-Helikase ist Teil eines großen Komplexes, des so genannten prä-replikativen Komplexes (pre-RC). Er spielt eine wichtige Rolle bei der Erkennung spezifischer Stellen auf der DNA, an denen die Replikation beginnen soll, den so genannten Replikationsursprüngen. Der prä-RC besteht aus dem Origin Recognition Complex (ORC1-6) und den Proteinen des Zellteilungszyklus 6 (Cdc6). Die ORCs sind in der Lage, DNA an die Replikationsursprünge

zu binden, während Cdc6 dazu dient, die ORCs ordnungsgemäß zu lokalisieren und auch dabei hilft, MCMs auf ATP-abhängige Weise zu binden. Zunächst bindet ORC1 an die Replikationsursprungsstellen, die dann als Nukleationspunkt für die übrigen ORCs dienen. Sobald die ORC-Plattform etabliert ist, werden Cdc6 und MCMs-CDT1 auf die DNA an diesen Stellen geladen. Alle Untereinheiten nutzen die aus der ATP-Hydrolyse gewonnene Energie, um sich aneinander zu binden, wodurch die Bildung dieses großen multimeren Komplexes ermöglicht wird (Fernandez-Cid, 2013).

Die MCM-Helikase wird mithilfe der ORCs-Cdc6-Plattform auf die DNA-Faser geladen. Sobald der gesamte Komplex geladen ist, phosphorylieren die Cyclin-abhängige Kinase (Cdc7) und die Dbf4-abhängige Kinase (DDK) MCM. Dann wird der Komplex durch andere Proteine ergänzt: Cdc45 und GINS, die den Cdc45-GINS-MCMs-Komplex (CMG) bilden. Die Hauptfunktion dieser komplexen Maschinerie innerhalb des Prä-RC in Zellen ist der korrekte und rechtzeitige Beginn der Replikation.

Alle erforderlichen Proteine werden während bestimmter Zellzyklusphasen produziert und aktiviert. MCM2-7-Proteine werden am Ende der Mitose produziert, aber sie werden während der G1-Phase auf das Chromatin geladen, und ihre Konzentration erreicht beim Übergang von der späten G1- zur frühen S-Phase ihren Höhepunkt. ORCs sind normalerweise während des gesamten Zellzyklus vorhanden: ORC1 wird in M-G1 gebildet und bleibt bis zur G1/S-Grenze an das Chromatin gebunden, wo es ubiquitiniert und abgebaut wird. Die anderen ORCs binden sich stromabwärts von ORC1 an die DNA, werden aber in der späten G1- und frühen S-Phase von ihr abgelöst (Kara, 2015). Die DNA-Replikation wird also durch viele verschiedene Mechanismen und verschiedene Arten von Proteinen streng kontrolliert, und jedes wird in einer präzisen räumlich-zeitlichen Weise reguliert.

Diese synchron regulierten Aktivitäten haben ihren Grund, denn sie stellen sicher, dass die Zellen jeden Replikationsursprung nur einmal pro Zellzyklus nutzen. In Eukaryonten beginnt die DNA-Replikation gleichzeitig an vielen Replikationsorten, um sicherzustellen, dass das gesamte längere Chromosom in angemessener Zeit dupliziert wird.

Interessanterweise verfügen eukaryotische Zellen oft über mehr Replikationsursprünge, die mit Prä-RC beladen sind, als für die DNA-Verdopplung benötigt werden, sogenannte "schlafende Ursprünge" (Das, 2014). All diese vielen Stellen haben eine spezifische Funktion: Sie können initiiert werden, wenn Gabeln an DNA-Filamenten hängen bleiben, um zu verhindern, dass der Replikationsprozess im Falle einer DNA-Schädigung zu sehr verzögert wird. Während der DNA-Replikation kann sich die gesamte Replikationsmaschinerie

verlangsamen und sogar stoppen, wenn endogene oder exogene Faktoren wie oxidativer Stress, DNA-Schäden oder geringe Mengen an DNA-Synthesevorläufern auftreten. Die Integrität des Genoms ist jedoch gefährdet, wenn die Replikation über einen längeren Zeitraum verzögert wird, weil die großen Komplexe an den Replikationsgabeln nicht über einen längeren Zeitraum aufrechterhalten werden können. Infolgedessen können die Zellen viele Fehler wie dsDNA und Chromosomenumlagerungen enthalten.

Die "schlafenden Ursprünge" sind in der Lage, diese Fehler zu verhindern: Wenn die Replikationsgabel anhält, können die alternativen Ursprünge aktiviert werden, und die Replikation wird von diesen alternativen Stellen aus fortgesetzt. Auf diese Weise kann die DNA-Replikation ohne Verzögerung abgeschlossen werden, und die DNA wird weitgehend ohne Fehler oder Umlagerungen repliziert. Daher sind korrekte Konzentrationen von MCM-Proteinen für die genomische Stabilität von wesentlicher Bedeutung.

Viele Studien an Mausmodellen und Zelllinien haben gezeigt, dass niedrige und unausgewogene MCM-Konzentrationen Zellen anfällig für Krebs machen: Verschiedene Arten von Krebs oder Krankheiten können aufgrund einer Unter- oder Überexpression einer oder mehrerer spezifischer MCM-Untereinheiten auftreten.

Wir haben festgestellt, dass die MCMs-Konzentrationen sowie die Konzentrationen anderer prä-RC-Faktoren in aneuploiden Zellen herunterreguliert sind. Darüber hinaus werden MCMs-Untereinheiten auch durch einen Defekt von CDK2/Cyclin E dysreguliert. Diese Checkpoint-Faktoren werden tatsächlich herunterreguliert und ihre Akkumulation in den Kernen verzögert.

Eine unzureichende Menge von MCM2-7 und die Deregulierung seiner Phosphorstellen führen somit zu einer unzureichenden Lizenzierung von Replikationsursprüngen und einer unzureichenden Replikation im Falle von Replikationsstress. Dies kann zu DNA-Schäden, DNA-Unterreplikation und in der Folge zu genomischer Instabilität führen. In der Tat haben wir beobachtet, dass aneuploide Zellen vermehrt DNA-Schäden, eine Anhäufung von de novo-Strukturumlagerungen und eine veränderte Replikationsdynamik aufweisen.

Darüber hinaus kann eine Zunahme der MCM-Helikasen einige der Defekte beheben. Somit könnten niedrige MCM-Helikasewerte für die in aneuploiden Zellen beobachteten DNA-Schäden verantwortlich sein. Die Ursachen für die Herabregulierung der MCM-Helikase und anderer replikativer Proteine sind jedoch nicht bekannt.

Defekte in der Proteinfaltungsmaschinerie beeinträchtigen die Replikation als eine Folge der Aneuploidie. Andere und wir haben gezeigt, dass die Funktion des Chaperons

Hitzeschockprotein 90 (HSP90), des wichtigsten Faltungspoteins, in aneuploiden Zellen herabreguliert ist.

Darüber hinaus wurde eine Herunterregulierung des Transkriptionsfaktors, der die Transkription von HSP-Genen fördert, des Hitzeschockfaktors 1 (HSF1), beobachtet. Die Herunterregulierung von HSP90 oder HSF1 kann zellulären proteotoxischen Stress verursachen. Wir stellen die Hypothese auf, dass proteotoxischer Stress und die in aneuploiden Zellen beobachtete Herabregulierung von HSF1 und HSP90 zu einer Herabregulierung der MCM-Spiegel führen können.

Folglich kann sich proteotoxischer Stress auf die Prä-RC-Aktivität auswirken, indem MCMs entweder auf mRNA- oder Proteinebene oder auf beiden Ebenen herunterreguliert werden (Sharma, 2012).

4. Aim of the thesis

Aneuploidy arises from chromosome segregation errors and is associated with several pathologies such as trisomy syndromes or cancer. In cancer, aneuploidy correlates with poor prognosis and high malignancy.

To analyze the consequences of aneuploidy, we have established a series of model aneuploid cell lines created by transferring a specific extra chromosome copy into diploid cells. Many cellular pathways are deregulated in response to chromosome(s) gain, and DNA replication and repair pathways are strongly downregulated. Early analyses revealed low abundance of minichromosome maintenance proteins (MCMs) in aneuploid cells, causing impaired DNA replication and accumulation of DNA damage.

The main aim of my project is to elucidate the mechanisms underlying the replication defects in response to chromosome(s) gain. To this end, we sub fractionated cells during their cell cycle phases. Immunoblotting analysis revealed that a significantly lower amount of MCMs in the DNA-binding fractions. During G1-S transition, chromatin-bound MCM2-7 helicase levels decreases in aneuploid. Using time-resolved mass spectrometry in nucleoplasmic and chromatin-bound fractions, of diploids and aneuploids, we analyzed the molecular mechanisms that are responsible for the deregulated binding of the MCM2-7 helicase in response to aneuploidy. Deregulation of MCM2-7 loading reduces the licensing of replication origins mainly due to defects in the post translational modifications (PTM) on key serines of MCM2 and the 121 of MCM7. Simultaneously, chromosome gain brings to defective cell cycle kinases, Accordingly, we observed changes in the main phosphorylated residue of proteins that interact with cell cycle regulators such as CDKs.

As consequence of chromosomes gain, changes in replication dynamics are due to malfunctional PTM in many serines of MCM2 and the 121 of MCM7. We propose that the presence of even a single extra chromosome leads to genome instability, where DNA damage arising from defects in replication accumulates in daughter cells, generation after generation.

5. Introduction

Organisms pass hereditary information to their progeny in the form of macromolecules called nucleic acids. In eukaryotic cells, the genome is compartmentalised into the nucleus, a specialised cellular region separated from the cytosol by the nuclear envelope, which regulates the inward and outward movement of proteins, nucleic acids such as RNA and other molecules. In this sense, the nucleus is crucial to protect (safeguard) the precious information carried in DNA. Inside the nucleus, the genome is condensed into compact structures called chromosomes. Chromosome numbers vary between organisms: fungi, algae and germ cells often have haploid sets of chromosomes. In contrast, the vast majority of metazoans contain diploid sets, meaning that each chromosome is present in two homologous copies, one inherited from the mother and the other from the father. Humans have forty-six chromosomes: twenty-two pairs of autosomes and one pair of sex chromosomes.

During each cell cycle, the genetic information is first duplicated and then transferred to daughter cells. Cells have many dedicated surveillance mechanisms to ensure the proper replication and distribution of DNA to their progeny. When these mechanisms fail, then daughter cells are generally nonviable. However, some of these abnormal progenies may survive. Surviving abnormal cells can have a different number of chromosomes and/or chromosomes with varying structures; this condition is known as aneuploidy.

5.1. Aneuploidy

Aneuploidy is defined as a change in the normal set of chromosomes and comes in two main categories: a) numerical, when one or more entire copies of chromosomes are gained or lost as a result of abnormal or non-functional chromosome segregation; b) structural, when segments of chromosomes are amplified and joined together with different chromosomes, or lost (Figure 1). Theodor Boveri studied the effect of the chromosome number deviation on the development of sea urchin embryos (Boveri, 2007). Aneuploidy was described for the first time by Lindsley and colleagues (1972), who investigated the effect of structural aneuploidy on the development of flies. Later, Robertson's studies (Magnuson et al, 1982) on translocations in mice embryos revealed the lethality of the aneuploid condition in mammals. Recently, extensive investigations on disomic yeast demonstrated the negative impact of aneuploidy on proliferation (Torres, 2007).

Deviation from the haploid set of chromosomes can occur also in human cells. One of the most common diseases associated with aneuploidy is the trisomy of chromosome 21 or Down syndrome (Mary Kay McCormick 1989; Roper RJ, 2006). In this syndrome, cells carry an extra copy of chromosome 21, which exerts a detrimental effect on cognitive and developmental function (Lebedev, 2004). Other trisomies that are life-threatening in the early stages of life are also known: for example, trisomy for chromosomes 8, 13 and 18, respectively known as Mosaic, Patau and Edwards syndromes (Agrawal, 2011; Loane, 2013, Tamara , 2013). In addition, aneuploid cells are found in the brain during ageing, implying that aneuploidy may contribute to the development of neuronal diseases such as congenital hear diseases, Alzheimer's, schizophrenia, autism or even cancer (MacIntyre, 2003; Wimalasundera, 2004; Tamara A, 2013; Jin Zhu, 2018).

Although aneuploidy is mostly considered a detrimental condition for cells, this is not always true and instead, it can be a normal physiological condition. In yeast, for example, aneuploidy arises as a response to stress conditions, providing the organism with an alternative function that aids survival (Yona et al., 2012). Also, in humans, it was observed that 20–25% of hepatocytes are polyploid and aneuploid (Duncan, 2010). It has been proposed that hepatocytes adopt aneuploid karyotypes to adapt to stress conditions (Duncan, 2012). Further, 30–35% of neuronal cells in foetal brains show deviation from diploidy (Yurov, 2007). Deviation from the haploid set of chromosomes can confer drug resistance to pathological organisms such as fungi (*Candida albicans*) or yeast (*Cryptococcus neoformans*) (Selmeki et al., 2006; Sionov et al., 2010). In addition, plant germlines can tolerate aneuploidy well, suggesting that it can be a temporary way to introduce genetic variation (Henry, 2010).

Despite the above-mentioned examples, aneuploid cells are found in 85% of solid tumours, and a high rate of aneuploidy correlates with poor prognosis and drug resistance (Carter, 2006; Birkbak, 2011; Lee, 2011). This suggests that tumour cells can gain a selective benefit from aneuploidy. Other characteristics that are frequently associated with aneuploid cancer cells are chromosomal instability (CIN) and genomic instability (GIN).

GIN indicates genomic alterations such as micro- and minisatellite instabilities, or it can refer to genomic variation in general, including chromosomal instability (Ninomiya, 2006). For simplicity, GIN can be described as an increased rate of structural chromosomal rearrangements.

In contrast, the term CIN indicates whole chromosomal numerical abnormalities caused by an increased frequency of missegregation. Cells suffering from CIN are also aneuploid, but aneuploid cells do not necessarily exhibit CIN. For example, cells from individuals with Down syndrome do not exhibit CIN, although they carry an extra copy of the chromosome 21 (Valind, 2013). This is also true in tumours, where CIN occurs often, but not always together with aneuploidy.

Currently, it is thought that typical mutations of tumours are accumulated rapidly in changing cells, and GIN is crucial for this rapid mutation rate (Beckman and Loeb, 2006). However, an understanding of the direct link between GIN and aneuploidy is still missing, although a few studies have described links between these two chromosomal conditions (Necchi, 2015; Natarajan, 2015).

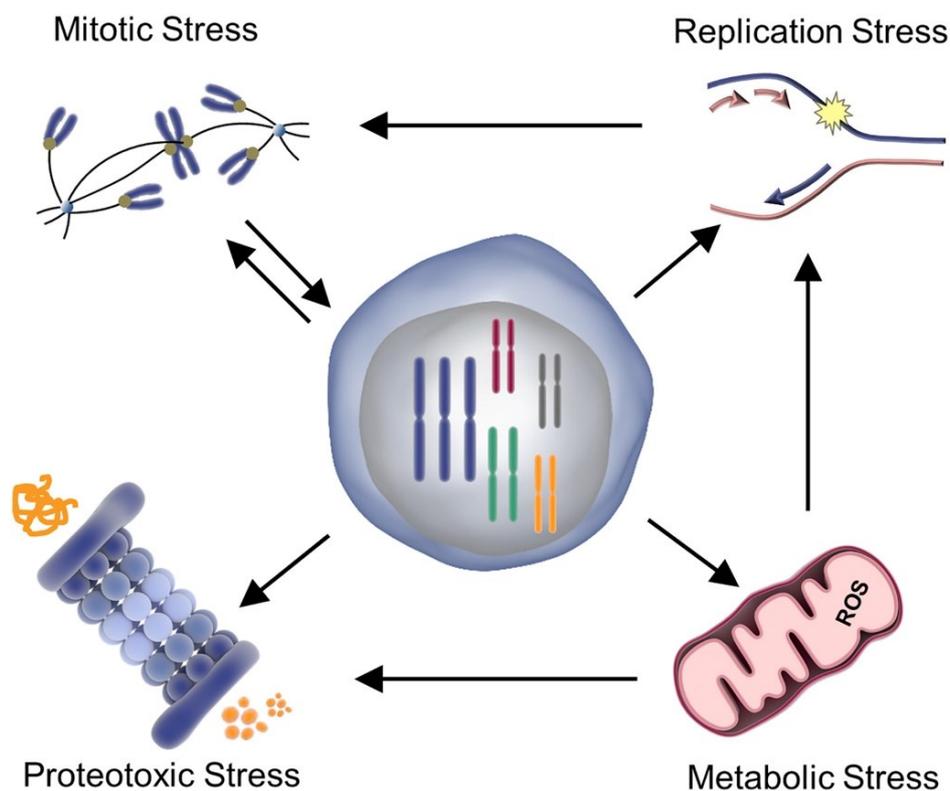


Figure 1. Causes of aneuploidy. Aneuploid cells can be generated as a result of dysfunction in various cellular processes. Reprinted from Cellular Stress Associated with Aneuploidy, 44 /4, Jin Zhu, , Pages No420-431., Copyright (2018), with permission from Elsevier.

5.2. Causes of aneuploidy

Aneuploidy arises from errors in chromosome segregation and their distribution to daughter cells during cell division (Thompson & Compton, 2008, Gordon 2012). Usually, cells have monitoring systems to prevent GIN and CIN. Failure of these systems leads to mitotic catastrophe, which can eventually lead to the onset of aneuploidy (Figure 2) (Chunduri, 2019). One such system is the spindle assembly checkpoint (SAC) (Zirkle, 1970). The SAC is sensitive to the mechanical tension that is generated once chromosomes are connected by microtubules (Santaguida, 2009). The SAC can sense that kinetochores are not attached to microtubules and whether or not chromosomes are aligned to the mitotic plate (Bolanos-Garcia, 2009). In these cases, the SAC delays anaphase, allowing cells to restore the proper attachment between chromosomes and microtubules. It is also possible that microtubules from only one pole bind both kinetochores of the same chromosome. As a result, an entire chromosome is then pulled into one of the daughter cells. Mis-segregation can also be due to defective chromatid cohesion. Chromatid sisters are held together by the cohesin ring complex. This system ensures that chromatids are not split before anaphase onset. Once a cell reaches anaphase, the cohesin ring is opened and the two sisters can be pulled into daughter cells. Sometimes, the ring is not cut, and then one of the daughter cells gains both of the chromatids of a chromosome, which is lost from the other cell (Guacci, 1997; Tanakan 2000; Solomon, 2011).

Centrosome amplification is another way by which aneuploidy might arise. In eukaryotic cells, bipolar spindles are formed by a pair of organelles (one at each pole), which are called centrosomes. Daughter cells gain only one copy of the organelle: it is duplicated again during the S phase. This system ensures that two spindle poles are formed per division, which in turn enables the formation of bipolar mitotic spindles essential for the segregation of a full set of chromosomes to daughter cells. However, sometimes a single cell may acquire more than two centrosomes due to, for example, cytokinesis failure, cell fusion or by centrosome overduplication (Rieder, 1995). As a consequence, multipolar centrosomes form multipolar spindles and chromosomes are randomly segregated into the daughter cells (Cimini, 2003). In a specific condition defined as pseudo-bipolar, multipolarity is resolved, leading to the generation of cells with diploid genomes (Wong & Stearns, 2003; Quintyne, 2005).

Aneuploid cells can also be generated by sporadic errors in the DNA replication and repair processes or by defects in the checkpoints that monitor these processes (Wilhelm, 2016; Xu, 2017). Mistakes can result in the stalling and collapse of the replication fork at specific sites

called common fragile sites (Awate, 2019). This leads to the formation of single-stranded DNA (ssDNA) or the persistence of double-strand breaks (DSB) (Asaithamby, 2011; Zhang, 2015a; Kneissig, 2019). In addition, lagging chromosomes are susceptible to cleavage during cytokinesis. Subsequently, the daughter cells gain pieces of the lagging chromosome. Also, lagging chromosomes can form micronuclei (Janssen, 2011). In these structures, DNA replication is defective, leading to incomplete replication and subsequent chromosome breaks (Crasta, 2012).

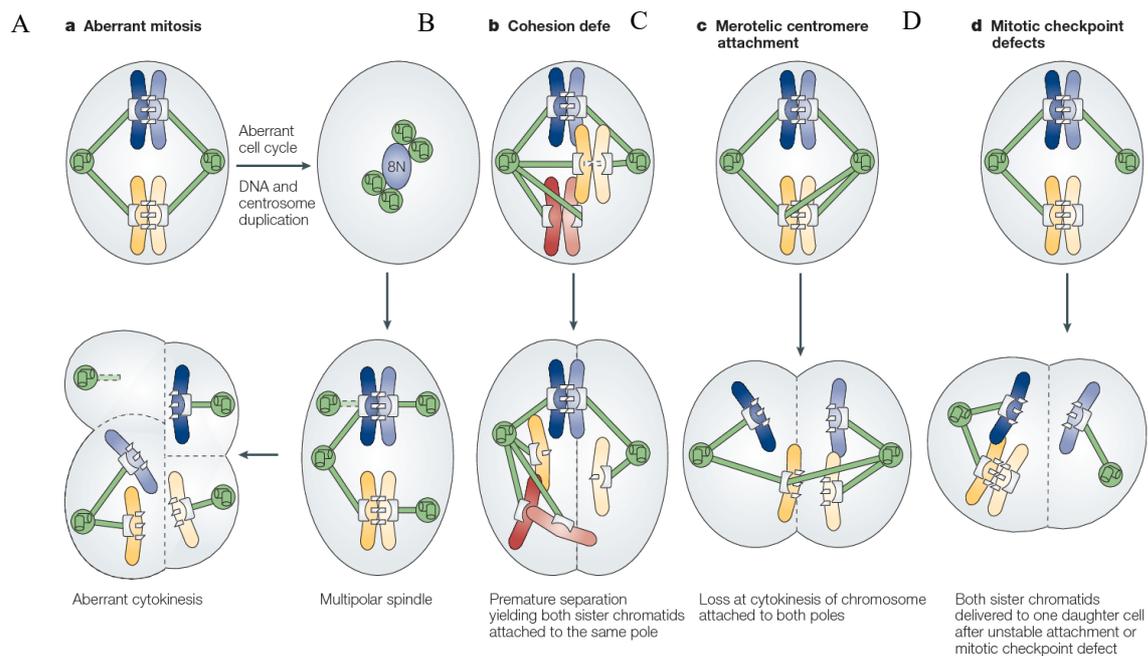


Figure 2. SAC failure and other defects that contribute to aneuploidy. A) Aberrant mitosis. B) Cohesin defects. C) Merotelic attachments. D) SAC defect. Copyright Clearance Center: [SpringNature, Nature Reviews Molecular Cell Biology, Short- and long-term effects of chromosome mis-segregation and aneuploidy (Stefano Santaguida), [COPYRIGHT] (2015)

5.3. Model systems

The role of aneuploidy in pathologies has been difficult to study, as the mechanisms that account for the physiological changes typical of conditions such as cancer or Down syndrome are not well understood (Fonseca, 2001).

A major reason for this gap in knowledge is the lack of proper controls that would allow comparison between aneuploid and normal cells. Once cells have become aneuploid, comparisons cannot be made because the resulting cells are too different from the parental cell line. For example, it is difficult to study the link between aneuploidy and CIN, especially

because aneuploid cells may not necessarily exhibit CIN, which means that it is challenging to distinguish the effects of aneuploidy *per se* from those of chromosome instability (Potapova, 2013, Joshua M. Nicholson, 2015). However, many groups have developed model systems to overcome this problem, resulting in several different model systems based on different organisms, from yeast to mice, which are suitable for the study of aneuploidy (Figure 3) (Miyabara, 1982; Giam & Rancati, 2015; Santaguida 2017). In yeast, diploidization is induced in these usually haploid organisms (Figure 3A–B).

Other model systems follow basically two main approaches in which cells or organisms are generated with either acute or constitutive aneuploidy (Thompson, 2008). To induce acute aneuploidy, the chromosome segregation process is impaired by drug treatment or by manipulating genes required for the mitotic checkpoint and mitotic spindle functions. This system is suitable for cells, tissues or even whole organisms, as the cells very soon acquire an aneuploid karyotype. This approach generates complex aneuploidy: the targeted genomes gain or lose one or more whole chromosomes or their pieces. Cells with complex aneuploidy resemble observed cancer cells (Storchova, 2007). However, it may be difficult to understand whether the consequences of aneuploidy are generated by chromosome copy number changes *per se*, or whether they arise as a side-effect of the drug treatment or the mutation. In the second approach, constitutive aneuploid cells are generated. Here, one copy of a specific chromosome is transferred into recipient cells arrested in mitosis. Then, aneuploid cells are selected by using the specific selection marker that is carried on the transferred chromosome. Using this approach, the resulting aneuploid cells differ from their isogenic counterparts only by the presence of one or two copies of a specific chromosome (Stingele, 2012). Low complexity aneuploidy allows the study of the long-term effects of this condition on cellular physiology (Siegel, 2012; Dürrbaum, 2014).

Many organisms have been modified to study aneuploidy. For example, haploid yeast strains carrying an extra copy of one chromosome have been generated by the random chromosome transfer strategy (Torres, 2007). Mating of yeast strains, one of which has a mutation in the gene required for karyogamy (KAR1), results in defective nuclear fusion. Mating is thus abortive, and at low frequency, a chromosome is transferred from one nucleus to the other. Finally, aneuploid strains can be selected through the use of specific markers. Trisomic mouse embryonic fibroblast (MEFs) are generated by taking advantage of the heterozygosity of two Robertsonian translocations, which occur in male mice (Figure 3C). These mice are mated with

wild-type females, and trisomic cells are generated as a result of meiotic non-disjunction in the male germline (William, 2008). However, trisomic MEFs are highly unstable and the cells soon become polyploid. Therefore, aneuploid MEFs are not suitable for experiments involving repeated passaging (Todaro and Green, 1963).

Human-induced pluripotent stem (iPS) cells can be derived from fibroblast or mesenchymal cells, which are taken from patients with various pathologies, including Down syndrome (Park, 2008); these cells are useful for study, however, it may be difficult to determine the general impact of aneuploidy because only cells from humans with certain trisomies can be studied by using this approach. To study the overall effect of aneuploidy without any of these limitations, a method called micro-cell mediated transfer can be used in human cells (Uponder, 2004; Nawata, 2011; Stingle, 2012). With this technique, a defined human chromosome is introduced into karyotypically diploid human cells from the donor A9 mouse cell lines. Prolonged colchicine treatment inhibits microtubule polymerization, which prevents the formation of a functional spindle during mitosis and thus induces micronucleation (Figure 3D). Micronuclei are collected by centrifugation in the presence of cytochalasin B. Each microcell consists of an intact plasma membrane, a small portion of cytoplasm and a single micronucleus containing from one to five chromosomes (Killary and Lott, 1996). Microcells are then purified by filtration to avoid donor cell contamination and fused to recipient diploid cells by using polyethylene glycol (PEG). Recipient cells containing the human chromosome can be selected for and stably propagated in a suitable medium with appropriate antibiotics (Killary and Lott, 1996).

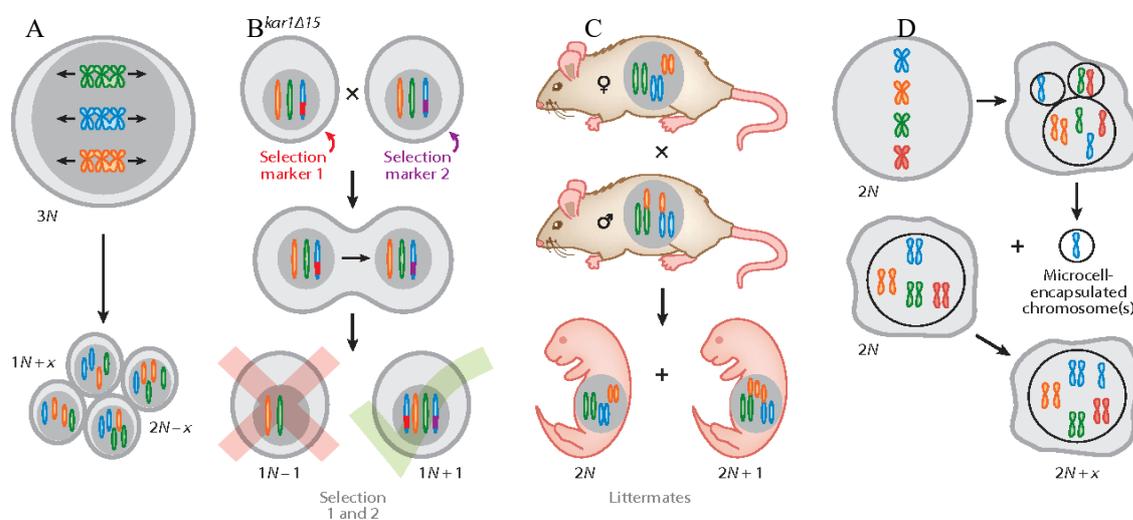


Figure 3. Models systems. A) Yeast strains with uneven ploidy produce highly aneuploid meiotic products (spores). B) Karyogamy-defective yeast strains (KAR1–15) can be used to produce rare chromosome transfers between nuclei during abortive mating by simultaneously selecting two different markers present on homologous chromosomes. C) Aneuploid mouse embryos can be generated through meiotic non-disjunction during gamete formation in male mice with two heterozygous Robertsonian fusion chromosomes. D) Chromosome transfer by fusion of microcell-encapsulated chromosomes with recipient cells. Used with permission of Annual Reviews, Inc., from *New Insights into the Troubles of Aneuploidy*, Siegel, Jake J. Amon, Angelika, 28,1, 2012; permission conveyed through Copyright Clearance Center, Inc.

5.4. Consequences of aneuploidy

The immediate consequence of chromosome missegregation is often the activation of the tumour suppressor p53, although the upstream trigger remains unclear (Tomasini, 2008). Further studies have shown that p53 is activated after DNA damage induction (Hanel, 2012). In these studies, aneuploidy was generated by interfering with the SAC by depletion of mitotic centromere-associated kinesin (MCAK) or of SAC components (Li et al., 2010; Thompson and Compton, 2010; Janssen et al., 2011).

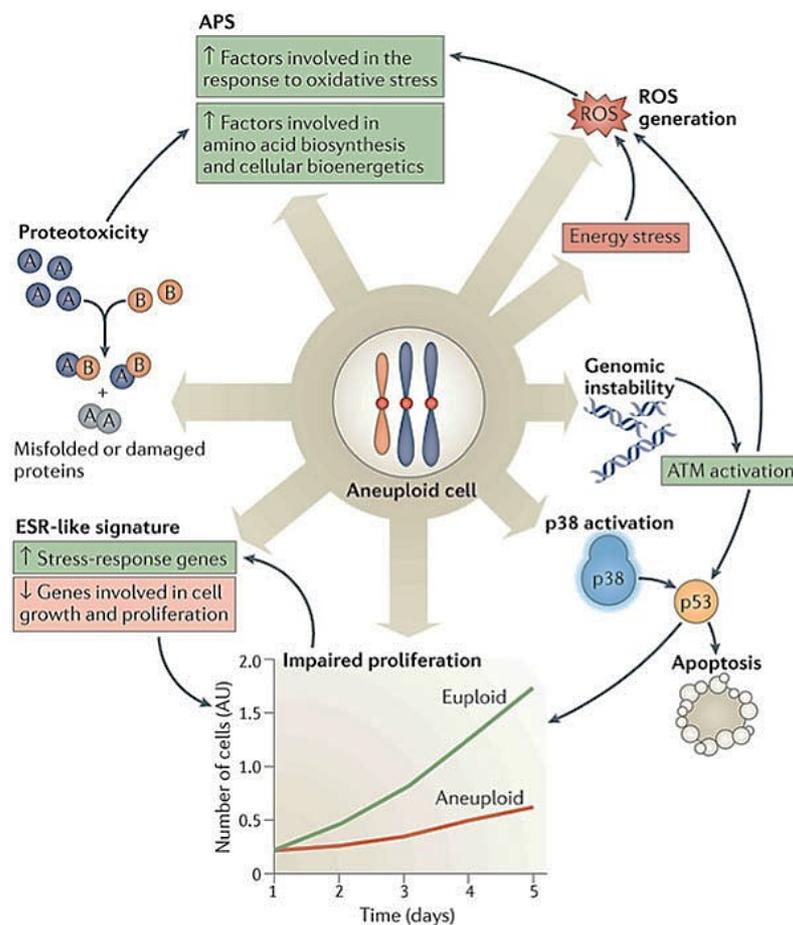


Figure 4. Consequences of aneuploidy. Copyright Clearance Center: SpringNature, Nature Reviews Molecular Cell Biology, On the road to cancer: aneuploidy and the mitotic checkpoint (Geert J. P. L. Kops), [COPYRIGHT] (2005)

These depletions result in the activation of DNA repair due to the presence of reactive oxygen species (ROS), ataxia telangiectasia mutated (ATM) or ataxia telangiectasia and Rad3 related (ATR). The tumour suppressor p53 is activated by these pathways and not because of lagging chromosomes *per se*. However, another study showed that p53 is activated by H3.3 phosphorylation on the lagging chromosome. Indeed, this p53-based phospho-H3.3 in G1 serves as a sensor for chromatin damage (Hinchcliffe, 2016). Recently, it was found a counteractive effect of p53 in eliminating aneuploid mitotic progenies originated by cell-in-cell engulfment (Liang, 2021).

However, the effects of aneuploidy in mammalian cells are not limited to the p53 activation and involve the entire physiology of a cell or an organism. Further, it was shown that all these changes are conserved among species and are not related to the identity of the extra chromosome. Thus, the effect of aneuploidy on cellular physiology is dependent on the unbalanced karyotype only. The stereotypical aneuploid phenotype includes alterations of the transcriptome and proteome, proteotoxicity, proliferation impairment and cell cycle delay (Torres, 2007; Tang, 2011; Oromendia, 2012; Stingle, 2012; Donnelly, 2014; Ohashi, 2015), metabolic alterations (Williams, 2008; Tang, 2011; Torres, 2007) and genomic instability (Sheltzer, 2011; Zhu, 2012; Necchi et al, 2015; Passerini, 2016) (Figure 2).

5.4.1. Gene dosage imbalance

The key question regarding aneuploidy-induced defects is whether the detrimental consequences are due to the presence of extra DNA or whether they are caused by the expression of the specific genes located on the extra chromosome(s). Several studies demonstrated that gene dosage imbalance might be responsible for the expression of the stereotypical aneuploid phenotypes.

In one of these studies, mammalian DNA was transferred into budding yeast where it could be replicated but not transcribed and translated. These cells did not show the usual aneuploid

phenotypes. The yeast could still grow normally and did not suffer from any pathway deregulation, although the cells were slightly bigger (Torres, 2007).

Studies on *Drosophila melanogaster* have demonstrated that the introduction of one extra copy of a chromosome is detrimental for flies. However, if an extra chromosome within a polyploid karyotype is generated, the observed effect is mild. The same result was found for yeast: if an additional chromosome is added to a diploid yeast strain, then the condition is less severe compared to the addition to haploid yeast (Torres, 2007; Oromendia, 2012). Moreover, the only viable trisomies in humans are those carrying extra copies of chromosomes 13, 18 and 21, which are all relatively small and contain only a few protein-coding genes.

Another question is whether the genes on the extra chromosome are expressed at increased levels or whether they are balanced by some intrinsic dosage compensation mechanism such as is utilised for sex chromosomes. Various studies with different organisms and models, including yeast, mouse trisomic cells, Down syndrome patient cells and human constitutive aneuploid cells, have shown that an increase in gene copy number is enough to increase transcription levels for the genes on the extra chromosome (Torres, 2007; Kahlem, 2004; Mao, 2004; Stinglele, 2012).

Importantly, silencing these extra genes or the entire extra chromosome would rescue the aneuploid phenotype. This has actually been proven through several methods. In one approach, cells from Down syndrome patients could be reverted to inducible pluripotent stem cells (iPSC); then, the extra chromosome 21 was removed by selecting for a reporter gene (thymidine kinase with neomycinphosphotransferase reporter gene or TKNEO). These iPSC cells proliferated faster than the original trisomic cells (Li, 2012).

Through another method, a mechanism that is used by female cells to silence the extra X chromosome was employed (Yurov, 2007). This factor, called Xist, covers the second X copy, silencing the chromosome. This system was engineered to target and silence the extra copy of chromosome 21 in Down syndrome cells (Jiang, 2013). Another recently developed method is based on CRISPR/Cas9, in which specific unique sequences on the Y (or other) chromosome are recognised. This system can be used to cut and destroy the extra DNA material within cells (Imaimatsu, 2018).

5.4.2. Deregulation of biological processes

Many biological processes are affected by chromosome gain (Sheltzer, 2012). However, reliable quantification of the changes in the transcriptome and proteome is difficult because the expression of genes on the extra chromosome(s) is only slightly increased (by 50% when one chromosome is gained in diploid cells). Furthermore, gene expression changes are not limited to the genes on the extra chromosome(s) but also include genes on other chromosomes (Upender, 2004; Torres, 2007; Sheltzer, 2012; Stingele, 2012). Strikingly, the same kinds of pathways are always deregulated as a consequence of aneuploidy, regardless of the identity of the extra aneuploid chromosome (Torres, 2007; Stingele, 2012; Dürrbaum, 2014). Moreover, similar pathway changes were observed in cells with complex aneuploidy or in cells taken from individuals with trisomy (Dürrbaum, 2014; Sheltzer, 2012).

Transcriptome and proteome data show that many pathways are downregulated in both human and mouse cells in response to aneuploidy, specifically, DNA replication and repair, cell cycle progression, RNA metabolism, splicing and ribosome biogenesis. On the other hand, some processes are upregulated: Golgi vesicles, endoplasmic reticulum, lysosome functions and the inflammatory response (Sheltzer et al., 2012; Stingele et al., 2012; Dürrbaum et al., 2014). Surprisingly, the innate immune system seems to be stimulated by aneuploidy, and arrested aneuploid cells with complex karyotypes can be cleared by immune cells (Santaguida et al., 2017). In aneuploid budding yeast, the transcriptome changes are reminiscent of the environmental stress response (ESR); there is an upregulation of genes involved in oxidative stress and heat shock, and downregulation of those factors involved in ribosome biogenesis and the nucleolus (Sheltzer et al., 2012).

Moreover, studies on Down syndrome cells revealed an increased activation of oxidative stress genes and decreased levels of cell proliferation genes in human cells and mouse models (Contestabile et al., 2009; Slonim et al., 2009). Although the overall physiological response to aneuploidy is similar across different aneuploidies, cells adapt in different ways, making it impossible to identify individual genes that are invariably deregulated (Dürrbaum et al., 2014). It is also not clear how aneuploidy can globally affect many biological processes when the identity of the extra chromosome is not a critical factor.

In yeast, similarities were found between aneuploidy and the ESR; the ESR is activated in response to many different stresses and also causes lower proliferation. Thus, it was proposed

that the transcriptional response to aneuploidy could also be an artefact caused by the associated defects in cell cycle progression (Regenberg et al., 2006). However, this seems not to be true for human cells: indeed, cells with complex karyotypes can proliferate as fast as diploid cells, although they show the typical aneuploidy response pattern (ARP).

The stress response of aneuploid human cells was analysed upon treatment with compounds such as actinomycin D, bafilomycin A1 and many others. Data from diploid and aneuploid cells were compared and differences in the way that diploid and aneuploid cells respond to stress were revealed. Further, the response to aneuploidy exhibited similarity to the response to drugs interfering with autophagy or transcription as well as to chaperone system deficiency.

Further comparison between aneuploid and cancer cells (depleted of HSF1 and in response to HSP90 inhibition) again revealed a partial overlap (Tang, 2011; Oromendia, 2012; Donnelly, 2014). Taken together, the extra chromosome within human cells causes proteotoxic stress and this might be the cause of the global transcriptome and proteome changes in aneuploid cells.

5.4.3. Protein homeostasis is impaired in aneuploid cells

As mentioned above, proteins are expressed according to the gene copy number in aneuploid cells. However, sometimes protein levels are lower rather than higher as a consequence of chromosome gain. The affected factors are specific subclasses of proteins, especially subunits of multimolecular complexes. In fact, the levels for these proteins are not elevated although their mRNA is more abundant (Torres et al., 2007; Stingele et al., 2012).

Kinases were also found to be downregulated by this compensation mechanism (Stingele et al., 2012). The explanation for these observations may lie in the altered protein homeostasis. As a consequence of the increased protein abundance, the chaperon surveillance systems required for protein folding become overloaded, which may lead to protein aggregation.

The chaperone system is mainly composed of heat shock proteins (HSP family) and their regulators, which function to ensure proper protein folding (McClellan et al., 2007).

Proteins can be degraded by the ubiquitin-proteasome system (UPS). The main regulators of this pathway are proteins of the UPS family, which help ubiquitin mark proteins as degradable substrates for the proteasome. Proteins can also be degraded by autophagy. Together, the UPS and autophagy degrade proteins that are irreversibly mis-folded. Chaperone and protein degradation systems are controlled to maintain protein homeostasis (Chen, 2011; Sin, 2015).

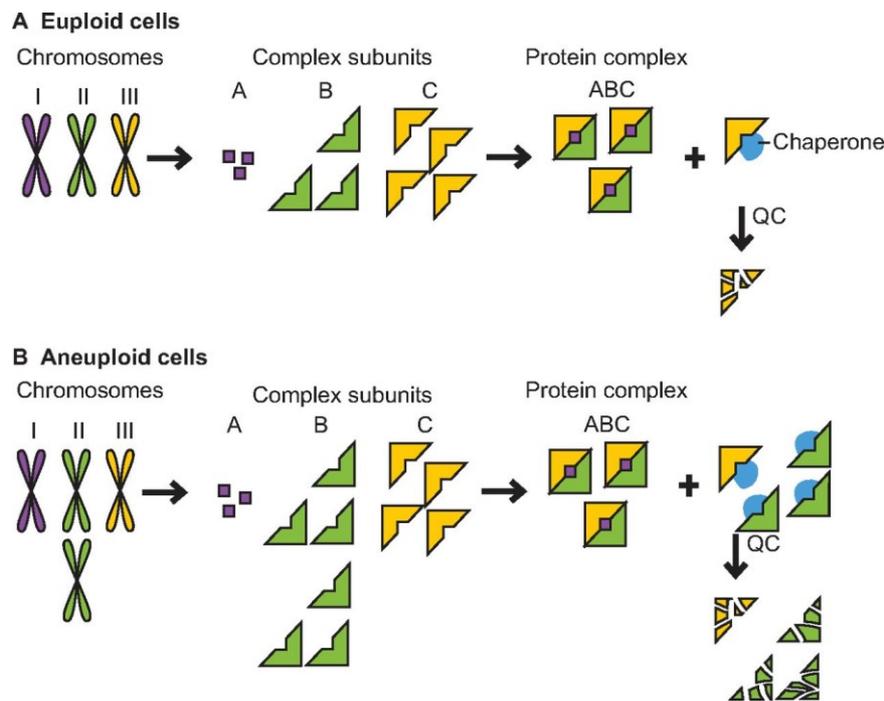


Figure 5. Changes in protein homeostasis as a consequence of chromosome gain. Reproduced/adapted with permission: The Company of Biologists' journals *Dis. Model. Mech.* 7, 15–20, , Aneuploidy: implications for protein homeostasis and disease (Oromendia A. B. & Amon, A) [COPYRIGHT] (2014).

Defects in protein homeostasis can lead to several diseases such as neurodegenerative conditions, dementia, cancer, cystic fibrosis and cardiovascular diseases (Morimoto et al., 2008). As previously mentioned, aneuploidy overwhelms protein homeostasis. It is known that aneuploid cells are more sensitive to chemical inhibition (by the 17-AAG drug) of the main protein folding factor, heat shock protein 90 (HSP90) (Torres et al., 2007; Stinglele et al., 2012; Donnelly et al., 2014).

In yeast, aneuploid human cells and trisomic MEFs, lysosome-mediated degradation and p62-dependent autophagy are upregulated. In fact, aneuploid cells accumulate cytoplasmic protein inclusions, and as a consequence, HSP90 is inactivated and non-properly folded proteins overwhelm the lysosome system (Stinglele et al., 2012; Donnelly et al., 2014; Santaguida et al., 2015; Ohashi et al., 2015).

A previous study from our group confirmed that aneuploidy negatively affects the protein folding system by impairing HSP90 function. Possible reasons for such an effect are the downregulation of the HSP90 transcription factor and heat shock factor 1 (HSF1). Overexpression of HSF1 can alleviate the impairment of the heat shock response (Donnelly et al., 2014). HSP90 defects can have severe consequences for cell physiology. Indeed, HSP90 clients are mostly kinases and signal transduction factors (Sharma et al., 2012; Taipale et al., 2014). Furthermore, HSP90 also plays a role in protein complex assembly (Makhnevych and Houry, 2012; Gopinath et al., 2014). Therefore, the abundance of kinases and multimolecular complexes is lower in aneuploid cells, as a consequence of the defects in HSP90 activity. Interestingly, protein folding and degradation pathways are often upregulated in tumours, conferring stress resistance to cancer cells (Kang et al., 2008; Rouschop et al., 2009; Kon et al., 2011). As a result, in some recent studies, several groups have targeted cancer cells with drugs that interfere with the protein folding system and autophagy (Kraus et al., 2015; Lazenby et al., 2015; Ishitsuka et al., 2015; Spreafico et al., 2015; Rangwala et al., 2014).

5.4.4. Metabolic alterations due to chromosome gain

Tumour cells require elevated amounts of energy and thus exhibit altered metabolic requirements. Changes particularly occur in the glycolytic pathway, and it has been proven that cancer cells harbour higher concentrations of glucose than non-transformed cells (Hirayama et al., 2009). Further, tumour cells are also more sensitive to glucose limitation (Jain et al., 2012), and glycine consumption is related to the proliferation rate (Birsoy et al., 2014).

Recently, it was shown that aneuploidy induces metabolic alterations as well. Indeed, aneuploid yeast strains produce low levels of biomass per glucose molecule that they take up, and, interestingly, aneuploid strains can take up more glucose than haploid strains. The biomass generation seems to be inversely proportional to the proliferation rate (Torres et al., 2007).

Trisomic MEFs, on the other hand, showed slightly different metabolic changes: they do not take up more glucose, but increase their consumption of glutamine and lactate and upregulate ammonium production (William et al., 2008). In our constitutive aneuploid cells, there is an upregulation of energy metabolism as well as mitochondrial respiratory and carbohydrate metabolisms (Stingele et al., 2012). According to the evidence described above, it can be speculated that chromosome gain results in increased energy requirements, possibly due to the

translation, transcription, folding and degradation of factors, which are encoded on the extra chromosome(s). The ensuing metabolic changes and increased energy requirements might affect the proliferation rate of aneuploid cells.

As there are similarities between the metabolic alterations in cancer cells and those in aneuploid cells, it was proposed that in cancer cells these metabolic changes arise due to the aneuploid state of tumour cells (Santagiuda, 2015b). However, more studies are needed to prove this hypothesis.

5.4.5. Aneuploidy negatively affects cell proliferation

In the 1970s, growth defects were observed in cells derived from Down syndrome patients (Segal and McCoy, 1974). More recently, similar defects were also seen in aneuploid yeast strains, which attributed to a specific elongation of G1 in diploid compared to haploid yeast strains (Torres et al., 2007). Cell proliferation defects were also observed in cells derived from trisomic mice, which harboured a mutation in BUBR1, a component of the SAC, which often results in chromosome missegregation (Torres et al., 2008; Baker et al., 2004). Consistently, the same growth defects were observed in constitutive human aneuploid cells. The extent of the growth defect is proportional to the size of the extra chromosome. In constitutive human aneuploid cells, only the G1 and S phases of the cell cycle were negatively affected, and G2 and mitosis could be completed within the normal physiological timeframe in these modified cells (Stingele et al., 2012).

It is still poorly understood whether the growth defects of aneuploid cells occur as a consequence of detrimental overexpression of genes that control critical cellular pathways or whether the impaired proliferation might be a consequence of the simultaneous deregulation of multiple genes, whose altered expression is not harmful when taken in isolation. In other words, gene copy number changes lead to growth defects in aneuploid cells, although these genes are not harmful when they are overexpressed singularly (Tang, 2013; Iourov, 2015; Dürrbaum, 2016; Kaya, 2020).

Studies on trisomic 21 iPSCs showed that proliferation can be rescued when one copy of chromosome 21 is silenced (Li et al., 2012; Jiang et al., 2013). However, cancer cells grow

faster than aneuploid models, meaning that tumours must acquire adaptive changes to overcome the proliferation defects caused by aneuploidy.

5.4.6. Aneuploidy leads to increased genomic instability

Genomic instability comprises many different modifications, which cause inheritable changes in the genomes of cells. Such modifications range from single nucleotide variations to structural and/or numerical chromosomal abnormalities.

Recent studies suggested that genomic instability can be a consequence of changes to the karyotype. Indeed, aneuploid budding yeast carrying only one extra chromosome showed increased rates of chromosome loss, mutation and mitotic recombination. As a consequence, levels of the DNA damage marker Rad52 were higher in these aneuploid yeast strains (Sheltzer et al., 2011). It was also shown that the presence of extra DNA *per se* does not induce genomic instability: the presence of yeast artificial chromosomes (YACs) carrying human DNA did not lead to DNA lesions or genotoxic stress. However, severe gene dosage imbalance was observed in disomic yeast strains, which was milder in trisomic yeast. In disomic yeast, the extra chromosome copy leads to a two-fold induction in protein production. In contrast, the increase in protein levels is only 50% in trisomic strains, and, therefore, these strains are more resistant to genotoxic stress than disomic strains (Sheltzer et al., 2012). Moreover, increased genomic instability was found in cells from Down syndrome patients. It was proven that Down syndrome lymphocytes accumulate DNA damage that cannot be repaired efficiently (Natarajan et al., 2015; Morawiec et al., 2008). Similarly, Down syndrome skin fibroblasts exhibited a higher incidence of genomic instability due to DNA damage and defects in DNA repair, although the checkpoint was found to be functional (Necchi et al., 2015). Therefore, gene dosage imbalance induces genomic instability. However, more studies are needed to elucidate the molecular mechanisms that lead to genomic instability in aneuploid cells.

5.5. Causes of genomic instability in aneuploid cells

Maintenance of a stable genome is an absolute requirement for cells in order to avoid the emergence of pathological states (Figure 6) (Yurov, 2014). As discussed above, GIN is crucial for cancer development because the high mutation rate leads to heterogeneity, conferring selective advantages on cancer cells (Beckman and Loeb, 2006). Many forms of GINs have been defined: mini- and microsatellite instability, point mutations, chromosomal

rearrangements and copy number variations. These aberrations were shown to result from defective DNA replication, DNA repair and checkpoint systems (Hakim et al., 2012; Roberts et al., 2012; Waddell et al., 2015; Blank et al., 2015). Alterations to DNA can arise during normal cellular metabolism, but some events can introduce alterations more often than others. Importantly, cells have many different mechanisms to prevent the accumulation of DNA damage and to ensure that the fidelity of the genetic information is preserved for daughter cells. Maintaining the integrity of the genome, proper DNA replication, functional and efficient activation of the checkpoint and DNA repair are all essential.

5.5.1. DNA replication as a source of DNA damage

DNA replication defects are a source of DNA damage, and it is vital that the entire genome is replicated before mitosis starts. Eukaryotes have evolved different mechanisms to tightly regulate replication owing to the large size and structural complexity of their genomes.

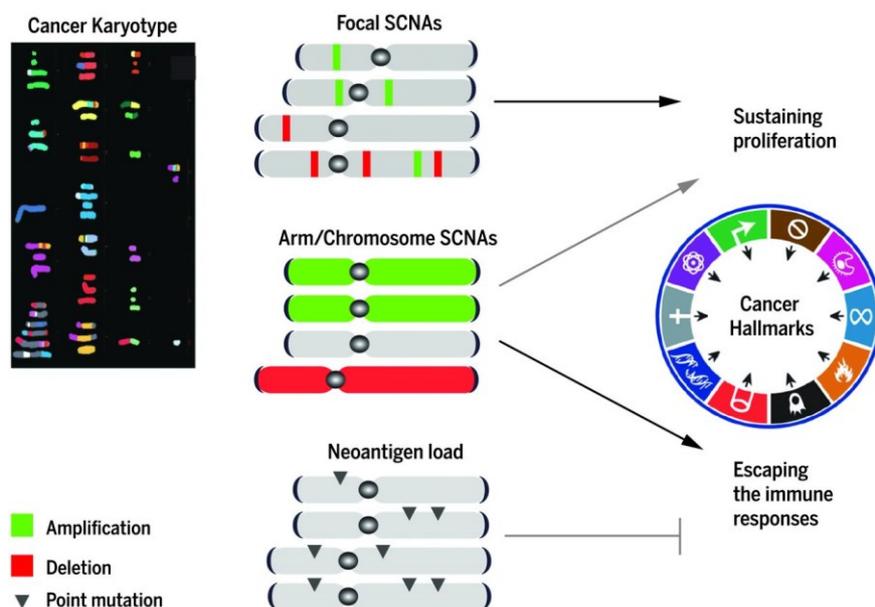


Figure 6. Across several human tumour types, high somatic copy number alterations (SCNAs) levels correlate with increased expression of cell cycle markers and decreased expression of markers of cytotoxic immune cell infiltrates. A high load of tumour neoantigens (reflecting a high level of point mutations) promotes the detection of tumours by the immune system, limiting immune evasion. The relative contribution of focal, arm/chromosome and neoantigen load to the prediction of proliferation and immune evasion is shown. Reproduced from: Davoli T, Uno H, Wooten EC, Elledge SJ., Tumor aneuploidy correlates with markers of immune evasion and with reduced response to immunotherapy. *Science*. 2017 Jan 20;355(6322):eaaf8399. doi: 10.1126/science.aaf8399. PMID: 28104840; PMCID: PMC5592794.]. Reprinted with permission from AAAS.

Replication starts from specific sites on DNA called origins of replications (ori sites). These sites are clustered in groups of up to five origins per cluster. Due to the large amount of DNA in eukaryote cells, replication involves sequential activation of many clusters, which allows replication to be achieved at the proper time (Guilbaud et al., 2011). Moreover, there is a mechanism that ensures that origins of replication are activated only once per cell cycle, as otherwise DNA damage or overamplification might be introduced. The control of ori sites is achieved in many ways. There is a temporal separation between the recruitment of the necessary factors to the origin of replication (origin licensing), and its activation (origin firing) (Yeeles et al., 2015). Specifically, the licensing process occurs during the G1 phase, and cascading activation of many proteins is needed for recognition of the ori sites. These proteins form a large complex termed the pre-replication complex (pre-RC), which is comprised of origins of replication complex (ORC1-6), cell division control protein 6 (CDC6), chromatin licensing and DNA replication factor 1 (CDT1) and mini-chromosome maintenance proteins (MCM2-7).

The pre-RC factors have to bind DNA through a specific sequence of events to properly license an origin of replication. ORC1-6 recognises and binds ori sites on DNA followed by CDC6, and subsequently, CDT1 recruits MCM2-7 to the rest of the complex and the pre-RC is formed. As soon as MCM2-7 is associated with the rest of the complex, CDC6 and CDT1 are immediately released. This ensures that a specific origin of replication is activated only once per cell cycle (Méndez and Stillman, 2000; Remus et al., 2009). Furthermore, pre-RC loading is allowed when cyclin-dependent kinases (CDK) activity is low, ensuring that the complex stays inactive during the G1 phase, but is activated in the S phase (or rather in G1/S) when CDK activity is higher (Yeeles et al., 2015).

There are many more levels of surveillance to avoid premature initiation or reactivation of the pre-RC. For example, the single subunits are targeted by post-translational modifications (PTM) that function in the transport to different cellular compartments or that regulate DNA binding. Phosphorylation of certain amino acids of the MCM2-7 subunits occurs in response to low CDK2 and cyclin E (CycE) activity and promotes DNA binding. In addition, in the S phase, metazoans stabilise another factor called Geminin. CDT1 is then bound by Geminin and the interaction with MCM2-7 is disrupted. Later during anaphase, the APC degrades Geminin, thereby restoring the CDT1–MCM2-7 interaction (McGarry and Kirschner, 1998). Many studies have shown that overexpression of either CDC6 or CDT1 triggers re-replication and leads to genomic instability (Zhong et al., 2003; Thomer et al., 2004; Mailand, 2005). Over the

course of the cell cycle, the pre-RC matures into a fully functional replication complex (RC) through the addition of many other replication factors. The events involved in this maturation and in activation of the pre-RC are not well understood, but the kinase activity of CDK2/CycE and CDC7/Dbf4 on the pre-RC are required during the G1/S or S phases. Finally, in the S phase, origins are activated, but not all at the same time (Guilbaud et al., 2011).

Cells harbour excess amounts of MCM2-7, which allows them to potentially license all origins. However, not all origins are activated. These are called dormant origins, and they serve as a back-up system in the case of replication fork stalling. Dormant origins are activated only when one adjacent fork is stalled and replication stress occurs. Then, a new fork can bypass the stalled one to ensure that replication is accomplished in the proper physiological timeframe (Ge et al., 2007; Woodward et al., 2006; Ibarra et al., 2008).

Upon origin firing, the cell needs to balance the speed of replication and the consumption and distribution of all these proteins. Damage to DNA can be physically bulky and usually results in the formation of ssDNA due to the action of the helicases, which unwind the helix and the stalled replication fork (Pacek et al., 2004). The general mechanism involves the binding of replication protein A (RPA) to ssDNA, which serves to build a platform of proteins that initiate the activation of the checkpoint cascade. The two major activated proteins are ATM and ATR (Marechal et al., 2013; Gralewska, 2020). There are many causes of replication stress, with profound effects on DNA replication. Nicks, gaps and stretches are the main factors, because once encountered by the replication machinery they can be converted into DSBs. Other types may represent physical barriers for protein complexes, but can be bypassed by DNA damage tolerance pathways (Mailand et al., 2013). Both replication and transcription occur on DNA, and sometimes they can interfere with each other, resulting in the slowing or blocking of both processes. This can lead to the formation of DSBs, and some researchers have found correlations between such collisions and fragile sites in highly transcribed regions replicated early in the mammalian S phase: for example, collision of replication and transcription processes results in breaks in the DNA helix (Pomerantz, 2010; Barlow, 2013; Wang, 2017; Marnef, 2017). Loss of RNA processing components might be involved in these collisions between helicases and topoisomerases (Tuduri et al., 2009), or the RNA behind the transcription bubble could re-hybridise with DNA, forming a three-stranded chain containing a hybrid called an R-loop, which is usually resolved by RNaseH (Yuce et al., 2013; Skourti-Stathaki 2014; Hamperl, 2017; Rinaldi, 2021).

Replication stress can be caused by external factors such as chemical compounds or UV-induced lesions. However, endogenous factors also hamper the replication machinery, such factors include defects in dNTP production inside cells, the formation of secondary structures, DNA damage, common fragile sites, telomeric regions or downregulation of replication machinery components such as the MCM2-7 helicase (Zeman and Cimprich, 2014).

Whenever the replication bubble is slowed down or stalled due to the presence of one or more of these conditions, dormant origins are activated to preserve genome integrity (Woodward et al., 2006; Ge et al., 2007; Ibarra et al., 2008). Sometimes, replication stress might be a source of damage to DNA; for instance, areas of replicating DNA might persist as ssDNA due to poor coordination between the fork and the helicase (Pacek and Walter, 2004). Importantly, it was demonstrated that a lower abundance of functional MCM2-7 (the chromatin-bound fraction) does not impair replication in unperturbed cells (Ge et al., 2007; Ibarra et al., 2008), although increased levels of DNA damage and increased numbers of micronuclei are subsequently evident in these cells (Ibarra et al., 2008). However, additional perturbation of the replication does not allow completion of DNA synthesis and the cells are non-viable (Ibarra et al., 2008).

In mice engineered to express hypomorphic mutated alleles of MCM2 and MCM4, MCMs could not efficiently bind DNA, and as described above, dormant origin activation failed, replication forks stalled on DNA and DNA damage was increased in these non-perturbed mice. In addition, the tumour development rate was higher in these mice, suggesting that dormant origins might be tumour-suppressive (Shima et al., 2007; Kunnev et al., 2010; Klotz-Noack and Blow, 2011).

5.5.2. Cell cycle and checkpoint defects lead to GIN

Different steps, each of which corresponds to a different juncture in the process of growth, DNA replication and cell division, characterise the life cycle of a cell. Only two major steps of the cell cycle were originally detected, mainly thanks to microscopy studies: the interphase and M phase. In the former, the cell grows, replicates its DNA and synthesises the proteins needed for the next step; the M phase involves the segregation of chromosomes and the physical separation of mother and daughter cells. Following those initial studies, it was discovered that the interphase was comprised of more steps called G₀, G₁, S and G₂ (Norbury and Nurse, 1992;

Conti, 2001). Cells in the G₀ phase are in a quiescent and non-proliferative state. Once a cell enters G₁, it starts to synthesise all the proteins that are involved in the progression of the cell cycle including the replication machinery, which is kept in an inactive state until entry into the S phase. In the S phase, the DNA is replicated and during this step an enlarged nucleus containing twofold DNA content can be observed. In the G₂ phase, the cell has replicated the entire genome and checks if everything has been completed before going into mitosis.

Cells can regulate the expression of proteins during each phase; nevertheless, once they overcome the restriction point, which is a point of no return, the cells are committed to completing replication and mitosis. The proteins that drive cell cycle progression are known as cyclin-dependent kinases (CDK). These kinases, once activated, phosphorylate downstream targets and initiate a complex regulatory cascade that leads to cell duplication (Morgan, 1996; Ekholm, 2000; Lygeros, 2008; Blow, 2011). Usually, the CDK levels during the cell cycle are relatively constant; they are synthesised, but are present in an inactive state until activation by other proteins called cyclins (Cyc). The execution of each cell cycle phase is dependent on the interaction between CDK and Cyc.

Cyclins are produced and activated only at specific times of specific cell cycle phases in an orderly fashion. They interact with the repressor domains of the CDKs, releasing their catalytic site and rendering them active. It is now known that CDK4, CDK6 and CDK2 are activated by a member of the CycD family (D1, D2 and D3) during the G₁ phase (Sherr et al., 1999; Mukherjee, 2010; Sherr et al., 2016) or CycE in late G₁, whereas the main complex that is active during the S phase is composed of CDK2/CycA (Girard et al., 1991). Both CDK1/CycA, at the early stages (Walker et al, 1991), and then CDK1/CycB are needed during the G₂ and M phases to overcome the final restriction point and enter mitosis (Abraham, 1995; Arellano et al., 1997; Vermeulen, 2003) (Figure 7). In addition to the cyclins, another level of CDK regulation is achieved by phosphorylation and dephosphorylation events, which occur on some of their threonine or tyrosine residues: Wee1 and Myc are involved in phosphorylation whereas cdc25 is responsible for the dephosphorylation (Lew et al., 1996; Pei, 2005). Finally, another level of control is exerted by CDK inhibitors (CKIs), which can bind CDKs individually or in CDK/Cyc complexes, abolishing their activity (Sherr et al., 1995). The two major families of CKI are known as INK4 and Cip/Kip. The former is active during the G₁ phase and has the ability to bind CDK before Cyc, thus blocking the activating partner. In this family of proteins are the Cip/Kip proteins p16, p19 and p18, which are able to inhibit CDK4 and CDK6

(Malumbres, 2006). Although the Cip/Kip proteins usually inhibit CDK/Cyc complexes, they can also inhibit the activation of proliferating cell nuclear antigens (PCNAs), thus blocking DNA synthesis (Mukherjee, 2010; Gan, 2017; Wong, 2020). As mentioned above, the cell cycle is very intricately regulated, and it is important to stress that both internal and external signals have a role in regulating the CKIs. One protein responding to such stimuli is the p53 tumour-suppressor gene, which controls the expression of p21 (el-Deiry, 1993; Hills, 2014; Galanos, 2016). For example, in p53-deficient mice, the transition from a precancerous lesion to cancer is accelerated (Bartkova et al., 2005; Gorgoulis et al., 2005; Bartkova, 2006). These proteins are active only in a specific intracellular compartment and inactive in the others. In most situations, the cell cycle progresses without any perturbation, but sometimes errors occur during the cycle. This could be caused either by an endogenous source or by some external factor like mutagenic substances or irradiation; one source of DNA damage is UV irradiation. In such cases, the cell is capable of recognising the damage and eventually, it can correct the problems by employing a complex network of DNA damage checkpoints, collectively termed the DNA damage response (DDR). The DDR can intervene and limit the potential difficulties for cell duplication and growth. Genetically defined control mechanisms called checkpoints are important elements of the DDR. Usually, there are three checkpoints: G1/S, G2/M and intra S phase (Johnson, 1999; Kastan, 2004; Piunti, 2014). At each checkpoint, a different set of proteins monitors the cellular status and if errors or DNA damage are found, they stop the cell cycle progression (Dungrawala, 2015; Park, 2017; Macheret, 2018). This occurs by inhibition of the CDKs that normally drive the progression of the cell cycle. The proteins whose role it is to recognise such damage are the PI3 kinase family and include the ATM and ATR. In response to different kinds of damage, both kinases trigger a complex signal transduction cascade, which results in a cell cycle delay. The G1 checkpoint is regulated upstream by a tumour-suppressor gene known as retinoblastoma (Rb). Usually, during G1, Rb inactivates the E2F transcription factor by sequestering it, but when Rb becomes phosphorylated, E2F is free to diffuse to the nucleus where it binds to DNA, promoting the transcription of proteins involved in cell cycle arrest. In addition, the p53 levels are increased after DNA damage at the G1/S checkpoint. This induces p53 activation, which promotes the transcription of p21, Mdm2 and Bax, the collective action of which stops the cell cycle and, if the damage is too severe, stimulates cell death (Siliciano et al., 1997).

Different lines of evidence suggest that these events are very tightly controlled. Indeed, entry into the S phase has to be slowed down until all ori sites are licenced, a control mechanism

called the licensing checkpoint (Shreeram et al., 2005). It was shown that reduced amounts of MCM2-7 on DNA lead to delayed entry into the S phase (Shreeram et al., 2002; Machida et al., 2005a; Nevis et al., 2009). Interestingly, many cancer cells can enter the S phase normally, although the number of licensed origins is reduced (Shreeram et al., 2002; Feng et al., 2003; Liu et al., 2009; Nevis et al., 2009). Another checkpoint is the intra S checkpoint where either the initiation or elongation phases of DNA replication are inhibited. Some studies also indicate the involvement of ATM-mediated phosphorylation events in this pathway (Lim et al., 2000). Mutations in both alleles of ATM result in the development of the ataxia telangiectasia disorder characterised by breast cancer predisposition (Renwick et al., 2006). Moreover, in the intra S phase, dNTP depletion leads to the activation of RPA by ATR, and the ssDNA is coated (Branzei and Foiani, 2010).

Finally, the cell cycle is arrested with or without p53 in G2. The aim of this arrest is to maintain CDK1 in its inhibited form. This is achieved by activation of the Chk1 and Chk2 kinases, which are controlled, respectively, in an ATR- or ATM-dependent manner. The DNA damage checkpoints are not the only ones present in cells; for example, another checkpoint known as the SAC is active during mitosis before the metaphase starts. It recognises the improper alignment of chromosomes through spindle fibre tension, and involves the activation of Mad and Bub proteins, which results in metaphase arrest (Fang et al., 1998).

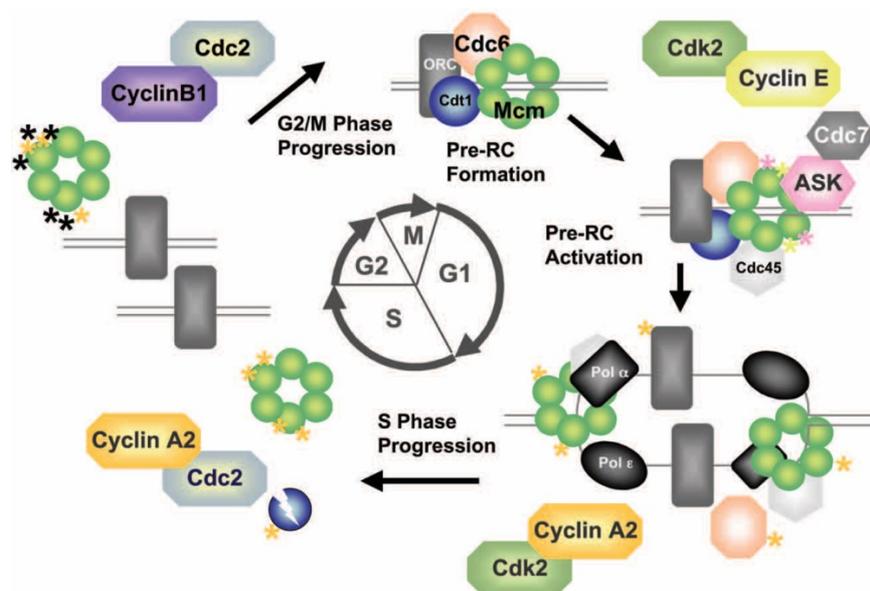


Figure 7. Cell cycle checkpoints and MCM2-7 regulation. MCM-7 and the entire pre-RC are tightly regulated throughout the cell cycle by kinase activity. Copyright Clearance Center: IUBMB Life, Critical Review, Control of DNA replication: Regulation and activation of eukaryotic replicative helicase, MCM. (Masai, H), [COPYRIGHT] (2005)

6. Results

6.1. Generation of constitutive aneuploid cells

To study the effects of aneuploidy on cellular physiology, a system to generate cells carrying one or two copies of a specific chromosome was established in our lab (details of the procedure are given in the Materials and Methods section).

To generate constitutive aneuploid cells, two different cell lines were used: the cancer cell line HCT116 and non-cancerous immortalised RPE1. The use of cells with different origins allowed the characterisation of all common features that are specific for aneuploidy. For all the experiments, the parental cell lines HCT116, RPE1 as a control and the respective aneuploid cells were tested.

The extra chromosome copy was carried by the A9 mouse cell line. Thus, the formation micronuclei were induced chemically by colchicine treatment for 48 h. Subsequently, micronuclei were collected by centrifugation. Then, micronuclei were fused with recipient human cells (HCT116 or RPE1), which were chemically induced to progress slowly through the M phase. Finally, cells carrying an extra copy of a specific chromosome were selected based on antibiotic resistance (G418, blasticidin or zeomycin).

Metaphase spreads were performed to confirm the presence of the extra chromosome within the new aneuploid clones. For example, DNA probes were used to identify a specific centromeric region of human chromosome 5 (Figure 8A), whereas DNA probes for chromosome 2 were used as a control. Indeed, four signals for chromosome 5 were detected, indicating that the cells had become tetrasomic for this chromosome (5/4).

To verify the genome integrity of the new aneuploid cell lines, next-generation sequencing (NGS) analyses were performed. Through identification of specific chromosome sequences, the newly generated cells were proved to be harbouring two extra copies of chromosome 5 specifically (i.e., 5/4) and that there were no other genomic rearrangements (Figure 8).

All the aneuploid cell lines were generated by using this method. These modified cells were used for the experimental procedures described herein, namely HCT116 tetrasomic for

chromosome 5 and trisomic for chromosomes 3 or 5. Additionally, the following RPE1-derived trisomic cells were used: 3/3, 5/3–12/3, 21/3, 7/3 and 8/3.

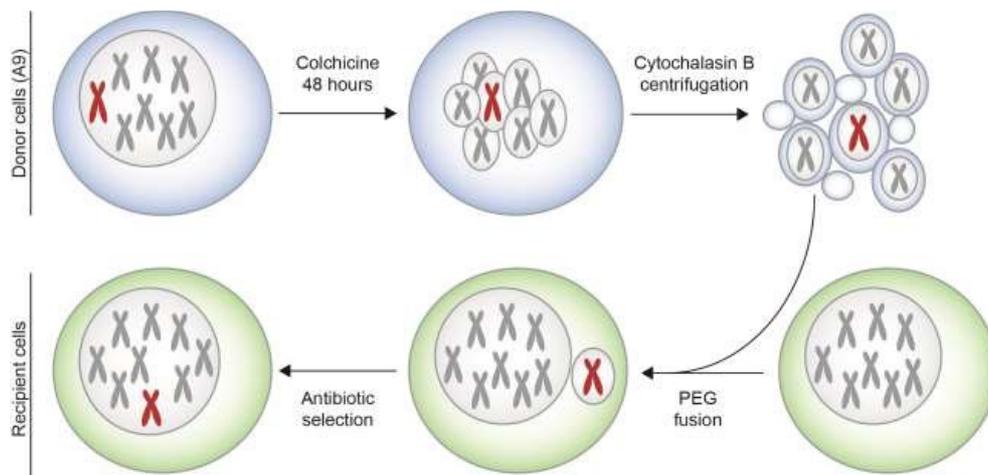


Figure 8. Microcell-mediated chromosome transfer. Microcells with micronuclei generated from a mouse donor cell line carrying a specific human chromosome (depicted in red) are transferred into a human acceptor cell line. Subsequent selection for the presence of the transferred human chromosome is achieved by culture in antibiotics. (Passerini, 2016).

6.2. Prolonged cell cycle in aneuploid cells is due to extended G1

Our group has reported that the gain of one or more extra chromosome copies results in slower proliferation (Stingele, 2012). In light of this, the question as to which phases of the cell cycle are altered by aneuploidy becomes intriguing. To this end, cells were synchronised in G0/G1 by removing growth factors using media without foetal bovine serum (FBS). Thus, HCT116 cells and derived aneuploid cell lines were cultured in media deprived of FBS for 72 h (Figure 9). RPE1 and derived aneuploid cells were cultured in media without FBS for 48 h rather than 72 h. After synchronization, cell proliferation was induced by the addition of 10% FBS and the cells were collected at the following time points: 0, 4, 6, 8, 12, 16 and 24 h for HCT116, and 0, 8, 12, 14 and 18 h for RPE1. Subsequently, cell cycle progression was analysed based on the incorporation of the thymidine analogue 5-ethynyl-2'-deoxyuridine (EdU, 10 μ M). EdU was added to the media 30 min before sample collection (Figures 9 and S1A, in the Supplementary Material). Finally, cell cycle analyses were performed by flow cytometry.

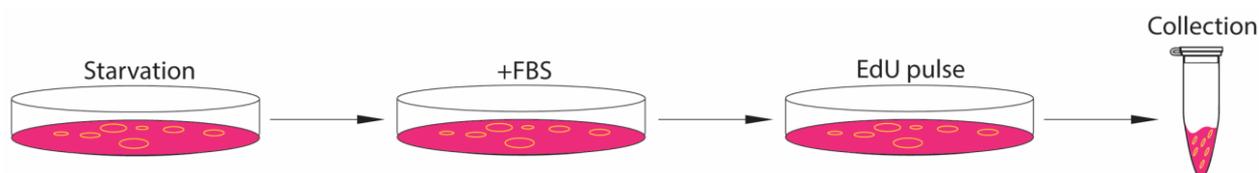


Figure 9. Scheme of cell synchronization procedure. Experimental strategy used to synchronise human cells: first, growth factors are removed, then 10% FBS is added, the cells are pulsed for 30 mi with EdU before finally being collected (details can be found in the Materials and Methods section).

As expected, cell cycle analysis confirmed that aneuploid cell lines progressed slower through the cell cycle than their wild-type counterparts. In particular, it is demonstrated that the G1 phase is significantly longer in cells that had gained an extra chromosome (Figure 10).

In euploid HCT116, most of the cells (approximately 80% of the cells) were in the G1 phase from 0 to 6 h. Between 8 and 12 h after the release, most of the cells (60–80%) entered the S phase. After 16 h, the cells entered the G2 phase and completed the cell cycle between 24 and 28 h (Figure 10A). In contrast, in the aneuploid HCT116 5/4 cell line, entry into the S phase occurred more rapidly, at only 12 h, which is 4 h later than in the control (Figure 10B). At 8 h, approximately 70% of the aneuploid cells were still in the interphase, but they subsequently progressed through the other cell cycle phases with the same timing as the parental control.

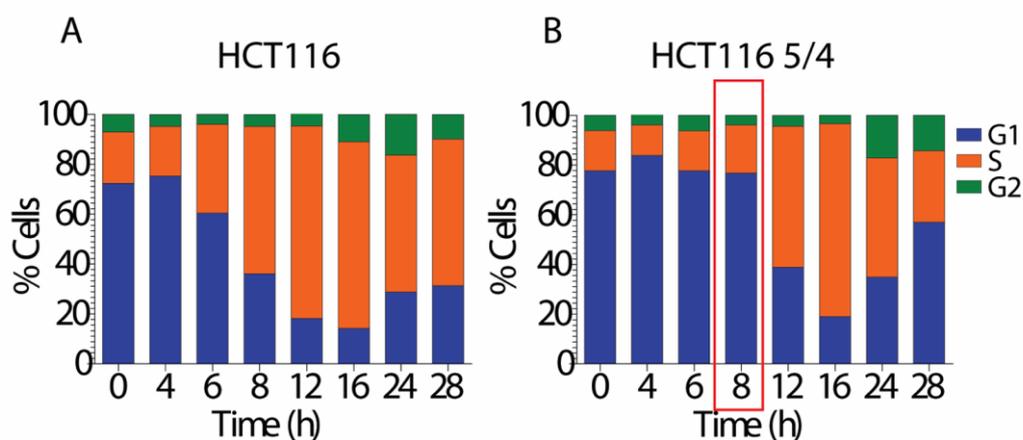


Figure 10. Cell cycle analysis of aneuploid cells. A) Cell cycle analysis of HCT116 euploid cells. B) Derivative aneuploid cells treated with EdU. The different cell cycle phases are discriminated as EdU-positive (cells in the S phase), 2N EdU-negative (cells in G1) and 4N EdU-negative (cells in G2 and M) (Figure S1).

Cell cycle delay in the G1 phase was also observed in other aneuploid cell lines (Figure S1B). Similar results were also confirmed in aneuploid RPE1 cells, although these cells required more time to restart the cell cycle after starvation.

Nevertheless, the aneuploids (RPE1 3/3 and 21/3) progressed slower through the G1 phase than the euploid cells, although the timing was different in these cell lines (Figure 11). Taken together, these data show that aneuploidy specifically affects the length of the G1 phase in human cells.

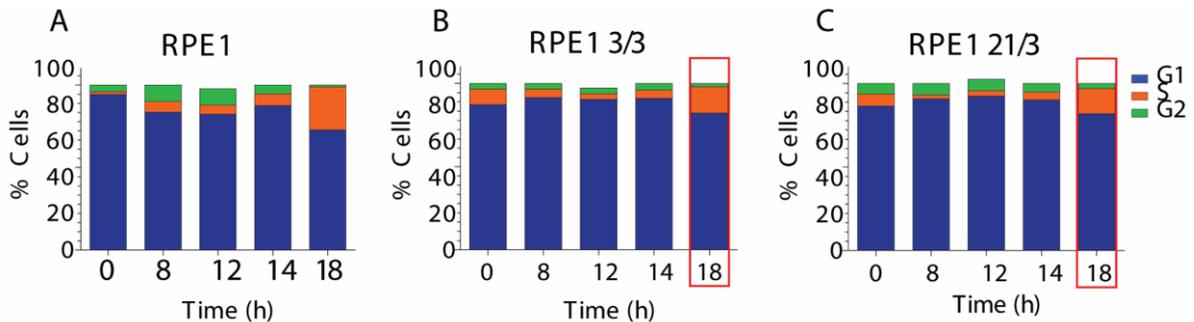


Figure 11. Cell cycle analysis. A–C) Cell cycle analyses of euploid and aneuploid RPE1 cells.

6.3. Licensing of origins of replication is defective in aneuploid cells

Given the extended G1 phase and the delay in the initiation of the S phase in aneuploid cells, the question of whether the loading of the MCM2-7 helicase might be affected was investigated. It has been previously shown that the MCM helicase is downregulated in aneuploid cells (Passerini, 2016). These proteins can critically affect licensing of the replication origins as well as the stability of the replication fork. Thus, cells might need to spend more time in the G1 phase of the cell cycle to reach the appropriate concentration of MCM2-7 helicase loaded on chromatin.

To address this question, time-course experiments were performed again, synchronising cells by FBS starvation. Cells were collected at 0, 4, 6, 8, 12, 16, 24 and 28 h and pellets sub-fractionated into cytoplasmic, nuclear and chromatin-bound fractions. Specifically, attention was focussed on the members of the pre-RC, including MCM2 and MCM7 subunits, CDC6 and ORC6 (Figures 12B and S3).

It was found that the pre-RC levels were lower in aneuploid cells than in euploid cells, which is similar to our previous observations. Also, the ability to be loaded onto DNA was compromised in aneuploid cells.

The levels of the entire pre-RC complex were found to be higher in euploid than aneuploid cells in both the cytoplasmic and nucleoplasmic fractions (Figures 12, 13 and S3A–D). This suggests that the proteins can be translocated from the cytoplasm to the nucleus in a timely manner.

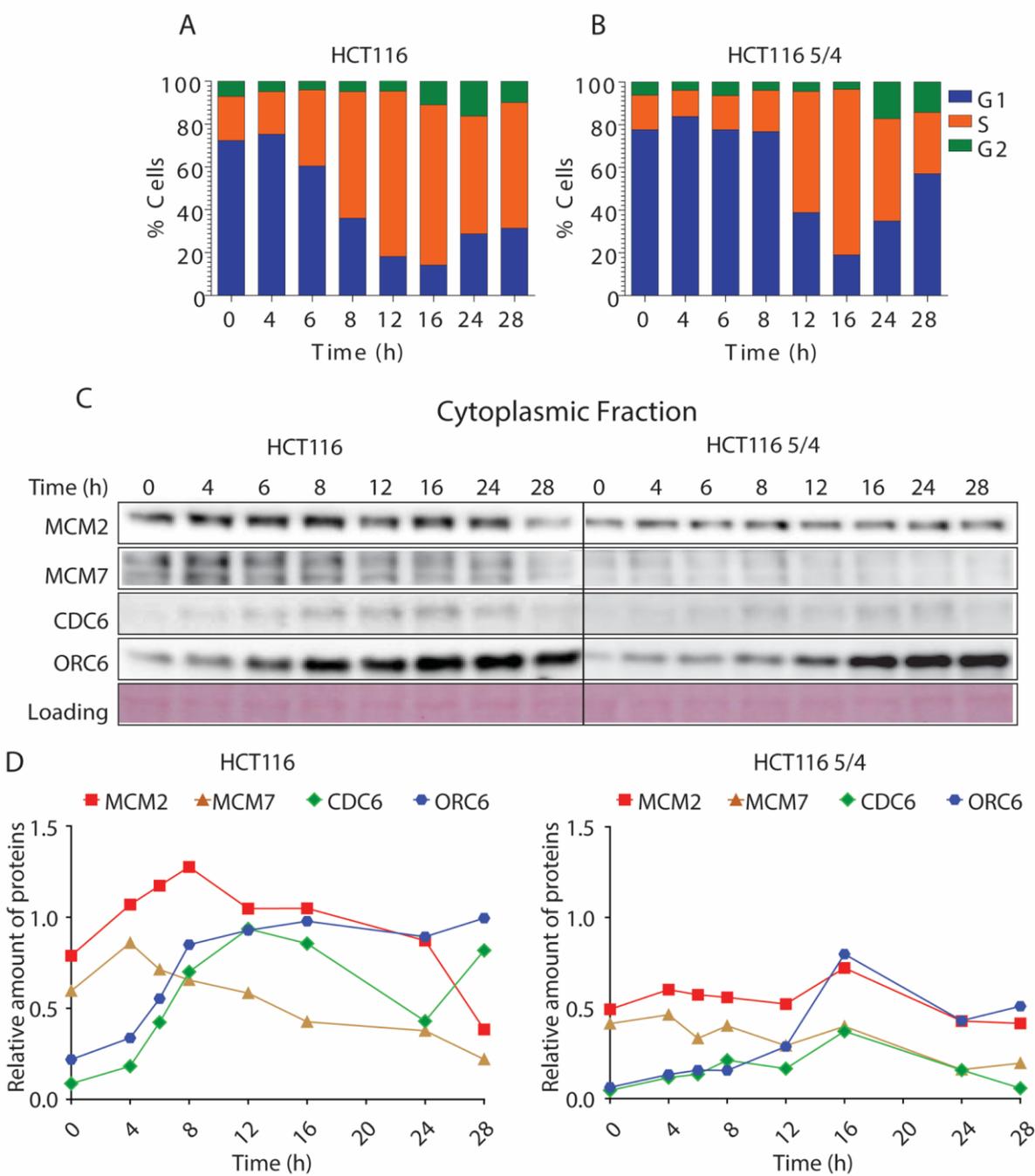


Figure 12. Cytoplasmic levels of the pre-RC members over the course of the cell cycle. A and B) Fluorescent activated cell sorting (FACS) analyses of HCT116 and HCT116 5/4 cells showing the percentage of EdU-positive and EdU-negative cells relative to DNA content. C) Western blot analysis of pre-RC subunit levels in the cytoplasmic fractions of HCT116 and derived aneuploid cells. D) Quantification of protein levels, performed by comparison of the proteins of interest and the loading control (Ponceau) for each time point (each lane represents the protein/Ponceau ratio).

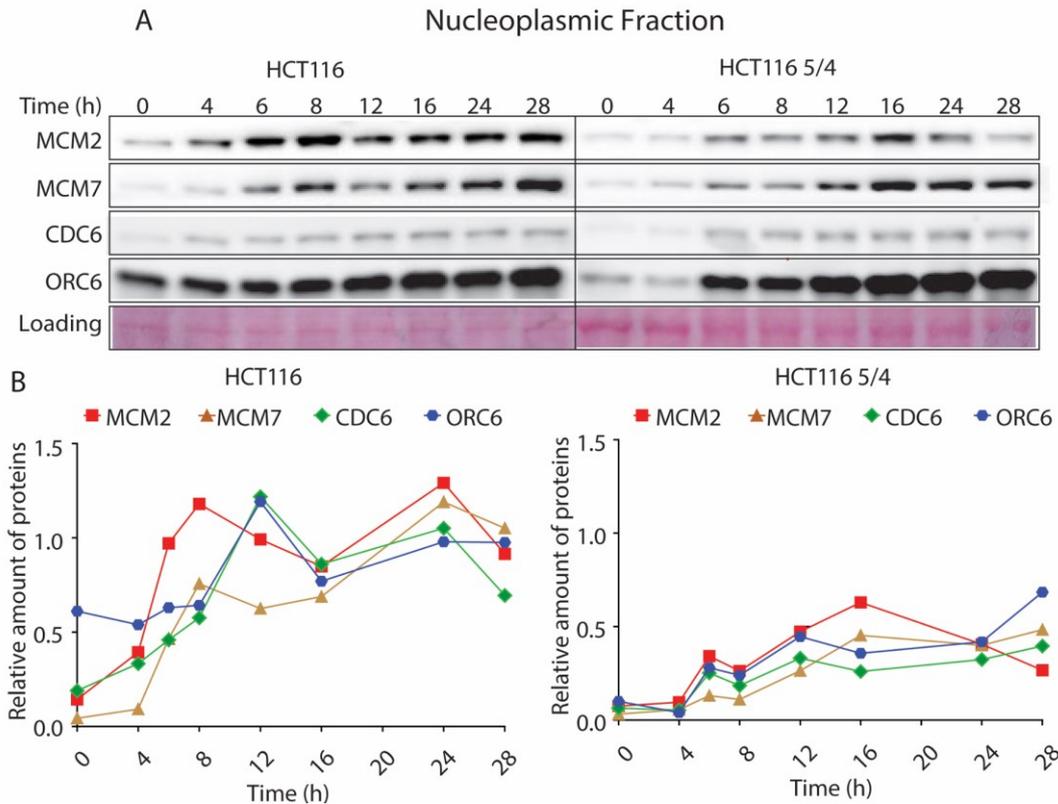


Figure 13. Nucleoplasmic levels of the pre-RC members over the course of the cell cycle. A) Western blot analysis of pre-RC subunit levels in the nucleoplasmic fraction of HCT116 and derived aneuploid cells. B) Quantification of the protein levels, performed by comparison of the proteins of interest and the loading control (Ponceau) for each time point (each lane represents the protein/Ponceau ratio).

The cytoplasmic protein levels of the pre-RC were lower in aneuploid cells than in diploid cells (Figure 12), but there were no significant differences in the time courses for HCT116 and HCT116 5/4. In addition, MCM2, MCM7, CDC6 and ORC6 levels were slightly lower over time (Figure 13). The accumulation dynamics of the pre-RC subunits were also very similar in the nucleoplasmic fractions. Here again, protein levels were higher in the wild-type cells than in aneuploids. However, MCM2, MCM7, CDC6 and ORC6 proteins entered and stayed within the nucleus in the same cell cycle phases in diploid cells and in cells with an extra copy of chromosome 5 (Figure 13). Identical results were also found in cells carrying an extra copy of chromosome 3 (either in the HCT116 or RPE1 cell lines) and 21 (RPE1 cell line) (Figure S3).

Next, the chromatin-bound fraction was analysed and a striking difference in the ability to recruit the pre-RC subunits to the DNA was observed. For example, the CDC6 subunit bound DNA at the same time point in both euploid and aneuploid cells, although this protein was less abundant in aneuploid cells (Figures 14 and S3A–D, lower panels).

In contrast, ORC6 bound chromatin later in aneuploid cells than in diploids: the levels of this subunit peaked at 16 h rather than at 12 h as in wild-type cells (Figures 14A and S3A–D). It was found that the binding of MCM2 and MCM7 subunits to the chromatin was also affected in aneuploid cells. Specifically, the chromatin-bound levels of both MCM2 and MCM7 increased from time point zero to 6 h after FBS addition. At this stage, both diploid and aneuploid cell lines were in the G1 phase and the accumulation of the helicase on DNA was similar in diploid and aneuploid cells, although the protein levels were lower in the latter cell line (Figures 14B and S3A–D, lanes 0, 4, 6).

However, the main differences were observed 8 h after FBS addition. At this stage, the levels of MCM2 and MCM7 dropped in the aneuploid cells but not in the diploids. Later, at 12 h after release from starvation, the levels of both helicase subunits were increased in aneuploids (Figures 14A–B and S3A–D, lanes 8–12).

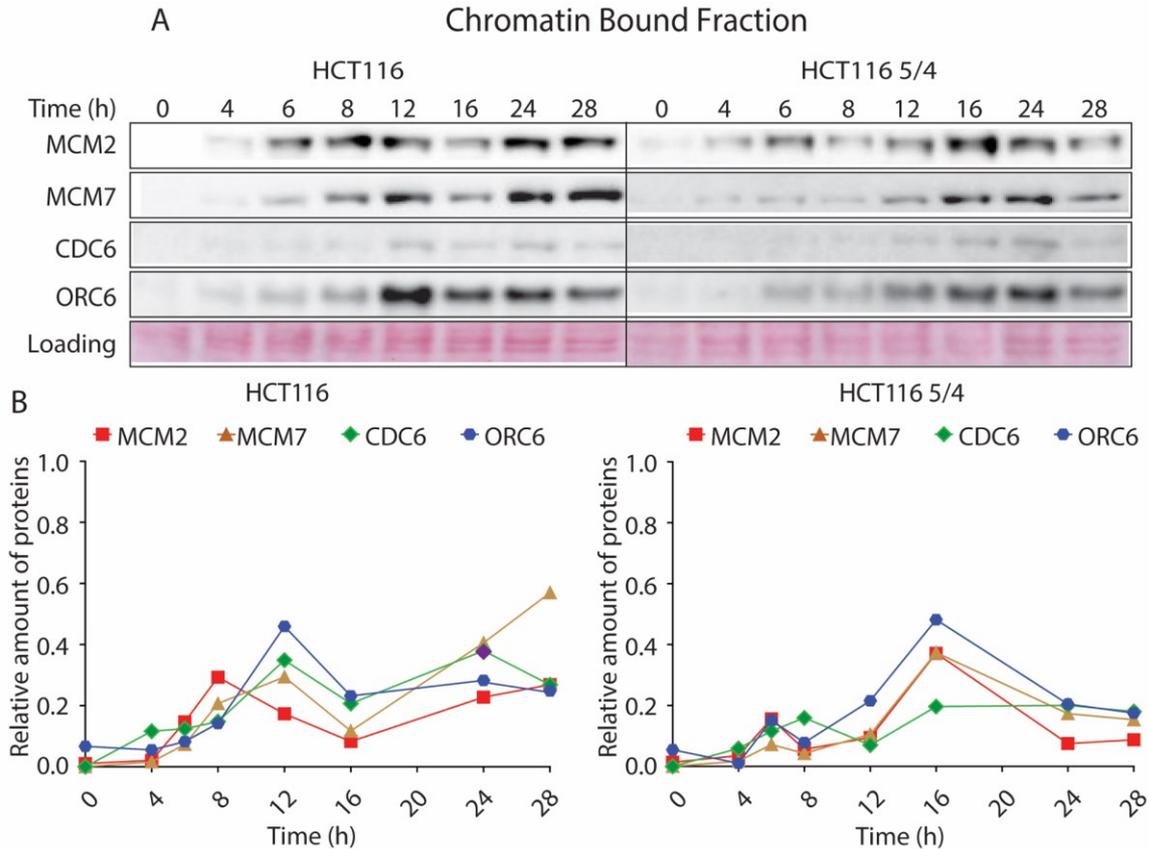


Figure 14. Differences in the accumulation of chromatin-bound pre-RC members over the course of the cell cycle. A) Western blot analysis of pre-RC subunits in the chromatin-bound fraction of HCT116 and derived aneuploid cells. B) Quantification of protein levels.

Along with the protein levels, the transcript levels were also determined by quantitative real-time PCR of MCM2 and MCM7. It was found that the mRNA levels did not change over the time course for the HCT116 WT, but the transcript levels of both helicase subunits sharply increased at 6 h after release from starvation in aneuploids (Figure 15). This evidence suggests that aneuploid cells recognise the lower levels of the MCM2-7 helicase proteins during the G1 phase and actively produce more mRNA to rescue the levels of the helicase subunits.

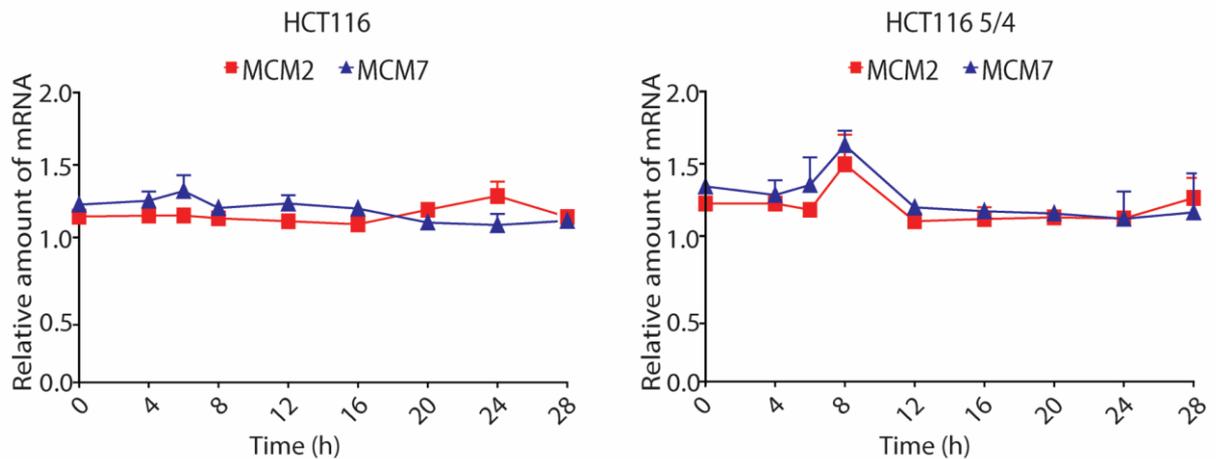


Figure 15. Differences in the pre-RC transcripts over the course of the cell cycle. mRNA levels of MCM2 and MCM7 subunits.

6.4. MCM2-7 helicase levels in cells released from mitosis

Many cellular processes can be affected by growth factor deprivation. To avoid any off-target effects due to starvation, the cells were also synchronised by treatment with nocodazole, a microtubule depolymerizing drug that arrests cells in the metaphase. Upon nocodazole arrest, cells were removed by shaking and re-plated to follow their progress into subsequent cell cycle phases. Cell cycle progression was determined by assaying the accumulation of the cyclin B1 protein in the nucleus (Figure S3). This protein is usually produced in the late S phase and reaches its highest concentration within cells during the G2/M transition.

By using pharmacological synchronization, it was confirmed that aneuploid cells suffered from an extended G1 phase, similar to the results observed in response to growth factor deprivation. In addition, cyclin B1 levels increased in wild-type cells at 16 h, whereas in aneuploid cells the protein levels did not increase.

However, this seems not to be due to a biological cause, but is instead due to unequal loading of the samples. In light of this observation, the 24 and 28 h time points in the aneuploid cells should be compared with the 16 and 24 h time points in wild-type cells (Figure S3). Furthermore, in euploid cells, the MCM subunits bind to DNA early during the G1 and S phases; however, this was less efficient in aneuploid cells.

In comparison with diploid cells, in aneuploid cells, these two helicase subunits were found to bind DNA earlier in G1 and at higher levels. As was shown previously, the levels dropped in late G1, and increased again 12 h later (Figures 16 and S3).

Taken together, these experiments suggest that the replicative helicase cannot bind stably to chromatin in constitutive aneuploid cells. In addition, the delay of the cell cycle and the longer G1 phase might be due to the observed differences in MCM2 and MCM7 accumulation on chromatin for diploid and aneuploid cells.

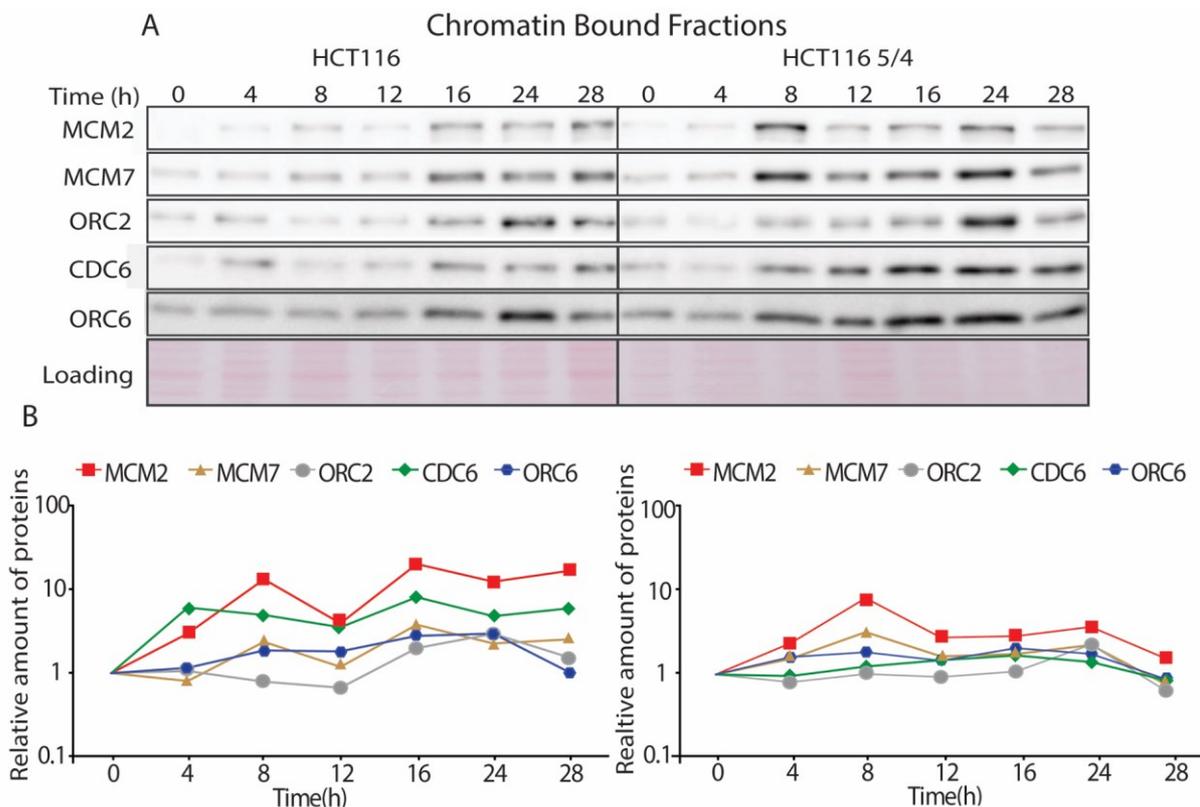


Figure 16. Differences in pre-RC levels over the course of the cell cycle after nocodazole synchronization.
 A) Western blot analysis of the chromatin fraction of cells synchronised in mitosis. B) Relative quantification of the proteins.

6.5. Mass spectrometry analysis of the nucleoplasmic and chromatin-bound fractions confirms MCM2-7 helicase downregulation

To gain insights into the biological processes that can be modified upon aneuploidy, proteomic analyses were performed by mass spectrometry (MS). Indeed, it is known that owing to chromosome gain, the MCM2-7 helicase is downregulated and thus binds DNA in insufficient quantities (Passerini et al., 2016). This has particular consequences for the transition from the G1 to the S phase of the cell cycle. Thus, it may be possible to observe the misregulation of the cell cycle by monitoring the regulation of key factors for the checkpoint within nuclei or on the chromatin. Thus, MS analysis was used to obtain an unbiased and comprehensive view of the dynamics of replicative proteins in cells.

For this purpose, the cells were synchronised by growth factor deprivation, as previously described. The nucleoplasmic and chromatin-bound fractions were collected at time points 0, 4, 6 and 8 h and processed for MS analysis as described in the Material and Methods section. For the nucleoplasmic fractions, samples were processed by Perseus software. First, data were filtered by different biological processes.

About 5,000 valid proteins were found from the data filtered by cell cycle and checkpoint regulation. Next, the valid proteins were clustered, and 4174 proteins were found in the hierarchical clustering. Hierarchical clustering was performed for each of the nucleoplasmic or chromatin-bound samples by calculating the Euclidean distance, and the K-means algorithm was used with 300 clusters being created.

Overrepresented cellular processes in the generated clusters were then identified by using GO term analysis. To compare the different protein levels and perform clustering, the data were *z*-scored; in this way, the measurement of standard deviations for each score could be taken into account. A protein with a positive *z*-score was relatively upregulated compared to the average protein levels, whereas a negative *z*-score indicates a downregulation.

The *z*-scores of the label-free quantification (LFQ) values for the nuclear or the chromatin fractions of HCT116 and HCT116 5/4 were calculated over time (Figure S3B–D). It was found that many biological processes were significantly enriched within seven clusters (details of how these clusters were calculated can be found in the Material and Methods section) for the nuclear

fraction (Table S4A) and six clusters for the chromatin-bound fraction (Tables 1 and 2). Finally, the value for each replicate was plotted separately as a trend over time (Figure 17).

The LFQ values of cluster 1 for the HCT116 cell line increased over time (Figure 17A). For HCT116 5/4, the values were higher at the beginning and dropped to close to zero over 4 h; however, at further time points, the values increased slightly again (Figure 17A).

Interestingly, the values at 4 h were consistently lower in all the plots of the aneuploid cell line. For plot 2 in HCT116, LFQ values oscillated from positive at the beginning of the cell cycle to slightly negative at 4 and 6 h, and became slightly positive again after 8 h.

In HCT116 5/4, the values increased over time, although with the usual exception at 4 h. The values were high in HCT116 plot 3, after which they steadily decreased to close to zero. The LFQ values of plot 3 in aneuploid cells were stable over time. No trend could be distinguished in any of the other clusters, although the LFQ values were slightly greater in diploid than in aneuploid cells.

The trend of the chromatin-bound fraction showed that MCM2-7 subunits were within the third cluster, which included many cellular processes. For the chromatin-bound fractions, there were about 5478 proteins in the hierarchical clustering. As shown in Table 2, MCM2-7 helicase was found within cluster 6 of the nucleoplasmic fraction, which is related to DNA/RNA associated factors and cell cycle regulation. The z-score was calculated as previously described and the value of each replicate was plotted separately as a trend over time (Figure 17B).

The curves of MCM2-7 were analysed in isolation from the other plots to better track the accumulation of helicase subunits (Figure 18). In the nucleoplasmic fraction, MCM2-7 accumulation oscillated from high (at time point 0 h) to low (at time point 4 h) in aneuploid cells (Figure 18).

On the other hand, diploid cells showed a slow, steady decrease of MCM levels over time (Figure 18A). In contrast, the trend for the chromatin-bound fraction of the MCM2-7 helicase revealed that the interaction of the helicase with the DNA was stable from 0 h to 6 h but was slightly diminished at 8 h in HCT116 5/4 (Figure 17B, grey lines).

Table 1. Protein clusters and related biological processes of the nucleoplasmic fraction.

Cluster number	Enriched cellular processes
Cluster 1	<ul style="list-style-type: none"> –positive regulation of hydrolase activity –microtubule cytoskeleton organization –positive regulation of GTPase activity –regulation of translational initiation in response to stress –regulation of translational initiation <p>For further results, see Table S9</p>
Cluster 2	<ul style="list-style-type: none"> –homeostasis –metabolic processes –regulation of T-cell mediated immunity –vesicle transport (Golgi) –membrane organization <p>For further results, see Table S10</p>
Cluster 3	<ul style="list-style-type: none"> –nucleic acid metabolic process <p>For further results, see Table S11</p>
Cluster 4	<ul style="list-style-type: none"> –protein transport –vesicle transport (Golgi) –membrane organization <p>For further results, see Table S12</p>
Cluster 5	<ul style="list-style-type: none"> –chemotaxis –tRNA aminoacylation/amino acid activation –response to external stimuli <p>For further results, see Table S13</p>
Cluster 6	<ul style="list-style-type: none"> –DNA/RNA associated processes –DNA recombination and repair –cell cycle regulation <p>For further results, see Table S14</p>
Cluster 7	<ul style="list-style-type: none"> –metabolic processes –translational processes –protein complex disassembly –mitochondrial translation <p>For further results, see Table S15</p>

Table from Braun's thesis, 2018. In the Supplementary Material, a hierarchical cluster is shown.

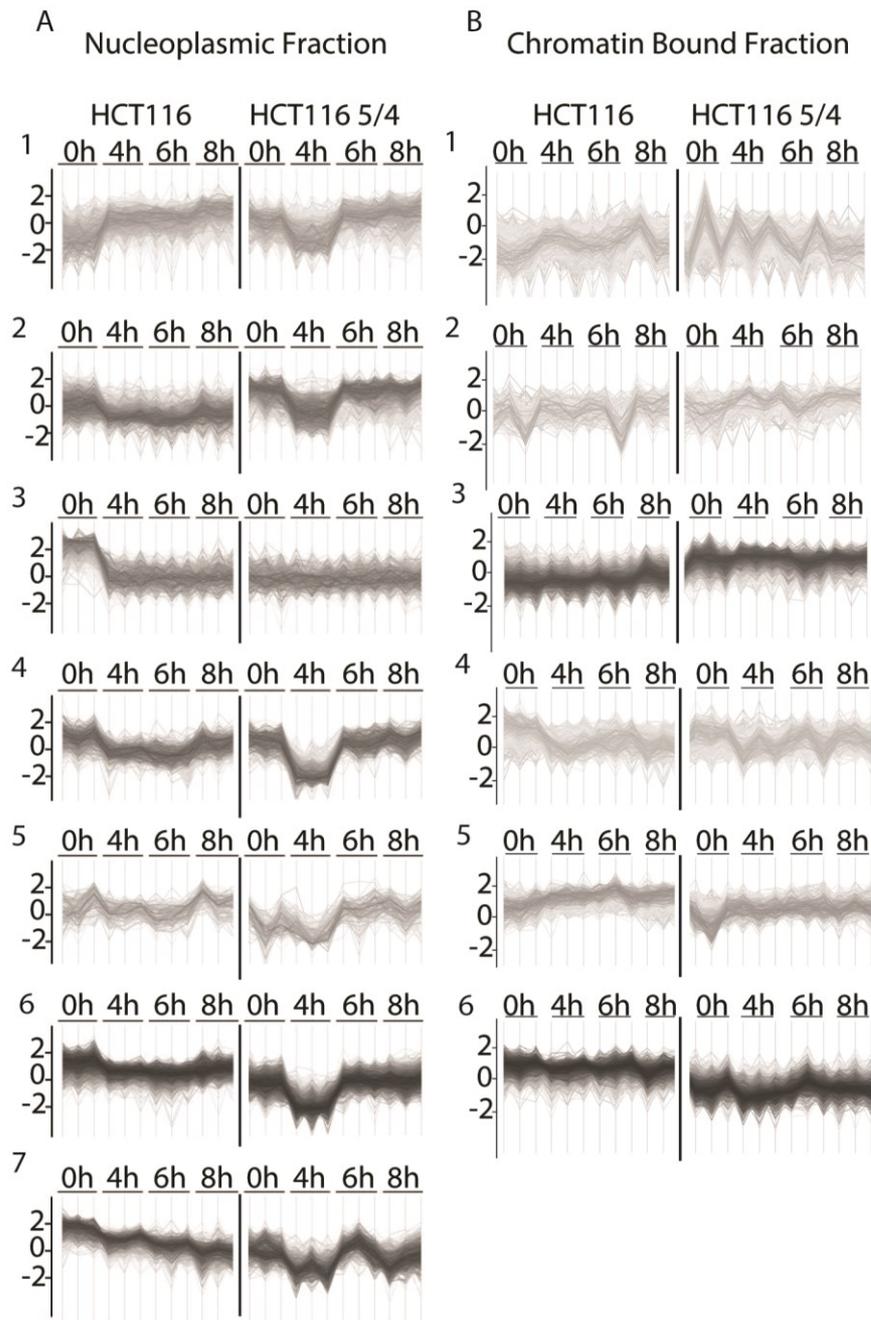


Figure 17. Cluster analysis of the HCT116 and HCT116 5/4 nucleoplasmic proteome over time. A, 1–7) Log₂ LFQ values of HCT116 and HCT116 5/4 over time for clusters 1–7. B, 1–6) Log₂ LFQ values of HCT116 and HCT116 5/4 over time for clusters 1–6. The vertical lines under each timepoint indicate the three individual biological replicates.

In diploid cells, the levels of helicase subunits increased slowly over time (Figure 18B, black lines). The intensities of the ORC complex as a representative of the rest of the pre-RC were also extracted from the dataset. In general, the levels of these subunits were lower in aneuploid than diploid cells (Figure S4E).

Table 2. Protein clusters and related cellular processes of the chromatin-bound fraction.

Cluster number	Enriched cellular processes
Cluster 1	<ul style="list-style-type: none">-metabolic processes-protein processing <p>For further results, see Table S16</p>
Cluster 2	<ul style="list-style-type: none">-positive regulation of TOR signalling cascade <p>For further results, see Table S17</p>
Cluster 3	<ul style="list-style-type: none">-signal transduction involved in mitotic cell cycle checkpoints-translational initiation-response to external stimuli/signal transduction-translation-membrane organization-regulation of apoptosis-proteolysis-protein transport <p>For further results, see Table S18</p>
Cluster 4	<ul style="list-style-type: none">-lipid metabolic processes-endoplasmic reticulum organization <p>For further results, see Table S19</p>
Cluster 5	<ul style="list-style-type: none">-catabolic/metabolic processes-mitochondrial translation-mitochondrion organization <p>For further results, see Table S20</p>
Cluster 6	<ul style="list-style-type: none">-DNA/RNA associated processes-cellular component organization or biogenesis-metabolic processes-histone involving processes <p>For further results, see Table S21</p>

Table adapted from Braun's MSc thesis, 2018.

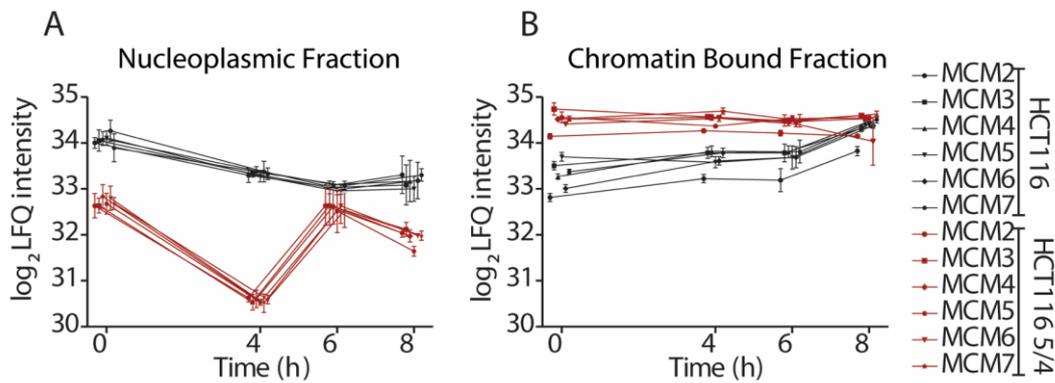


Figure 18. Intensity profile of the MCM2-7 clusters. A) Time-dependent LFQ profile of the MCM2-7 cluster in the nucleoplasmic fraction. B) Time-dependent LFQ profile of the MCM2-7 cluster in the chromatin-bound fraction.

Analysis of the mass spectrometry measurements allowed the identification of several clusters that were differentially regulated over time in HCT116 and derived aneuploid cells. All clusters could be matched to specific cellular processes. The loading of the MCM2-7 helicase was not maintained during the G1 phase, although the effect was smaller than in the western blot analysis.

6.6. Stability of the MCM2-7 helicase during the cell cycle in aneuploid cells

The experiments described above suggested that the helicase binding to DNA might be inefficient in aneuploids, and therefore it was interesting to determine the reason for the altered loading of MCM helicase on chromatin. Therefore, the possibility that MCM2-7 is affected by proteotoxic stress, which is common in trisomic cells, was considered.

To test this hypothesis, cells were treated with two different drugs: cycloheximide (CHX) and MG132. The first blocks translation, and thus the degradation of MCM subunits over time could be followed. In contrast, MG132 inhibits protein degradation and should therefore restore the levels of the proteins.

Samples were collected at different time points: 0, 15, 30, 45 and 60 min after CHX treatment (Figures 19 and S4A, C, E), and western blot analysis of MCM proteins, p53 (as a control of protein degradation) and ORC6 was performed on synchronised cells. For this purpose, HCT116 5/4, 5/3, 3/3 and the respective control cell lines were used. It was found that the pre-

RC subunits were stable both in aneuploid and diploid cells in the presence of CHX. In general, MCM2, MCM7, CDC6 and ORC6 appear to have long half-lives and are not degraded immediately upon shut-off of protein synthesis (Figures 19 and S5).

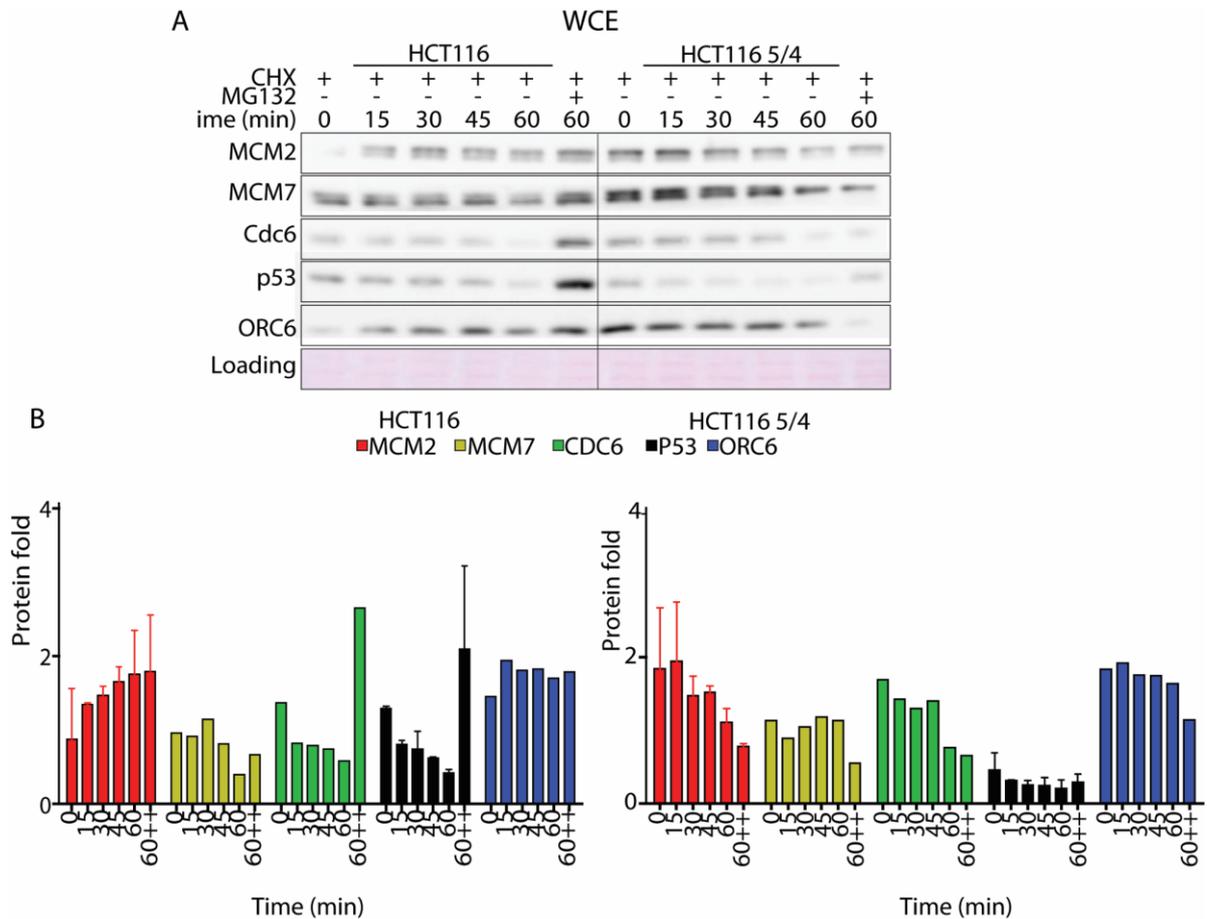


Figure 19. Stability of pre-RC proteins. Western blot analysis of cells treated with cycloheximide [100 ng/mL] and collected at different time points. Cells were also treated with MG132 (proteins are normalised to time point zero).

Indeed, pre-RC subunits were still detectable after 1 h of cycloheximide treatment. However, protein levels of the pre-RC subunits were lower in aneuploid than in control cells after the same length of treatment (Figure 20). This was not due to a faster degradation, but due to the generally lower expression of these subunits in aneuploid cells.

Next, the MCM stability over time was tested in different cellular compartments in HCT116, HCT116 5/4 and HCT116 3/3 cells synchronised by growth factor deprivation. During the time course, cells were treated with CHX. In the cytoplasmic and nucleoplasmic fractions, the stability of all pre-RC proteins was similar in diploids and aneuploids, and they were still detectable after 8 h of treatment.

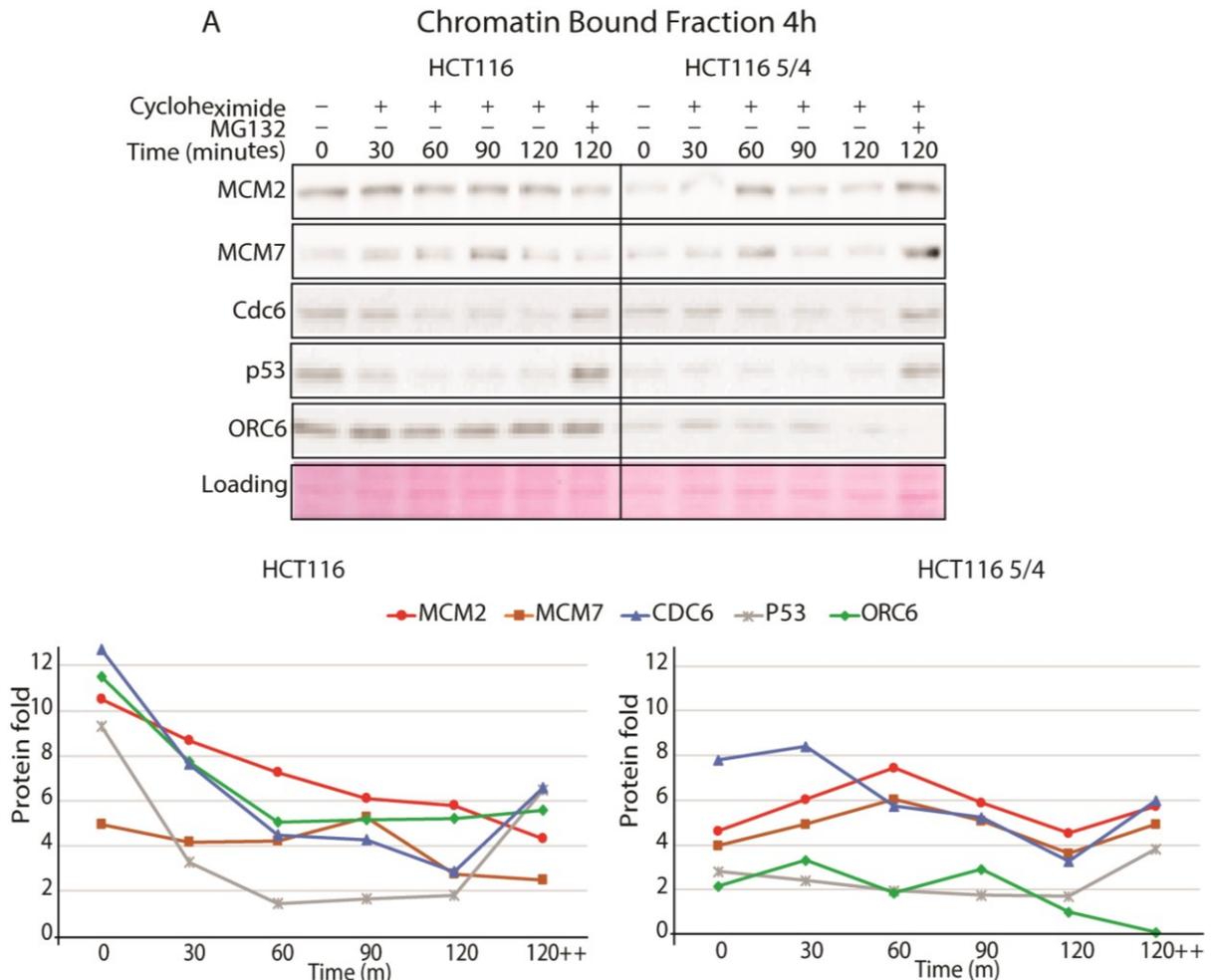


Figure 20. Pre-RC stability on DNA through the G1 phase. A) Western blot analysis of the chromatin-bound fraction of the pre-RC. Samples were treated with CHX (100 μ M) and/or MG132 (100 μ M) at 4 h after FBS addition, and collected every 30 min. B) Quantification of protein levels calculated by the formula: protein of interest/Ponceau, and normalised to time point zero.

Cells were released for 4 h and at exactly 4 h after release, the CHX was supplemented into the media. Samples were subsequently collected every 30 min for 2 h. As a control, one sample was treated with both CHX and MG132 for 2 h (Figure S5). At 4 h, when CHX was added, it was observed that the MCM2 and MCM7 levels began to increase and the protein levels were stabilised for at least 60 min (which is 5 h after the cells were released from starvation; Figure S5). CDC6 and ORC6 DNA loading were comparable in HCT116 and the aneuploid cells (Figure S5).

The same treatment was repeated, but instead, the cells were treated with CHX 6 h after they were released from starvation (Figure 21). The chromatin fraction was examined to understand whether MCM stability was responsible for the dissociation of the replicative helicase from DNA in aneuploid cells 8 h after FBS was added. The ORC6 subunit dynamics were identical

between all the tested cell lines over the entire time course: however, aneuploid cells showed an increased fluctuation of ORC6 levels on DNA (Figure 20A–B).

In contrast, differences in MCM2 and MCM7 loading were observed between wild-type and the respective aneuploid cell lines. In aneuploid cells, MCM2 and MCM7 were no longer bound to DNA after 60 min of cycloheximide treatment (Figure 21A, lanes 60–120). As described above, the MCM2 and MCM7 subunits were not able to stably bind to chromatin between the 6 and 8 h time points for the aneuploid cells.

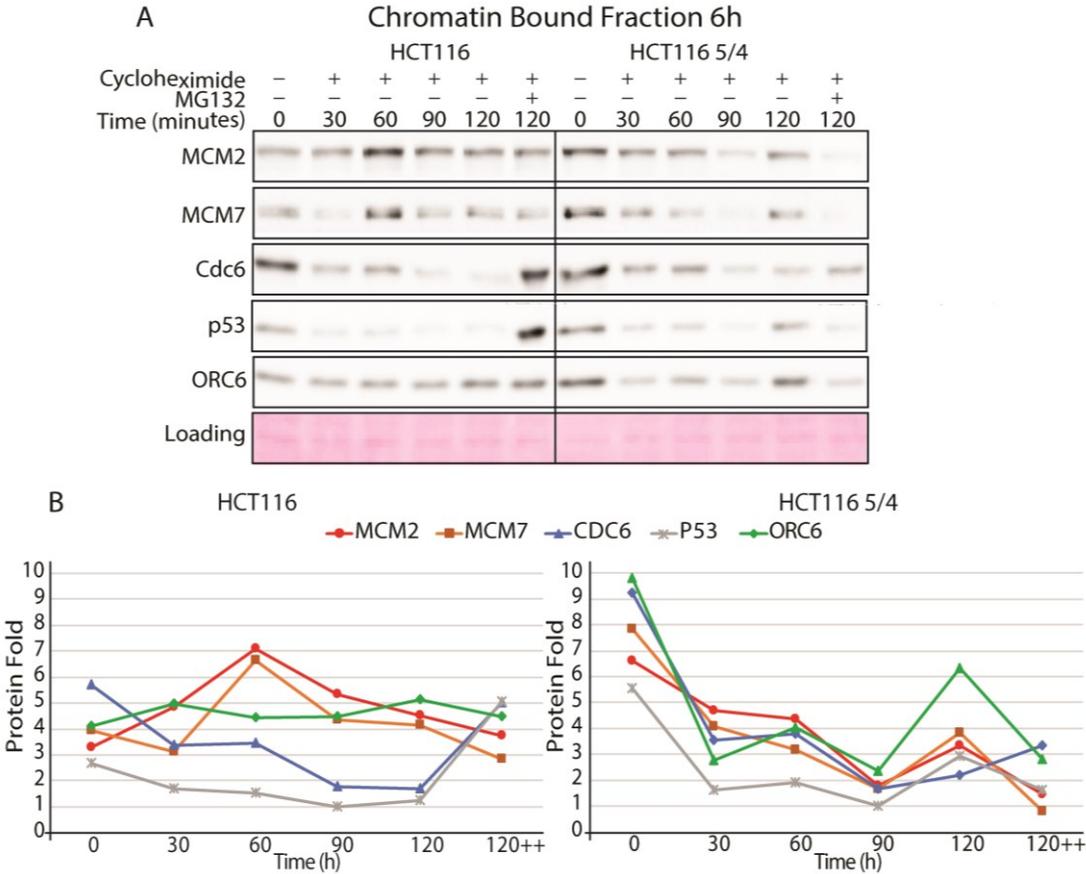


Figure 21. Pre-RC stability on DNA in the G1 phase. A) Western blot analysis of the chromatin-bound fraction of the pre-RC. Samples were treated with 100 μM CHX and/or 100 μM MG132 6 h after FBS addition and collected every 30 min. B) Quantification of protein levels by using the formula protein of interest/Ponceau, and normalised to time point zero.

The same results were also found when the HCT116 3/3 and the RPE1 3/3 and RPE1 21/3 cell lines were tested (Figure S5). In all these cell lines, the pre-RC subunits appeared to be very stable in diploid cells, whereas in aneuploid cells their abundances were markedly lower at one of the time points. Cycloheximide treatment thus allowed the differences in MCM2 and MCM7 subunit DNA binding between the diploid and aneuploid cell lines to be precisely determined.

This again demonstrates that the MCM2-7 helicase cannot efficiently bind DNA in aneuploid cells.

6.7. Impaired MCM2-7 loading is not due to the decreased expression of its subunits

Aneuploidy negatively affects the levels of MCM2-7 helicase and its ability to bind DNA to properly execute its function. This leads to the question as to whether the downregulation of MCM2-7 *per se* could be sufficient to cause the cell cycle delay that is observed in aneuploid cells. Previously, it was shown that cells transfected with an MCM7-expressing vector exhibited increased levels of at least two helicase subunits: MCM2 and MCM7. The accumulation of these proteins was also linked to decreased DNA damage, as demonstrated by less 53BP1 foci in cells transfected with MCM7 (Alexandrow et al., 2016).

Therefore, the goal was set to determine whether MCM7 overexpression might rescue the cell cycle delay in aneuploid cells. Thus, HCT116 and HCT116 5/4 cell lines were transfected with different constructs for MCM2, MCM7 or the C-terminal truncated form of MCM7 (MCM7CT). MCM7CT is deleted at the terminal portion of the protein that can interact with the retinoblastoma (RB) protein. The cells were also transfected with empty pcDNA3.1 to validate that the observed effects were due to the overexpression and not caused by any collateral effect of the nucleoporation. Western blot analysis was used to analyse the expression of the different proteins, either in whole-cell lysates (WCE) or the chromatin fraction.

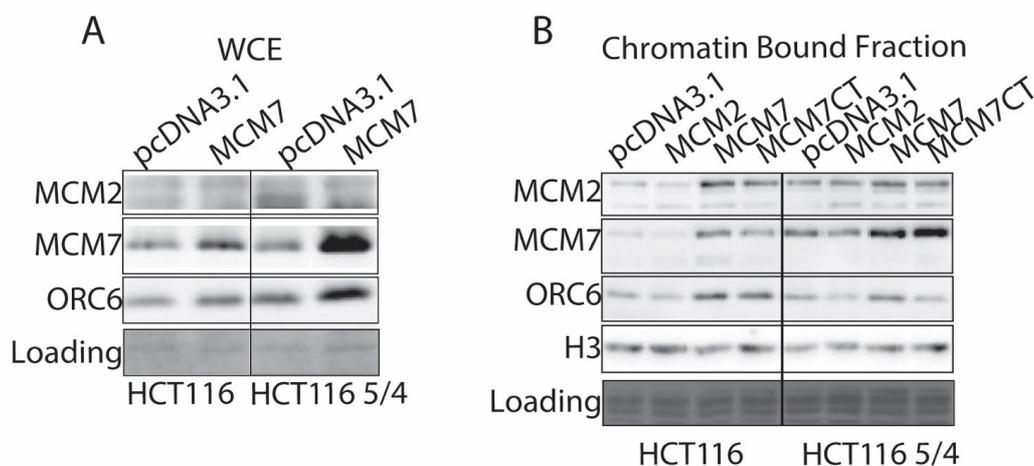


Figure 22. MCM7-overexpression in cells. A) Whole cell lysate of stable clones with empty vector or MCM7. B) Chromatin-bound fraction of stable clones with empty vector, MCM2, MCM7 or MCM7CT

As previously reported in the literature (Passerini et al., 2016), MCM2 overexpression did not increase the protein levels either in diploid or aneuploid cells (Figure 22A–B, MCM2 lanes). Protein levels did not change in cells transfected with an empty vector either (Figure 22A–B, pcDNA3.1 lanes), confirming that transfection with an empty vector alone did not affect the expression of the proteins of interest.

From HCT116 or HCT116 5/4 transfected with the MCM7 vector, cells exhibiting the highest levels of MCM7 either in WCE or in the chromatin fraction were selected. The new clones were tested to see if they expressed higher levels of functional helicase subunits (chromatin-bound fraction; Figure 23A–B).

Cells carrying the extra copies of MCM7CT were found to overexpress the truncated form of the protein (Figure S6A–B). This last result corroborated the hypothesis that the helicase could still bind DNA, although MCM7CT should not be able to fold into its proper conformation (Alexandrow et al., 2016).

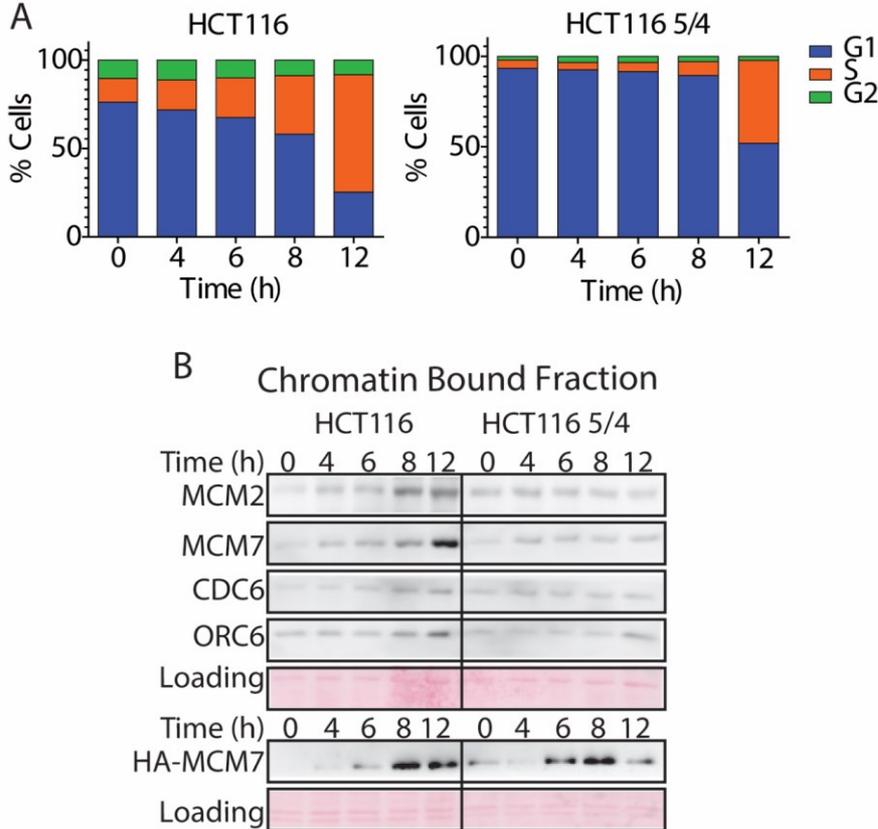


Figure 23. MCM7 overexpression. A) Cell cycle analysis of euploid and aneuploid clones stably overexpressing MCM7. B) Western blot analysis of the time course for the pre-RC proteins in the chromatin-bound fraction from the clones in A).

To determine whether the extra copies of MCM7 could rescue the G1 phase delay, cell synchronisation by starvation was performed as described above. Cell cycle analyses were performed after incorporation of the thymidine analogue, as well as immuno-blotting analysis on samples fractionated into cytoplasmic, nucleoplasmic and chromatin-bound fractions (Figure 23B). The overexpression was additionally confirmed by the detection of the exogenous MCM7 protein (HA-MCM7) during the time course. In HCT116 5/4^{MCM7}, it was evident that MCM7 overexpression did not rescue the delay in the G1/S phases in aneuploidy cells. In fact, 90% of HCT116 5/4^{MCM7} cells were still in G1 at 8 h, whereas only 55–60% of the HCT116^{MCM7} cells were in G1. The pre-RC proteins on DNA levels were also checked and it was found that aneuploid cells with higher levels of MCM7 did not show any increase in these proteins. The overexpressed MCMs could progressively bind to chromatin over time, and, importantly, no dissociation of the MCMs from DNA was observed, as described above (Figure 23B).

6.8. Lower levels of MCM2 do not affect the cell cycle

Next, it was decided to test whether the downregulation of the MCM helicase levels would be sufficient to cause the cell cycle delay in diploid cells, as was observed in aneuploid cells. Therefore, MCM2 was transiently knocked down by transfecting cells with siRNA and then synchronised cells by growth factor deprivation. The expectation was that there would be some changes in the cell cycle due to the lower levels of MCM2. To verify this hypothesis, HCT116 cells that were electroporated in the presence of siMCM2 were used along with those that had not been electroporated (mock).

However, knock-down of MCM2 did not lead to G1 delay in diploid cells. About 20% of siRNA-transfected cells were in G1, the same percentage as in the mock cells (Figure 24A). Protein levels of MCM2 and MCM7 decreased in siRNA-MCM2 cells, but the ability of MCM2 to stably bind DNA was not affected (Figure 24B).

These findings suggest that the MCM2-7 downregulation in aneuploid cells is not the primary cause of the cell cycle delay *per se*, as no shortening of the G1 phase in HCT116 5/4 cells carrying extra copies of MCM7 could be detected. Furthermore, MCM2 knock-down did not result in a longer G1 phase in HCT116 cells.

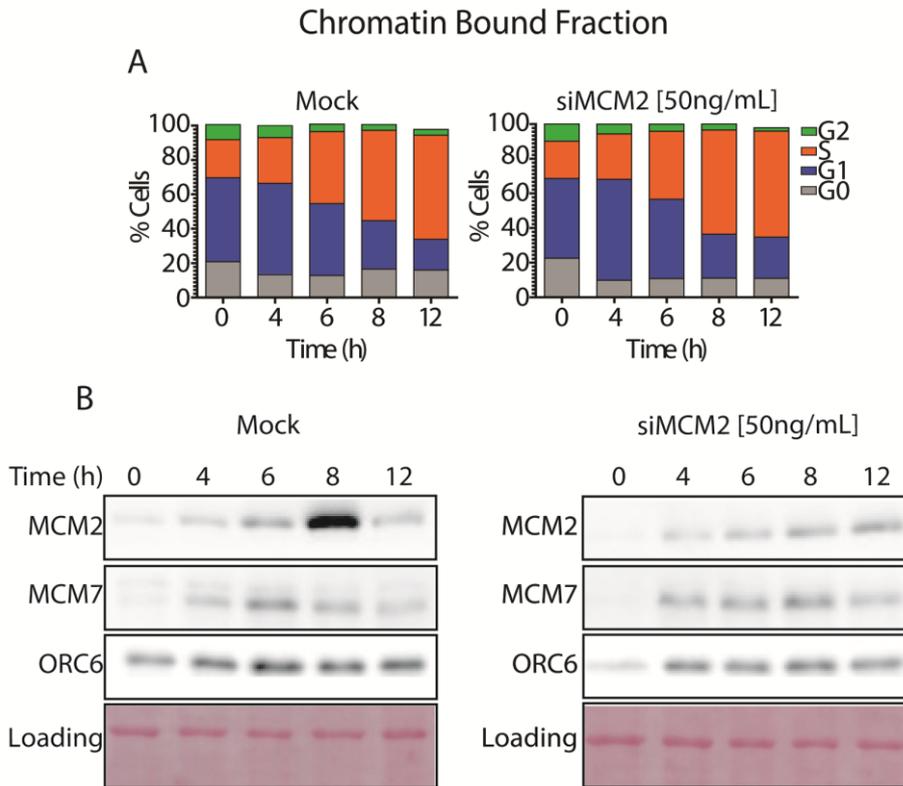


Figure 24. Analysis of the effect of MCM2 downregulation. A) Cell cycle analysis of HCT116 cells mock-transfected or transfected with siMCM2. B) Time course of pre-RC levels in wild-type cells transfected with siMCM2.

6.9. Endogenous overexpression of MCM7 does not rescue the cell cycle defects of aneuploid cells

The MCM7 overexpression possibly failed to affect the cell cycle because the transient overexpression was not sufficient. Therefore, another strategy was employed: an endogenous way to express more copies of the MCM7 gene in aneuploid RPE1 cells was used. Since the MCM7 gene is located on human chromosome 7, RPE1 cells were generated with an extra copy of this chromosome. Wild-type cells and RPE1 8/3 were used as the MCM levels control. RPE1 trisomic for chromosome 8 was used as a generic control for aneuploid cells, but MCM levels seemed to be positively affected in this cell line.

To verify the expression levels of MCM, WCEs were tested along with sub-fractionated cells, that is, cytoplasmic (Cyt), nucleoplasmic (Nuc) and chromatin fractions (Chr) (Figure 25). In western blots, no overexpression of MCM7 in RPE1 7/3 cells was observed (these cells carry an extra copy of chromosome 7 with the MCM7 gene). The intensities of the MCM7 bands did not reach the same levels as in the wild-type cells in WCE and in the cytoplasmic fraction of cells with extra chromosome 7 (Figure 25).

However, the intensities of the MCM7 bands were very similar between all the cell lines in the nuclear extract and chromatin-bound fraction (Figure 25). The MCM2 protein, in contrast, showed higher levels only in wild-type and RPE1 8/3 cells within all the fractions (in the Chr, MCM2 levels were even higher in RPE1 8/3 than wild-type). ORC6 levels were always high for diploid and 8/3 cells but lower in RPE1 7/3 (Figure 25).

As mentioned before, surprisingly, it was found that RPE1 8/3 cells expressed MCM7 and MCM2 at similar levels as the wild-type, which was especially evident in the cytoplasmic and nuclear fractions (Figure 25), and the chromatin-bound fraction of MCM2 was very strong in cells carrying an extra copy of chromosome 8.

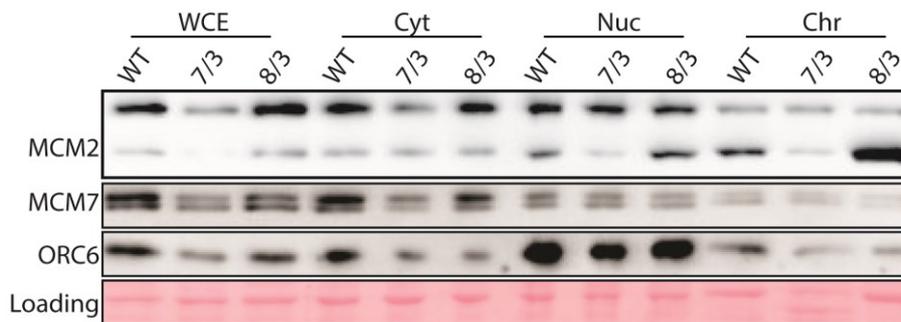


Figure 25. Pre-RC expression levels in response to extra gene copy number. Western blot analyses of MCM2, MCM7 and ORC6 pre-RC components in RPE1 and derived aneuploid cells carrying an extra copy of chromosome 7 or chromosome 8 in samples from the whole cell lysate (WCE), cytoplasmic (Cyt), nuclear (Nuc) and chromatin-bound fractions (Chr).

To test whether the cell cycle was affected in RPE1 7/3, the cell cycle profile of these RPE1 and aneuploid cells with extra copies of chromosome 7 or 8 were analysed. Additionally, the asynchronous cells were treated with low doses of aphidicolin, a DNA polymerase inhibitor that further increases defects in replication regulation (Figure 26). In this experiment, it was observed that RPE1 7/3 cells, either treated with aphidicolin or non-treated, were mostly in the G1 phase (~75%). The proportion of S phase cells was similar between treated and untreated cells with a difference of only 5%. In the wild-type, approximately 60% of cells were in G1 and 30% were in the S phase (Figure 26). The percentage of cells in the S phase was also smaller in RPE1 7/3 than in diploid cells. However, RPE1 8/3 cells did not show the same behaviour as described for the other cell lines: RPE1 8/3 cells had a lower percentage of G1 phase cells (~50%) than wild-type or RPE1 7/3 cells, but a higher percentage of S phase cells (~40%) than diploid cells (Figure 26).

Thus, it was possible to prove through another approach that the changes in MCM2-7 levels *per se* cannot explain the cell cycle delay and the longer G1 that was observed as a consequence of chromosome gain.

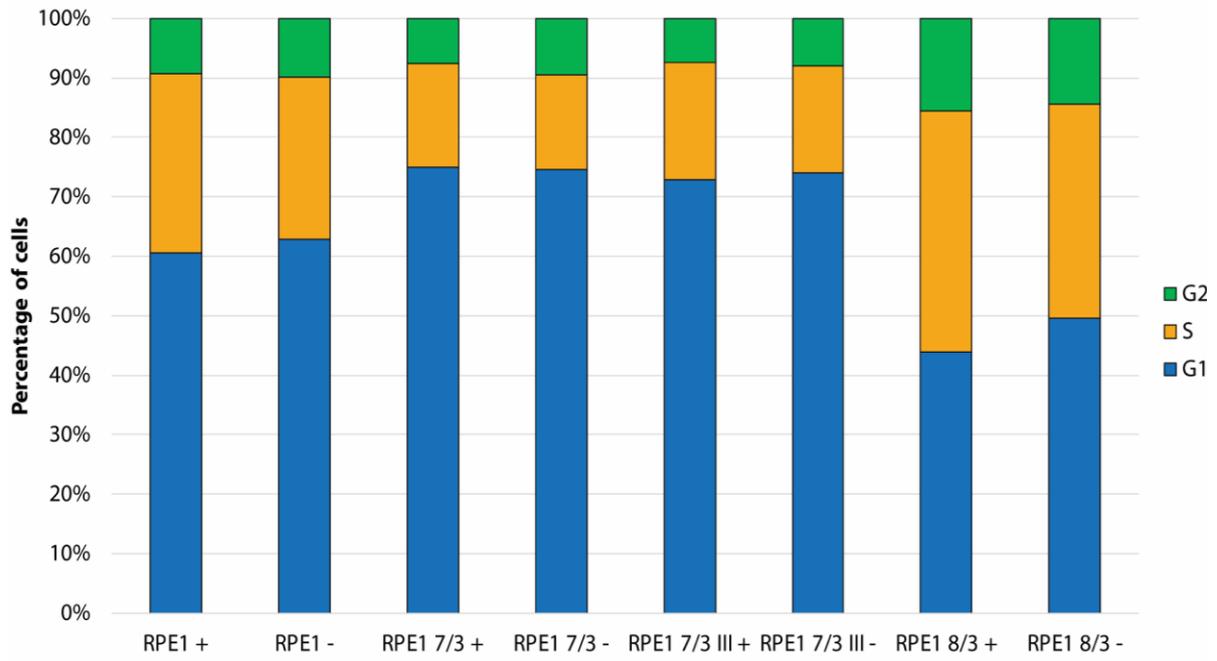


Figure 26. Cell cycle analysis of asynchronous cells. FACS analyses of RPE1 WT and aneuploid cells carrying extra copies of chromosome 7 or chromosome 8, either treated (+) or not (-) with aphidicolin [0.2 μ M].

6.10. Defective checkpoint factors and consequent impairment of MCM2-7 helicase regulation may be responsible for the extended G1 in aneuploid cells

As explained above, the low levels of the MCM2-7 helicase *per se* do not fully explain the altered cell cycle of aneuploid cells. As aneuploid cells spend more time in the interphase, it was hypothesised that the defective G1/S transition could be due to defects in checkpoint factor abundance and changes in their stoichiometry. To test this idea, HCT116 WT, 5/4 and 3/3 cells were synchronised by growth factor deprivation, as described above. To determine the changes in protein levels, cell fractionation was performed and the nuclear fractions were studied in detail.

In western blot analysis, differences in the nuclear levels of cyclin E1 and CDK2 were observed. The amount of cyclin E within the nucleus increased from 0 to 4 h; however, at 8 h, the levels

decreased both for HCT116 3/3 and 5/4 aneuploid cells (Figure 27). In addition, CDK2 was detectable in the nuclei only after 6 h. Unfortunately, the cycE1 results were poorly resolved (Figure 27B) and only the lower band shows an accumulation.

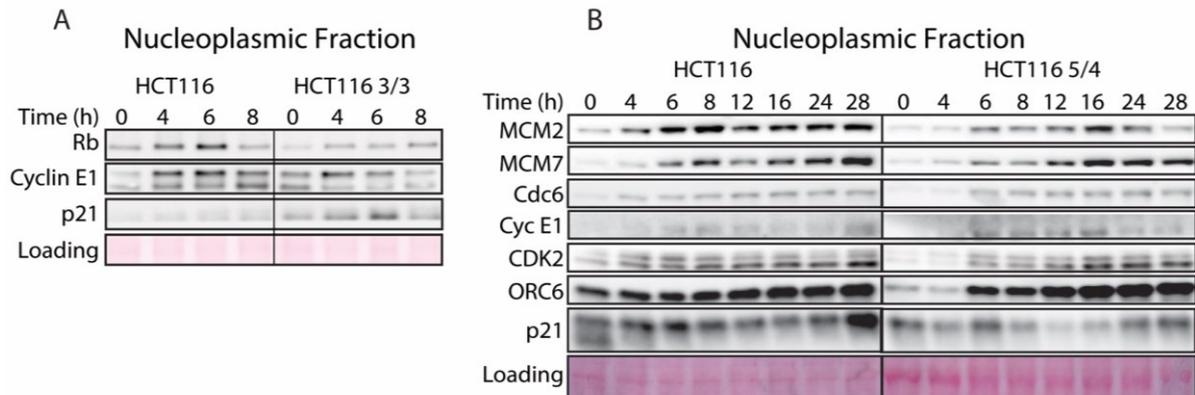


Figure 27. Time course of the expression of G1/S regulators in the nuclei. A) Western blot analysis of checkpoint factors in HCT116-H2BGFP WT and trisomic cells. B) Overview of the accumulation dynamics of pre-RC and G1 checkpoint factors in HCT116 and HCT116 5/4. All cell lines were previously synchronised by FBS deprivation and then released into a medium containing serum.

Next, a clonogenic experiment was performed in which cells were chemically treated for 13 days with inhibitors of cell cycle checkpoint kinases. Specifically, three different concentrations of SU9516 for CDK2, RO-3306 for CDK1, PD-0332991 for CDK4/6 and PHA-767491 for CDC7 were used.

In this experiment, the ability of cells to form colonies under conditions of CDK inhibition was tested. Strikingly, aneuploid cells were very sensitive to all of these kinase inhibitors. In detail, low doses of the CDK2 inhibitor were enough to impair colony formation of aneuploid cells (Figure 28A): at 0.25 μM , 100% of aneuploid cells could form colonies, whereas at 0.625 μM , this dropped sharply to 10–15%. No colonies were found in cells treated with 1.5 μM . In contrast, 55–60% of diploid cells could form colonies at 0.625 μM , but they showed similar sensitivity as aneuploid cells at the highest and the lowest concentrations (Figure 28A).

For the CDK1 inhibitor, the concentrations used to treat cells were 1, 2.5 and 5 μM . As shown in Figure 28B, only approximately 40% of HCT116 5/4 cells could form colonies at 2.5 μM , whereas approximately 60% of wild-type cells formed colonies at the same concentration. Neither aneuploid nor diploid cells survived at the highest concentration, although both could form colonies normally at the lowest concentration (Figure 28B).

The CDC7 inhibitor was administered at doses of 1, 2.5 and 5 μM . Similarly, in response to CDK2 inhibition, only 10–15% of aneuploid cells were still alive at the intermediate concentration (2.5 μM); however, 100% of cells remained alive at 1 μM and no colonies were found at 5 μM (Figure 28C).

Finally, the CDK4/6 inhibitor was administered at doses of 0.25, 0.5 and 1 μM . In this experiment, 80% of aneuploid cells and 100% of diploid cells formed colonies at the intermediate concentration (0.5 μM), and 100% of both HCT116 5/4 and wild-type cells could survive when treated with 0.25 μM . However, a significant difference was observed at the highest concentration (1 μM): only 50% of the aneuploid cells could form colonies in contrast to 80% of the HCT116 cells (Figure 28D). This survival experiment revealed that aneuploid cells are more susceptible to kinase inhibition than wild-type cells, with HCT116 5/4 being particularly sensitive to CDK2 and CDK4/6 inhibition.

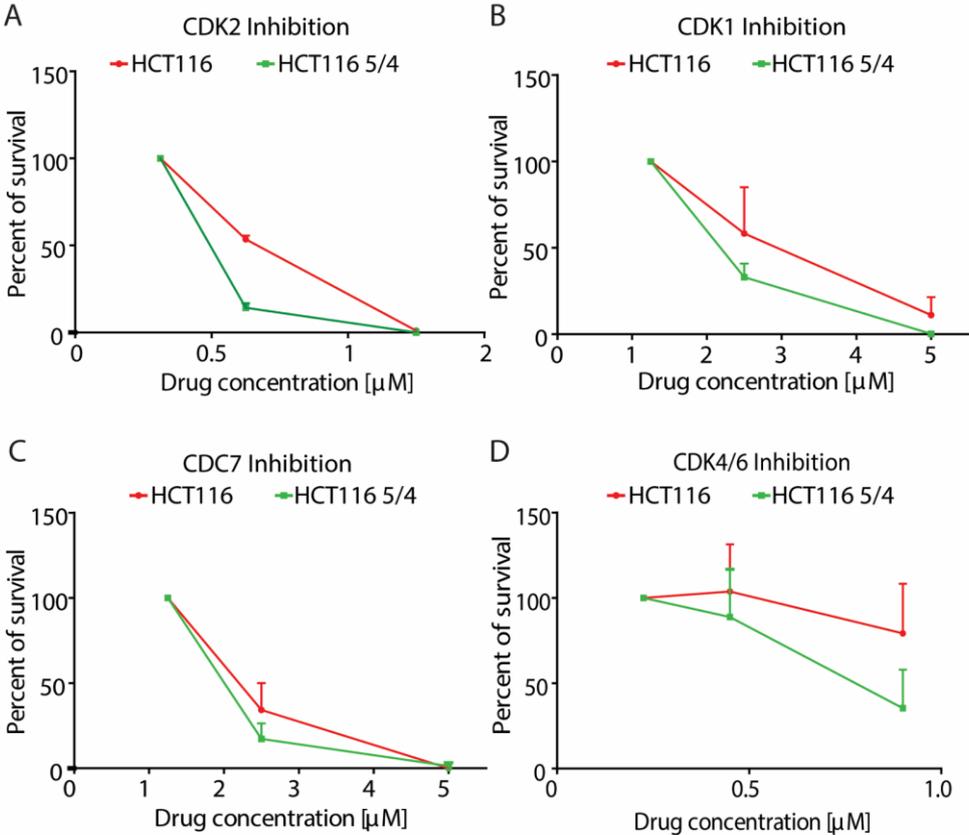


Figure 28. Aneuploid cells are sensitive to kinases inhibition. Clonogenicity of HCT116 WT and cells aneuploid for chromosome 5 treated for 13 days with different concentrations of A) CDK2, B) CDK1, C) CDC7 and D) CDK4/6 inhibitors.

Next, whether the reduced levels of CDK2 observed in aneuploid cells were responsible for the cell cycle delay was determined. For this purpose, cell synchronization of HCT116 was performed by growth factor deprivation. In addition, cells were treated with the CDK2 inhibitor (SU9616) at concentrations of 0.75 and 1 μM . Aneuploid and diploid cells were then released into media supplemented with 10% FBS and the CDK inhibitor. Samples were collected at 0, 4, 6 and 8 h and were tested by FACS analyses.

As shown in Figure 29, cells treated with the CDK2 inhibitor were more delayed than mock (non-treated) cells. Specifically, 50–55% of cells were in G1 upon CDK2 inhibition (either with 0.75 or 1 μM) at 8 h, whereas only 35% of mock-treated cells were in G1.

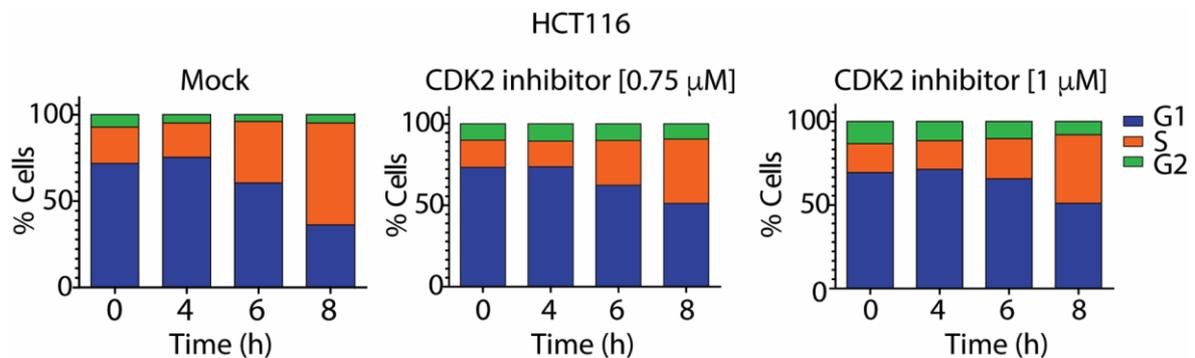


Figure 29. Cell cycle analyses of HCT116 cells upon CDK2 inhibition. Wild-type cells were treated with CDK2 inhibitor [0.75 μM] or [1 μM] or mock-treated. Cell cycle phase was determined by EdU versus DAPI (4',6-diamidino-2-phenylindole) visualization by FACS.

Furthermore, the effect of the CDK2 inhibition-based delay on the DNA binding of the MCM2-7 helicase was tested. Thus, HCT116 synchronization and CDK2 inhibition was carried out as described above. Analysis of EdU incorporation was performed to determine the differences between mock and CDK2-inhibited cells (Figure 30A). It was observed that CDK2-inhibited HCT116 cells (either with 0.75 or 1 μM) were delayed in the S phase. On the other hand, the mock cells could still incorporate EdU properly (Figure 30A). In addition, the DNA binding of the pre-RC subunits was tested by western blot analysis (Figure 30B). It was found that the CDC6 band was still visible at 8 h in CDK2-inhibited cells, but was not detectable in the mock cells at this time point. ORC6 levels were also higher in cells treated with the CDK2 inhibitor than in mock cells.

Regarding MCM2-7 helicase dynamics, there were similarities between CDK2-inhibited cells and aneuploid cells (as characterised in the previous section) only for the MCM2 subunit.

Specifically, MCM2 was loaded onto DNA from 0 to 4 h in cells treated with 0.75 μM CDK2 inhibitor, but the levels decreased at the later time points (6 and 8 h; Figure 30B). MCM2 accumulated on the chromatin also in cells treated with 1 μM of the drug (from 0 to 6 h), but the levels dropped again at 8 h. In contrast, in mock cells, MCM2 bound DNA from 0 to 8 h, as expected. MCM7 subunits did not seem to be affected by CDK2 inhibition. Indeed, MCM7 levels increased over time in all cells, that is, non-treated and those treated with 0.75 μM or 1 μM of the drug.

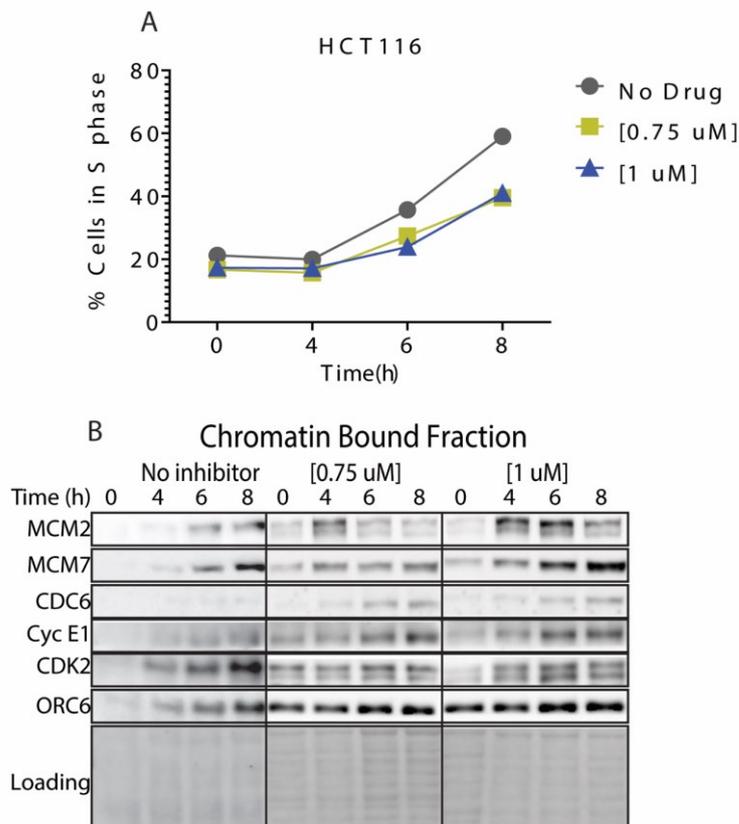


Figure 30. MCM protein levels upon CDK2 inhibition in wild-type cells. A) Percentage of cells in the S phase (EdU-positive cells only) for non-treated cells and cells treated with 0.75 μM or 1 μM of CDK2 inhibitor. B) Western blot analysis of treated and mock-treated HCT116 cells.

Finally, how the kinase activities of CDK1, CDK2, CDC7 and CDK4/6 changed with time was determined. For this purpose, mass spectrometry analysis of the nucleoplasmic fraction of synchronised HCT116 and HCT116 5/4 cells was performed. The LFQ intensities were again used to plot the proteins levels of CDK1, CDK2, CDK4/6 and the MCM2-7 helicase over time. It was found that CDK2 levels were lower in aneuploid cells than in diploids; the same dynamics were found for CDK4/6. As expected, the MCM2-7 levels were downregulated in aneuploids and the dynamics over time differed from the control cells. In contrast, CDK1 levels were similar between HCT116 5/4 and the control cells (Figure S9).

Furthermore, all the modifications of proteins that are known to be specifically altered by these cell cycle regulated kinases were analysed. The phosphorylated residues within all these were averaged and a table constructed of values of the serine-threonine-lysine (STY) modifications for each of the time points. In this way, it was possible to determine the specific phosphorylation trend for each of these kinases, which reflects the ability of CDKs to phosphorylate their downstream targets and thus regulate cellular functions (Figure 31). As shown in the graph, phosphorylation of CDK2 targets was not constant for all the time points. In fact, an increase from 0 to 8 h after the control cells were released from starvation was observed. In cells tetrasomic for chromosome 5, CDK2 targets were also phosphorylated, but the modification was lower than in the diploid cells even at the last time point (8 h; Figure 31). The same trend was evident for the other kinases. Specifically, CDC7 targets also appeared to be less efficiently phosphorylated in aneuploid cells than in diploids. Both CDC7 and CDK2 are functional in G1 and early S phases. Thus, the compromised activity of these two proteins may result in a compromised passage through the G1/S phase transition. The trend was milder for CDK1 and CDK4/6 kinases did not seem to be much affected (Figure 31B).

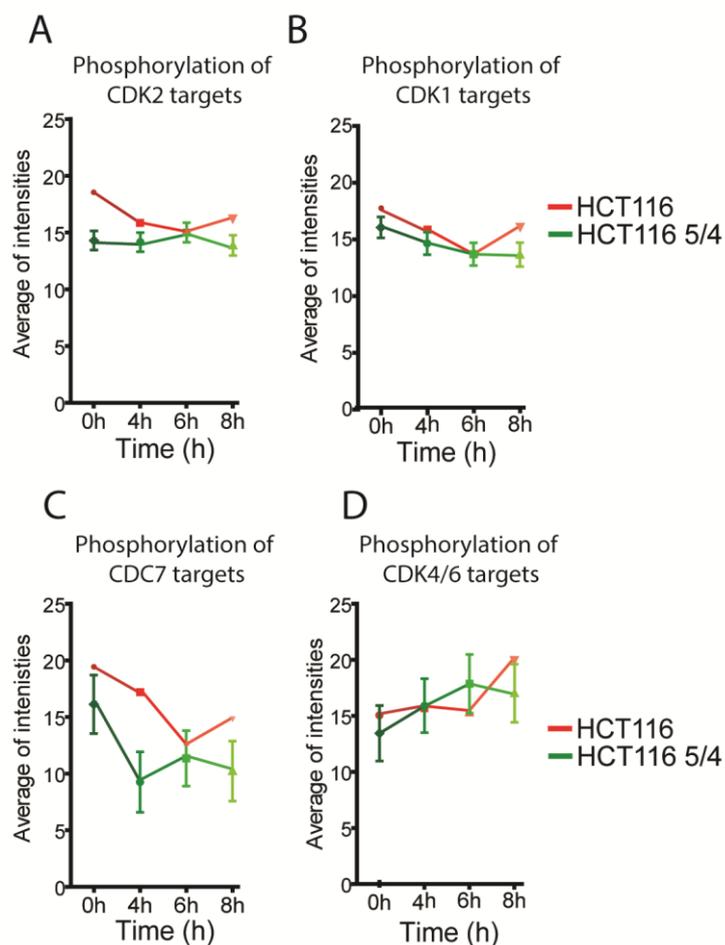


Figure 31. Trend of the phosphorylation of kinase targets. A) Phosphorylation of CDK2 kinase targets over time. B) Phosphorylation of CDK1 kinase targets over time. C) Phosphorylation of CDC7 kinase targets over time. D) Phosphorylation of CDK2 kinase targets over time. For each time point, the average of the modified targets is calculated.

Consistent with the observed delay in the cell cycle, it was thus observed that the key cell cycle-regulated kinases and interactors were downregulated.

6.11. Deregulation of MCM2-7 helicase phosphorylation in aneuploid cells

Constitutively aneuploid cells show an extended G1 phase likely caused by the downregulation and malfunction of CDK2 and cyclin E. It was speculated as to how the MCM2-7 helicase is affected by the deregulation of CDK2 and cyclin E. It is known that MCM subunits are targets of CDK2 during the whole G1 phase. Thus, suboptimal CDK2 activity might result in altered post-translational modifications (PTMs) on the MCM subunits.

To verify this hypothesis, mass spectrometry analysis of the phosphorylation sites (serine, threonine and tyrosine) that are normally targets of these kinases was performed. For this purpose, HCT116 WT and aneuploid HCT116 5/4 cells were used (with two extra copies of chromosome 5). As described above, diploid and aneuploid cells were synchronised by growth factor deprivation and then released by adding 10% FBS. Cells were also sub-fractionated and nuclear and chromatin-bound fractions were collected and analysed by mass spectrometry. Each MCM2-7 subunit can be modified on various sites and the addition of a phosphate group to a specific serine of a single helicase subunit drives the entire complex to carry out a particular function. It was shown that PTMs regulate the binding of the MCM2-7 helicase to DNA (origin of replication licensing) and activate the helicase activity (origin of replication firing). Two-sample tests (p^2 test) were used to determine significant differences between values. Many PTMs were detected on the MCM2-7 subunits, which have been previously found in other studies, as shown in Table 3. Next, the data were filtered by using the gene ontology browser for biological processes (GOBP), and heatmaps were generated to visualise the intensity changes. To determine whether the PTMs were increased in constitutive aneuploid cells over time, the values of aneuploid to euploid cells were normalised (Figure 32). Particular attention was paid to the phosphorylation of the MCM2, MCM3 and MCM7 subunits.

Regarding MCM2, it was found that there were less PTMs in aneuploid cells compared to the control parental cells. These residues were at serines 4-5-7, 13, 27, 40-41, 108 and 139 (Figure 32, red boxes). Specifically, phosphorylation of MCM2 at the S4-5-7 was lower at early time points (0 to 6 h). The other modified residues of MCM2 were S13-27; phosphorylation of these

sites was not maintained in constitutive aneuploids (Figure 32, red boxes). Thus, aneuploid cells fail to phosphorylate these serine moieties efficiently.

Table 3. Identified phosphorylation sites in nucleoplasmic fractions.

Number	Protein	Phospho-site position	Amino acid	Related kinase	Reference
1	MCM2	4	serine	CDC7	(Chuang et al., 2009)
2	MCM2	5	serine	CDC7	(Chuang et al., 2009)
3	MCM2	7	serine	CDC7	(Chuang et al., 2009)
4	MCM2	12	serine	unknown	
5*	MCM2	13	serine	CDK2, CDK1	(Chuang et al., 2009; Montagnoli et al., 2006)
6	MCM2	25	threonine	unknown	
7	MCM2	26	serine	unknown	
8*	MCM2	27	serine	CDC7, CDK2	(Cho et al., 2006; Chuang et al., 2009)
9	MCM2	39	threonine	unknown	
10	MCM2	40	serine	CDC7	(Montagnoli et al., 2006)
11	MCM2	41	serine	CDK2	(Montagnoli et al., 2006)
12	MCM2	53	serine	CDC7	(Cho et al., 2006; Montagnoli et al., 2006)
13	MCM2	59	serine	CDC7	(Cho et al., 2006)
14	MCM2	108	serine	CDC7, ATR	(Cortez et al., 2004; Montagnoli et al., 2006)
15	MCM2	139	serine	CK2	
16	MCM2	381	serine	unknown	
17	MCM3	535	serine	ATM	(Cortez et al., 2004)
18	MCM3	668	serine	unknown	
19	MCM3	672	serine	unknown	
20	MCM3	674	serine	unknown	
21	MCM3	711	serine	unknown	
22	MCM3	722	threonine	CDK2	(Li et al., 2011)
23	MCM4	2	serine	unknown	
24	MCM4	3	serine	CDK2	(Komamura-Kohno et al., 2006)
25	MCM4	120	serine	unknown	
26	MCM4	131	serine	unknown	
27	MCM4	326	serine	unknown	
28	MCM6	762	serine	unknown	
29	MCM7	121	serine	CDK2, CDK1	(Wei et al., 2013)

Adapted from Braun's MSc thesis, 2018.

A post-translational modification on a serine of the MCM7 subunit was also identified. Serine 121 was the only affected site (Figure 32, green box). Phosphorylation of MCM7 S121 was diminished specifically at 6 h.

Alterations in the phosphorylation of MCM3 at serine 722 was also found. Phosphorylation of S722 on MCM3 was slightly reduced only at 0 h in HCT116 5/4. At later time points, no differences between aneuploid and diploid cells were detected.

HCT116 5/4 vs HCT116				Position	Gene name
0h	4h	6h	8h		
0.34066	1.5	0.99034	0.99756	203	TERF2P
0.66245	0.94685	1.50413	0.63049	195	LIG1
0	0	0	0	53	MCM2
0.31891	0	0.62848	0.73458	27	MCM2
0.98467	0.91622	0.67265	2.37681	40	MCM2
0.98467	0.91622	0.67265	2.37681	41	MCM2
1.00964	0	1.04184	0	4	MCM2
0.32958	0	0.52092	0.3	5	MCM2
0.99728	0	1	0	7	MCM2
0	1.41551	0	0	67	CLSPN
0	0	0	0	1189	BRCA1
0	0	0	0	1191	BRCA1
0	0	0	0	51	LIG1
0.32984	0	0.97432	0.96009	91	LIG1
0.98822	0.90115	0.9913	0.92396	76	LIG1
0	0	0	0.30364	13	MCM2
0.48971	0	0	0	27	MCM2
0	0	0	0	277	RAD9A
0	0	0	0	691	TNKS1BP1
0	0.46095	0.95232	0	31	CDT1
0	0	0	0	5	MCM2
1.01092	0.96786	2.85081	0.89987	13	MCM2
0.51098	0.92607	0	0.47686	195	LIG1
0	1.97967	0	0	355	RAD9A
0.96288	0.65351	0.65909	0.94689	139	MCM2
0	0.46095	0.95232	0	29	CDT1
0.66093	1.44869	0.99729	0.97973	108	MCM2
0.97121	0	1.11255	0	91	LIG1
0.98125	0	0	0	53	MCM2
2.06426	0	0.96992	0	336	RAD9A
0	0	0.96992	0	328	RAD9A
2.06426	0	0.96992	0	355	RAD9A
0.97466	0.61499	1.00599	0.47852	51	LIG1
0	0	2.01619	0	91	LIG1
1.00356	0.98944	1.00957	0.99391	76	LIG1
0.98496	0.9493	0.93786	0.84708	27	MCM2
0.49905	0.96	1.97817	0	40	MCM2
1.00328	0.50515	1.56792	0.27219	41	MCM2
0.65276	0	0	0	722	MCM3
1.07813	1.55354	1.05726	1.01473	20	RRM2
1.52453	0.69636	0.96639	0.28908	11	DUT
0	0	0	0	210	LIG3
1.02049	0.67448	1.62554	2.90361	612	NUP98
0.6495	0.94861	0.31871	0.52814	323	TERF2
0	0	0	0	224	ATRIP
0.96512	0.32078	0.3201	0.97266	121	MCM7
0.6639	0	0	0	277	RAD9A
2.22857	0	0.50448	0	328	RAD9A
0.70451	1.03903	1.56237	1.57203	435	TNKS1BP1
0.70972	2.03226	1.53074	1.62633	691	TNKS1BP1
0.9469	0	0.92943	0.63014	31	CDT1

Figure 32. Heat map of phosphorylated sites. Mass spectrometry analyses of the phosphorylation occurring in the nucleoplasmic fraction along the G1 phase in aneuploid cells. The heat map depicts the post-translational modification of nuclear proteins and was generated after the STY matrix was filtered with the GOBP database specifically for DNA replication processes. Each of site was compared between HCT116 and HCT116 5/4. In the red boxes, the modifications detected on the MCM2, MCM3 and MCM7 proteins are highlighted.

This method allowed the identification of alterations in PTM profiles at specific residues and for specific MCM subunits in the constitutive aneuploid cells.

6.12. Generation of MCM2 and MCM7 mutants according to the MS results

It was found that CDK2 protein levels decreased in aneuploid cells and also that CDK2 kinase activity was reduced. It was also possible to identify changes in PTMs between aneuploid and diploid cells during the G1 phase. How the cell cycle might be influenced by the altered phosphorylation of the MCM2-7 helicase was thus considered.

To answer this question, the function of the individual phosphorylations occurring on specific MCMs subunits was addressed. Site-specific mutagenesis was performed to build a panel of different mutations, which were tested individually (like for MCM7) or combined (like MCM2). For each specific MCM subunit, serines (S) were changed to alanines (A) (phospho-mutant) or to aspartic acid (D) (phospho-mimic).

The MCM2 mutants tested were: S4-5-7A and S-4-57D; S13-26-27A and S13-26-27D; S4-5-7-13-26-27A and S4-5-7-13-26-27D (Figure 33). Then, HCT116 WT and HCT116 5/4 aneuploid cells were transfected with these vectors. Cell cycle analyses were performed for the following modified cell lines: HCT116-MCM2, HCT116-MCM2 S4-5-7A, HCT116-MCM2 S4-5-7D, HCT116 5/4-MCM2, HCT116 5/4-MCM2 S4-5-7A and HCT116 5/4-MCM2 S4-5-7D. The cell cycle analyses of asynchronous cells did not reveal any significant changes (Figure 33). Further, the percentages of cells in different cell cycle phases were different between aneuploid and diploid cells. Indeed, the G1 phases are longer in aneuploid than in diploid cells. Regarding the S and G2 phases, in aneuploid cells, these phases are generally not as long as in the wild-type cells.

Western blot analysis was performed to determine the expression levels of the mutant versions of MCM2. It was found that MCM2 S4-5-7A (the phospho-mutant) negatively affected the ability of the complex to bind DNA, as previously shown (Figure S11). Indeed, the protein levels of the MCM2 S4-5-7A mutant were diminished specifically in the chromatin-bound fraction. On the other hand, the phospho-mimic (MCM2 S4-5-7D) mutant bound DNA to the same extent as non-mutant protein in both diploid and aneuploid cells (Figure S12.1).

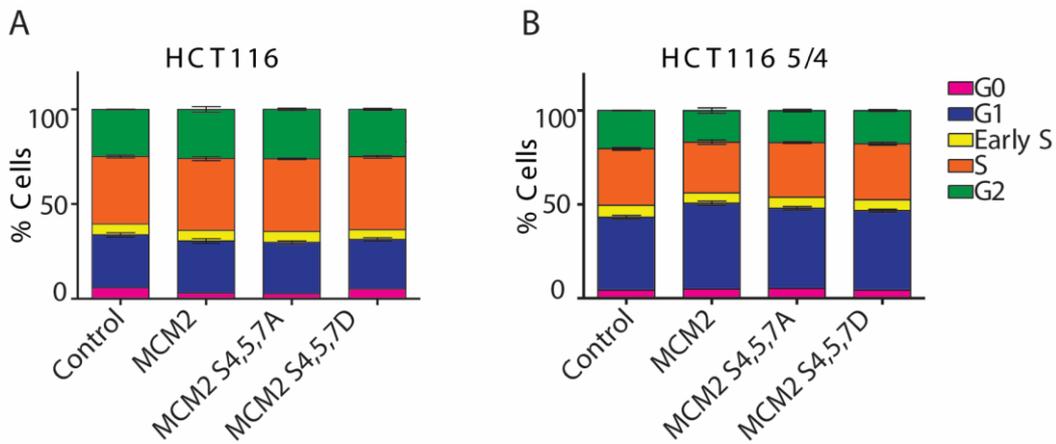


Figure 33. Cell cycle analysis upon MCM2 mutation. FACS analyses of MCM2 mutants in asynchronous HCT116 WT and aneuploid cell lines, EdU versus DAPI (this set of experiments was performed with Simon Braun and confirmed by western blot analysis).

MCM7 phospho-mutant and phospho-mimicking expression vectors were also generated by replacing a serine with an alanine (S121A) or with an aspartic acid (S121D), respectively (Figure S11). These vectors were transfected into HCT116 WT and cells tetrasomic for chromosome 5. The expression levels were confirmed by western blot analysis (Figure S11). To determine the differences in the cell cycle, the transfected cells were treated with low doses of aphidicolin (Aph) to increase the replication stress. Specifically, it was found that about 60% of cells with wild-type MCM7 or mutants (MCM7, MCM7 S121A and MCM S121D) were in the G1 phase in untreated transfected HCT116 5/4 (Figure 34B, red box) and about 50% of the control transfected cells (pcDNA) were in G1 (Figure 34B, red box). In the diploid cells, the percentage of G1 cells was always lower than in aneuploid, and there were no differences between the cells transfected with pcDNA, MCM7 and MCM7 S121A, whereas there was a slight increase in MCM7 S121D cells in the G1 phase (10% higher) (Figure 34A, red box).

However, the scenario changed in transfected cells with replication stress: indeed, the number of cells in the G1 phase decreased both for HCT116 5/4 as well as for wild-type cells (Figure 34A–B, blue boxes). Specifically, about 30% of HCT116 5/4-MCM7 cells were in the G1 phase, whereas that number was 35% for the control cells (pcDNA). Moreover, the number of MCM7 S121A-transfected cells in G1 increased to about 50%. In contrast, aneuploid cells transfected with the phospho-mimic (MCM7 S121D) behaved similarly to the HCT116 5/4-MCM7 cells (Figure 34B, blue box). The treated diploid HCT116-MCM7 cells progressed quickly through the G1 phase (although only some were in G1), whereas the control cells

(pcDNA) remained in the same cell cycle phase (Figure 34A, blue box). Further, 45% of the diploid cells transfected with S121A were in the G1 phase upon Aph treatment and the S121D cells showed an intermediate phenotype: the percentage of cells in G1 decreases, but there were still more of these cells in the G1 phase than for HCT116-MCM7-transfected cells subjected to replication stress (Figure 34A, blue box). The behaviour of diploid cells was comparable with that of aneuploid cells, but the effect of the phospho-mutant was comparable in aneuploid and diploid cells only when the cells experienced replication stress. Indeed, upon aphidicolin treatment, the amount of G1 cells was significantly higher in HCT116 cells and cells tetrasomic for chromosome 5. However, a large number of cells transfected with the wild-type (MCM7) or the phosphor-mimic (MCM7S121D) could transition to the S phase upon replication stress.

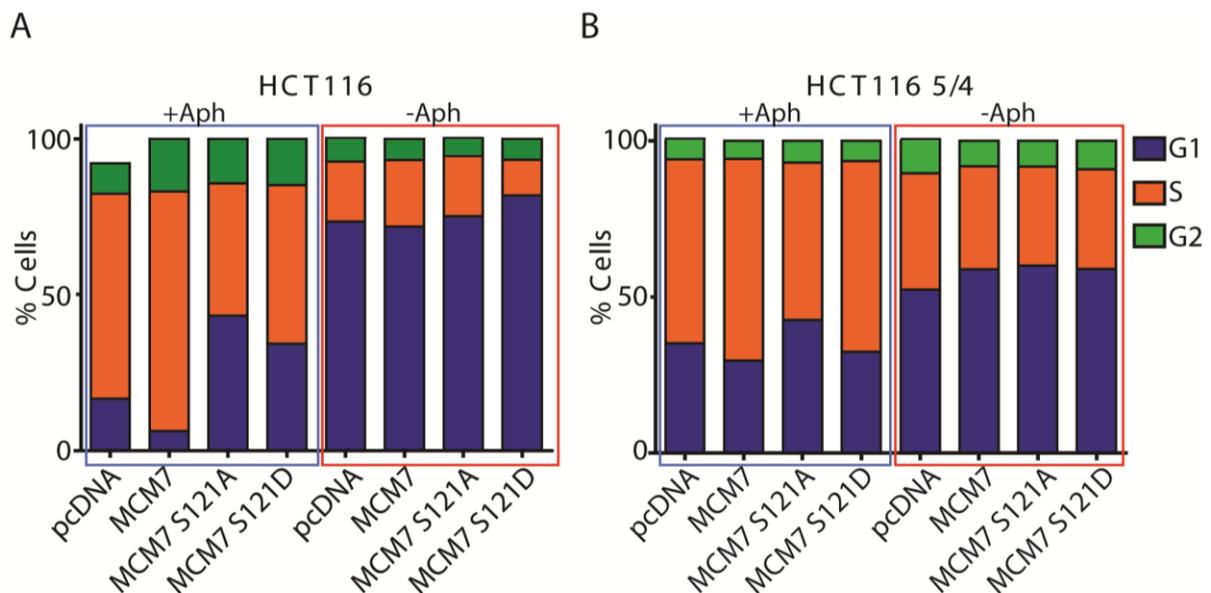


Figure 34. Impact of the MCM7 S121 phosphorylation site on the G1 phase. FACS analyses of MCM7 mutants in HCT116 WT and aneuploid cells with and without aphidicolin treatment [0.3 μ M].

Thus, MCM7 phosphorylation of S121 was revealed to be potentially involved in the longer G1 of aneuploid cells.

7. Discussion

Aneuploidy is detrimental to life: an unbalanced karyotype leads to detrimental changes in cell physiology and for organisms. The best characterised disease linked to aneuploidy is trisomy 21 (Down syndrome), and this is the only known trisomy where individuals can reach adulthood. Children show growth defects, distinctive facial features and reduced IQ, but they can still survive. There are three other known trisomic syndromes in which the baby is stillborn or dies immediately after birth. In these diseases, numerical changes occur in the germline. However, aneuploidy has also been found in other conditions that are harmful for human life. Indeed, complex aneuploidy (numerical and structural changes) are found in 90% of solid tumours. In addition, an increased rate of aneuploidy, so-called chromosomal instability (CIN), is associated with poor prognosis and drug resistance in cancer.

In our laboratory, cells were generated with changes in chromosome copy number by using the minicell chromosome transfer method. Our group found a phenotype that is shared by all analysed aneuploid cell lines, defined as the ARP. It has been demonstrated that the ARP overlaps with the response of cells suffering from proteotoxic stress; in fact, defects in the chaperone system have been described in our model systems of aneuploidy.

In this work, the focus was on identifying the reasons for the cell cycle delay in aneuploid cells, and whether this is interlinked with the previously observed downregulation of replicative factors. It is demonstrated that the expression of the MCM2-7 helicase and cell cycle regulatory kinases and other factors were reduced in cells with extra chromosomes and how these changes affect the proliferation of aneuploidy cells is characterised.

7.1. Cell cycle delay at the G1 to S phase transition is not solely due to reduced DNA binding of the MCM2-7 helicase

Our aneuploid model cells show a proliferation defect associated with cell cycle delay. Cell cycle phases were previously analysed and compared between diploid and aneuploid cells: from the comparison, it was evident that cells with chromosomes had longer cell cycles (Stingele et al., 2012). Cell cycle progression was investigated in cells synchronised by growth factor deprivation. Release of cells back into medium with growth factors and sampling of cells over time revealed the length of the G1 phase in cells carrying an extra chromosome. Roughly 70% of diploid cells went into the S phase 8 h after the cells were released. At this time, most

aneuploid cells were still in the G1 phase (80%). Therefore, G1 seems to be the cell cycle phase that is strongly negatively affected by aneuploidy. Thus, how progression through this cell cycle phase could be impaired just by the presence of an extra chromosome was investigated.

It is known that many biological processes are affected by aneuploidy, and specifically that factors required for DNA replication and repair pathways are downregulated in cells with extra chromosomes (Passerini et al., 2016). In particular, it was shown that all MCM2-7 helicase subunits are commonly less abundant in aneuploid cells. These helicase subunits are strictly regulated during G1. It has been demonstrated that MCM helicase can bind the chromatin upon post-translational modification due to key checkpoint regulators.

The regulation is accomplished by checkpoint proteins such as CDK2/cyclin E, and the phosphorylation of different sites of the MCM2-7 allows the licensing of the origins of the replication and later the firing of it. Therefore, the possibility that low levels of the replicative helicase might cause the cell cycle delay by prolonging the G1 phase was considered. However, another option was that the checkpoint was not operating correctly. Thus, aneuploid cells would need more time to pass through the G1 phase, as they would need to license the origins of replications. The last hypothesis involves proteotoxic stress. As a consequence of aneuploidy, cells suffer from misfolded protein accumulation. This might lead aneuploid cells to generate missfunctional protein complexes.

The hypothesis was tested by investigating the accumulation of MCM2-7 subunits and the entire pre-replicative complex (pre-RC) in the different cellular compartments (cytoplasm, nucleus and chromatin-bound fractions) by using various methods to exclude any off-target effects. Overall, the pre-RC factors CDC6 and ORC6 were found to be properly distributed between each compartment and seemed to be functional, although the levels of each of these factors were lower in aneuploids than in diploid cells. Furthermore, the subcellular distributions of MCM2 and MCM7 as representatives of the helicase complex were carefully determined. It was found that these subunits could be properly localised to the cytoplasm and then could be transferred to the nucleus without any particular defects. Although there is an overall downregulation of MCM2-7 in aneuploid cells, this replicative factor can still be distributed properly between the different cellular compartments.

The portion of proteins that bind DNA are particularly important as it represents the accumulation of functional factors. Indeed, MCM2 and MCM7 accumulation on chromatin proceeded as expected in diploid cells. The amounts of these subunits bound to chromatin increased over the course of the G1 phase (0–8 h), whereas the helicase complex dissociated from DNA in subsequent cell cycle phases. In aneuploid cells, on the other hand, the MCM2 and MCM7 proteins bound chromatin from 0 h to 6 h, but 2 h later the subunit levels decreased, before increasing again at 12 h. The mRNA levels of MCM2 and MCM7 were also investigated. The mRNA levels peaked at 8 h, demonstrating that aneuploid cells induced the expression to produce more subunits. This suggests that the aneuploid cells not only contain lower levels of replicative factors but also the helicase complex MCM2-7 is not able to stay stably associated with DNA as in diploid cells. This defect in chromatin association could cause a compromised transition from the G1 to the S phase of the cell cycle. This is likely because aneuploid cells need to restore a threshold of the level of chromatin-bound MCMs before they can proceed to the S phase, as otherwise replication can lead to DNA errors. Since the activity of the chaperone system is diminished in aneuploid cells, the stability of the helicase complex was tested when the transcription process was blocked. However, each of the subunits were stable within at least the cytoplasmic and nucleoplasmic fractions. Chromatin-bound proteins showed a drop in the helicase factors in aneuploid cells as previously described by Passerini (2016).

In this work, a novel behaviour of MCMs helicase along the cell cycle has been described. Indeed, in aneuploid cells, MCM2-7 levels decrease in the late G1 phase. Upon chromosome gain, this new behaviour can be explained by the MCM2-7 downregulation only, or by deregulation of key sites of the replicative helicase.

At this point, it was decided to vary the expression levels of the MCM2 or MCM7 subunits. To rescue MCM2-7 levels, cells carrying extra copies of the MCM7 gene were generated. It is known that overexpression of this subunit causes cells to express higher levels of the MCM2-7 complex on the DNA (Passerini et al., 2014). However, attempts by myself and others were unsuccessful in overexpressing the MCM2 subunit, either through transient transfection or by generating stable clones. However, overexpression of MCM7 alone can rescue the levels of the other subunits. But, this indirect overexpression of the entire MCM2-7 helicase did not shorten the G1 phase, although the MCM levels did not drop at 8 h, as in non-overexpressing cells.

A different strategy was also employed: since the MCM7 gene is encoded on chromosome 7, aneuploid RPE1 cells trisomic for this specific chromosome (RPE1 7/3) were generated. The results were the same as those obtained by using the previously described strategy (data not shown). Further, MCM2 was knocked down in WT HCT116 cells by siRNA, and in this case, the cell cycle was only slightly delayed: 10% more of transfected cells were in the G1 phase compared to mock-transfected cells. Altogether, these results show that the activity of the MCM2-7 helicase is negatively affected by aneuploidy. Indeed, as a consequence of chromosome gain, the replicative helicase is downregulated and its ability to stably bind DNA is compromised. These findings may explain why the G1 phase of aneuploid cells is extended by 4 h compared to diploid cells. However, the hypothesis that low levels of MCM2-7 helicase alone are responsible for the cell cycle delay does not seem to be true because changes in the levels of MCM2 and MCM7 subunits do not strongly affect the cell cycle either in HCT116 WT or aneuploid cells.

7.2. Impairments of CDK2/cyclin E affect the cell cycle

Different pieces of evidence suggest that low levels of MCM2-7 helicase *per se* are not responsible for the defective cell cycle in cells carrying an extra chromosome. Usually, cells contain an excess of each of the MCM subunits to avoid problems during the replication. This is called the MCM paradox (Das, 2014).

However, the levels of the replicative helicase can be affected by the defects in the chaperone system. Indeed, MCM subunits have to be folded properly to be incorporated in the complex.

A typical consequence of aneuploidy is the impairment of the protein folding system and subsequently the onset of proteotoxic stress. Additionally, chromosome gain leads to the accumulation of LC3 II protein and autophagosomes in the cytoplasm. Aneuploid cells are also more sensitive to heat shock protein 90 (HSP90) inhibition (Donnelly et al., 2014; Santaguida et al., 2015). The possible cause of the MCMs downregulation might be due to helicase subunit misfolding or, as hypothesised herein, that the replicative proteins may not be properly folded into their final quaternary form. As a consequence of the misfolding, many factors might be incorporated into lytic vesicles, and the protein degradation system would then be overwhelmed by the high levels of undigested proteins. This might lead to increased levels of misfolded proteins, which can partake in crucial molecular pathways. Many replicative factors are

interactors of HSP90 and therefore replication might be particularly vulnerable to the defects in protein folding.

In aneuploid cells, misfolded proteins might be integrated into heteromeric complexes, or the improperly folded factors might be deployed by cells even though they are not fully functional. It is known already that CDK2 downregulation can lead to cell cycle delay, specifically in the G1 phase (Nevis et al., 2009). Indeed, cells need to license enough origins of replication to progress through the late S phase. On the one hand, low levels of CDK2 can affect cell cycle progression, because, as a consequence, the CDC7 kinase is not active (Chuang et al., 2009). On the other hand, CDK2/cyclin E phosphorylate single MCM subunits, driving licensing and helicase firing (Bai et al., 2016). Furthermore, cyclin E affects MCM2-7 loading onto DNA in a kinase-independent manner. This interaction is required to direct the helicase complex to the right positions on the chromatin, which enables strong and stable interactions (Geng et al., 2007).

Thus, miss-functional CDK2 and/or CycE1 might result in the unusual accumulation of the MCM2-7 helicase in aneuploid cells. On the one hand, the non-sustained phosphorylation activity of CDK2 can cause a miss-loading of the replicative helicase. On the other hand, MCMs cannot seat on the DNA at the specific origin of replication sequence without the CycE1 activity (this activity is CDK2 independent) (Masai, 2005).

Analyses of checkpoint proteins, specifically in nuclei, revealed that two key factors were mainly affected in aneuploid cells along with the tested time courses: CDK2 and cyclin E1. As a consequence of chromosome gain, the increase in both CDK2 and cyclin E occurred with different kinetics along the time course. In diploid cells, cyclin E levels increased from 0 h after FBS addition, peaking at 8 h, when the cells entered into the S phase. In aneuploid cells, cyclin E levels reached this threshold level later. Similar behaviour was shown for CDK2: the levels of this kinase were stable along the time course in diploid cells, whereas aneuploid cells harboured less CDK2 within their nuclei already at 0 h after the cells were released from starvation. The levels of the kinase remained low for more than 8 h.

Furthermore, chemical inhibition of different cell cycle kinases proved that aneuploid cells are more sensitive to inhibition of CDK2 than diploid cells. Indeed, low doses of the CDK2 inhibitor were sufficient to decrease the clonogenic ability of the aneuploid cells.

Finally, chemical inhibition of CDK2 in synchronised cells suggested a role for this kinase in the MCM2-7 and cell cycle impairment of aneuploid cells. Indeed, when synchronised diploid cells were treated with the CDK2 inhibitor, the levels of chromatin-bound MCM2 and MCM7 subunits were reduced as previously described for the aneuploid cells. Moreover, the cell cycle profile exhibited a slight delay and an increased percentage of G1 cells. Thus, chemical impairment of CDK2 in diploid cells resulted in phenotypes similar to those of aneuploid cells.

Moreover, the same CDK2/CycE1 miss-accumulation was demonstrated by combining cell synchronization and label-free quantitative (LFQ) mass spectrometry. In the first instance, lower levels of CDK2 were observed in aneuploid cells than in diploids along the time course and within the nucleoplasmic fraction.

The downregulation and altered kinetics of CDK2/cyclin E accumulation confirm the hypothesis as to why these checkpoint regulators are negatively affected in aneuploid cells. As a consequence of the CDK2 and cyclin E downregulation, the G1 phase is elongated: in particular, the transition from the G1 to S phase is impaired. The reason for these defects appears to lie in the fact that an additional 4 h are needed for CDK2 and cyclin E to reach the threshold levels. Thus, in aneuploid cells, the transition from the G1 to S phase is accomplished later compared to diploid cells.

7.3. Deregulation of CDK2 affects the cell cycle through defective phosphorylation of MCM2-7 helicase

Checkpoint regulators are affected in cells with extra chromosomes. Nuclear accumulation of cyclin E and CDK2 is slower, in aneuploid cells.

This different accumulation of the CDK2/CycE1 might result in cell cycle delay due to mis-hyperphosphorylation of retinoblastoma protein (Rb), or by misregulation of the MCM2-7 helicase subunits. Indeed, besides the downregulation of these major factors that allow the G1/S transition, the kinase activity of CDK2 might not be fully functional. The miss-phosphorylation of Rb was tested in our lab by two different people, and briefly validated by myself as well (data not presented). The cells were synchronised and released at different time points. From this experiment, it was not possible to prove that Rb hyperphosphorylation was impaired in aneuploid cells. Next, the hypothesis of the miss-phosphorylation of the MCM2-7 subunits was

tested. In this case, a slightly different approach was used. Synchronised cells were fractionated, and mass spectrometry analysis based on LFQ and phosphorylation site detection was used to investigate the concentrations and the post-translational modifications of nuclear and chromatin-bound proteins. By using mass spectrometry, it was possible to detect sites modified by phosphorylation for all proteins either in nuclei or in chromatin-bound fractions.

A comparison of the detected phospho-sites between HCT116 5/4 and HCT116 showed how these modified sites were altered in aneuploid cells. First, the trend of target phosphorylation was examined and it was found that the phosphorylation could not be sustained efficiently 8 h after FBS addition in aneuploid cells. In contrast, CDK2 kinase activity increased with time in diploid cells.

This evidence could suggest a reason for the cell cycle delay in aneuploid cells. The hypothesis postulated herein is based on the lower abundance of MCM2-7 helicase and checkpoint regulators. More specifically, it is speculated that the impaired kinase function of CDK2 could cause deregulation of MCM phosphorylation, and that this might be the reason why the helicase could not remain stably associated with DNA throughout the G1 phase. To verify this hypothesis, heatmaps of the phosphorylated sites were generated for aneuploid and diploid cells and compared. Abnormal phosphorylation was identified on many serines for three of the helicase subunits: MCM2, MCM3 and MCM7. Mutations were generated at each of these sites and the resulting phenotypes determined.

However, no changes in the cell cycle were observed in cells that were transfected with MCM2 mutated on the sites S4-5-7, S13 and S27, although a slight decrease in the levels of the helicase complex could be detected in cells expressing the form of MCM2 mutated at S4-5-7. In fact, the function of these serines is already known in the literature, and the mutated forms cannot bind DNA because they cannot be phosphorylated by CDK2. More investigations are needed regarding the MCM2 mutants. First, to understand whether these sites are really important for the binding of the helicase complex to the chromatin, and second, to uncover new functions of these phosphorylated serines, such as sensors of replication stress or DNA damage.

The function of MCM7 S121 was also investigated, and as previously carried out for MCM2, mutated forms of this serine were generated. To determine the resulting phenotype, replication stress was induced in diploid and aneuploid cells transfected with the mutated MCM7.

It is known that the S121 of the MCM7 subunit can be phosphorylated by CDK2 in G1 or by CDK1 in late mitosis(Wei, 2017). Cell cycle analyses were performed on asynchronous cells previously transfected with the phospho-mutant (MCM7 S121A) and as a control with the phospho-mimic (MCM7 S121D). A higher percentage of cells carrying the MCM7 S121A mutant were G1 cells under replication stress, whereas the phospho-mimic mutant could slightly rescue the phenotype (a smaller percentage of G1 cells). Deregulation of MCM7 S121 made the cells more sensitive to replication stress and probably to DNA damage, as the concentration of the drug was high.

Aneuploidy leads to checkpoint factor deregulation. Specifically, cyclin E and CDK2 may be shuttled into nuclei later than in diploid cells. CDK2 kinase function is also not very effective for targets such as the MCM2-7 helicase. As a consequence, the already low-abundant subunits of the helicase complex are not properly regulated. This cascade of events causes the extended G1 and the defective G1/S phase transition in aneuploid cells. Moreover, downregulated and deregulated MCM2-7 helicase can presumably affect the replication process in aneuploid cells. Finally, the slower replication can promote increased DNA damage and therefore augments genome instability in aneuploid cells.

7.4. The role of aneuploidy in promoting genomic instability

This study has provided insights into the cell cycle defects caused by chromosome gain. In line with previous studies (Stingele et al., 2014; Passerini et al., 2016), the G1 phase is found to be extended in aneuploid cells. In particular, it was shown that the transition between the G1 and S phases is impaired due to deregulation of the MCM2-7 helicase subunits.

This work has employed the same model system that was set up in our lab for previous studies. In this model system, constitutive aneuploid cells were generated by using chromosome transfer (Stigele et al., 2012). In our lab, cells with cancerous (HCT116) or non-cancerous (RPE1) backgrounds were used. In this way, any cell line-specific phenotypes could be excluded and it was possible to study only those changes that are caused by aneuploidy. Thus, the newly generated cells carry three copies (trisomic) and/or four copies (tetrasomic) of a panel of many different chromosomes.

It was shown that replicative factors, MCM2-7 specifically, were downregulated as a consequence of aneuploidy. In a previous study, a lower abundance of the replicative helicase was linked with the induction of GIN in constitutive aneuploid cells (Passerini et al., 2016).

This work aimed to investigate the molecular causes and consequences of MCM2-7 downregulation. The results support the hypothesis that the longer G1 in aneuploid cells was caused by MCM2-7 helicase deregulation, and it was not strictly dependent on the levels of the MCM2-7 helicase. Previous studies showed a partial rescue of the MCM levels in aneuploid cells transiently overexpressing the MCM7 subunit. However, it was not possible to find the same rescue in aneuploid cells with stable overexpression of MCM7. However, it was found that the dynamics of checkpoint factor activity over the cell cycle were altered in aneuploid cells. Moreover, the levels of these cell cycle proteins were lower in aneuploid cells compared to diploid cells.

A previous study showed that cyclin E overexpression can reduce the amount of MCM2-7 helicase on chromatin, with the consequence that cells can license fewer origins of replication (Ekholm-Reed et al., 2004). Following the consequences of CDK2 and cyclin E misregulation, in our model system, it was found that phosphorylation of the functional serines of MCM2-7 helicase is impaired at many sites; specifically, regarding many residues of the MCM2, MCM7 and MCM3 subunits.

The combined effect of low levels of the MCM2-7 helicase in aneuploid cells, and the mis-phosphorylation on specific helicase subunits, result in aneuploid cells having an extended G1. Indeed, as a consequence of the reduced abundance and misregulation of MCM2-7, aneuploid cells might not have enough licensed origins of replication, since the helicase complex cannot stably associate with DNA. Furthermore, the licensing of dormant origins might be inefficient in aneuploid cells. This type of origins is used by cells as a surveillance system to ensure that DNA replication is accomplished in the proper physiological timeframe, and in such a way to prevent any introduction of errors to the DNA. Thus, the decreased number of origins (replicative or dormant) might cause an increase of GIN in aneuploid cells, due to the error-prone timeframe of the replication process. Preliminary results from DNA combing experiments showed an increased distance between replication forks in aneuploid cells upon induction of replication stress. Moreover, the replication complex is negatively affected and

forks proceed slower in cells that have gained an extra chromosome compared with in diploid cells (data not shown).

Aneuploid cells might engage a system to allow them to eventually complete G1, even though not enough dormant origins are licensed. It was shown, for example, that bypass of the arrested G1 phase is achieved by depletion of p53 or overexpression of HPV E7 oncoprotein (Liu et al., 2009; Nevis et al., 2009). Defective DNA replication is a major source of DNA damage. In addition, defects of DNA repair or failure of the checkpoint can also introduce mistakes in the genome, leading to subsequent genomic instability. For example, reduced levels of MCM2 cause a reduction in the phosphorylated form of Chk1 (Han, 2014). The checkpoint can fail as a result of the depletion of MCM7, and subsequently, DNA replication is no longer sensitive to stalled forks (Cortez et al., 2004).

Through the mass spectrometry analysis of nuclear and chromatin fractions, these observations could be confirmed in constitutive aneuploid cells. Indeed, it was possible to determine that many phosphorylation sites on MCM2 and MCM7 were negatively affected in aneuploid cells. In particular, an extension of the G1 length was detected in diploid and aneuploid cells carrying copies of a mutant form of MCM7 (MCM7 S121A) upon replication stress.

It would be interesting to examine how MCM2-7 and other checkpoint regulators are affected by chromosome gain. One explanation is suggested by the impairment of chaperone systems (mainly the HSP90 protein) in aneuploid cells. For example, it was shown that many factors of the DNA replication and repair pathways are clients of molecular chaperones (Taipale et al., 2014).

Furthermore, a comparison between HeLa cells treated with an HSP90 inhibitor and aneuploid cells showed an overlap in many of the downregulated pathways. DNA replication and repair were some of the commonly affected processes found in this comparison (Donnelly et al., 2014). In aneuploid cells, the HSP90 impairment might have consequences for protein folding. It might then be possible that misfolded proteins are integrated into macromolecular complexes regardless. As a result, the pathways involved will not be fully functional. Such an explanation might account for the impaired function of MCM2-7 helicase, CDK2, cyclin E and other checkpoint factors in aneuploid cells and the resulting defects in DNA replication and repair and cell cycle processes. In this work, no such strong effect on MCM2-7 upon HSP90 inhibition

was found. More studies on the check proteins could lead to some novel aspects of this kind of regulation.

Another possibility could involve the deregulation of E2F activity. It was shown that this transcription factor family can control DNA replication and cell cycle progression (Dyson et al., 1998). It is known also that E2F-1 regulation is linked to HSP90.

Some preliminary studies were performed; however, it was not possible to distinguish any significant differences in nuclear E2F-1 accumulation between diploid and the respective aneuploid cells over time. However, some other members of the E2F family (E2F-2 and E2F-4) showed decreased LFQ values in aneuploid cells in quantitative mass spectrometry analyses of nuclear G1 fractions (data not shown). Further investigations of E2F-2 and E2F-4 might better elucidate the role of these transcription factors and their involvement in the defective DNA replication and cell cycle progression in aneuploid cells. DNA replication might be affected by all these factors, and slowing fork progression might be a way to overcome the problem. It was demonstrated that aneuploid cells have many anaphase bridges (Passerini et al., 2014).

Aneuploid cells were found to be impaired in their activation of dormant origins with a resulting increase in replication stress. Subsequently, the cells can progress to anaphase without properly finishing replication. This then leads to an increased incidence of anaphase bridges. These bridges can lead to lagging chromosomes and/or DNA double-strand breaks, which are inherited by daughter cells, leading to further genomic instability.

Based on the data herein, a model can be proposed in which chromosome gain leads to downregulation of the MCM2-7 helicase as well as other replicative factors such as CDK2. This, in turn, leads to an altered pattern of post-translational modifications in aneuploid cells because of the dysfunctional checkpoint at the G1/S transition.

Moreover, the replication process might also be impaired due to the lower abundance and defective phosphorylation of the MCM2-7 helicase. As a consequence, the incidence of anaphase bridges in aneuploid cells is increased. Generation after generation, DNA damage is increased in the daughter cells, leading finally to genomic instability (Figure 35).

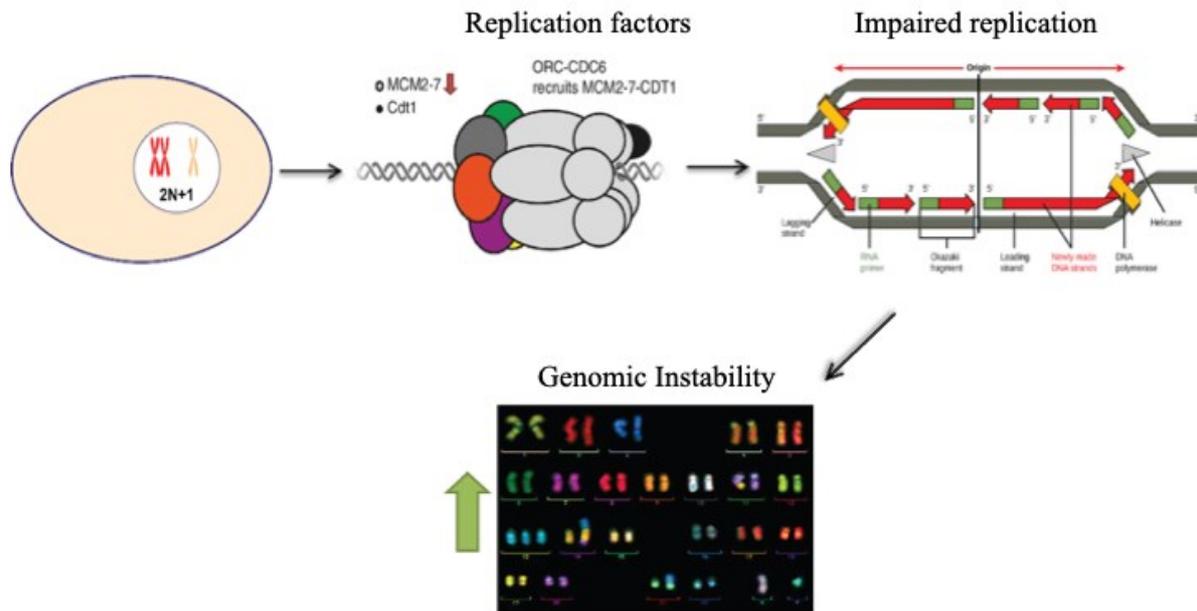


Figure 35. Model to explain the impaired proliferation in aneuploid cells. Impairment of cell cycle regulated kinases might be responsible for the deregulation of MCM2-7 helicase loading at the G1/S transition.

7.5. Aneuploidy, GIN and tumorigenesis

An unbalanced karyotype is common in cancer cells; thus, it was suggested that aneuploidy may exert tumorigenic effects (Holland and Cleveland, 2009). Indeed, aneuploidy was found in 90% of solid tumours and 50% of blood cancers (Beroukhi et al., 2010). The impact of genomic instability on the development of cancer is suggested by several lines of evidence.

In principle, several mutations in oncogenes and tumour suppressor genes have to occur in a relatively short time to provide the growth and fitness advantages typical of cancer. Cells can become tumorigenic due to germline or somatic mutations in genes involved in maintaining genome stability and DNA integrity (Edelmann et al., 1997; Prolla et al., 1998; Varley, 2003; Zhang et al., 2015b, Shlien et al., 2015). Finally, GIN promotes the karyotype heterogeneity that is the principal characteristic of cancer (Patel et al., 2014).

A typical hallmark of tumours is the deregulation of the cell cycle; therefore, any changes to genes related to proliferation could induce tumorigenesis. Since aneuploidy affects cell proliferation, its role in the onset of cancer remains under debate. Actually, it is still not understood whether aneuploidy is an intermediate station between normal cells and cancerous cells. Studies on cellular proliferation have proven that aneuploid cells can gain proliferative advantages after long-term passage (Weaver et al., 2007).

Recently, increasing evidence has begun to suggest that cancerous cells might become aneuploid as a last option to rescue their defective state (Amon et al., 2016). Aneuploidy is not the only way by which the cell cycle could be affected. Loss of E2F transcription factors leads to deregulation of the cell cycle and defects in proliferation and development (Wu et al., 2001). Additionally, mice carrying mutant forms of E2F-1 and E2F-2 were more prone to cancer (Zhu et al., 2001). Mutations of this class of transcription factor cause DNA replication defects in murine hemopoietic progenitors. Interestingly, a proliferative advantage occurred after oncogene mutation in the background of existing E2F-1 and E2F-2 mutations in hemopoietic progenitors. In contrast, oncogene mutations can lead to cancer and are selected against normal cells (Bilousova et al., 2005). In the same way, aneuploidy leads to proliferation defects and genomic instability is increased; as a consequence, cells acquire new genetic variations that allow them to adapt and to gain selective advantages under certain environmental conditions.

8. Material and Methods

8.1. Materials

8.1.1. Chemicals:

Acetic acid	Sigma-Aldrich Taufkirchen, Germany
Acrylamide	30% w/v SERVA Electrophoresis Heidelberg, Germany
Agarose	SERVA Electrophoresis Heidelberg, Germany
Ammonium persulfate	Merck Biosciences Darmstadt Germany
Ampicillin	Roth Karlsruhe Germany
2-Mercaptoethanol	Merck Biosciences Darmstadt Germany
Bradford reagent	BioRad Hercules USA
Bromophenol blue	Sigma-Aldrich Taufkirchen, Germany
DMEM + GlutaMAX™-I	Thermo Fisher Scientific Waltham USA
Dimethylsulfoxid	Roth Karlsruhe Germany
EDTA	Calbiochem La Jolla USA
Ethanol	Sigma-Aldrich Taufkirchen, Germany
Ethidium Bromide	Thermo Fisher Scientific Waltham
Fetal bovine serum	Sigma St. Louis USA
Glycerol	Sigma-Aldrich Taufkirchen, Germany
Glycine	MP Biomedicals Santa Ana USA
Hydrochloric acid	Sigma-Aldrich Taufkirchen, Germany
Hydroxyurea	Sigma-Aldrich Taufkirchen, Germany
Isopropanol	Sigma-Aldrich Taufkirchen, Germany
Lipofectamine 2000	Thermo Fisher Scientific Waltham
Magnesium chloride	Sigma St. Louis USA
Methanol	Thermo Fisher Scientific Waltham
Nocodazole	Sigma-Aldrich Taufkirchen, Germany
Penicillin/ Streptomycin	Thermo Fisher Scientific Waltham
Phosphatase inhibitor tablets	Roche Basel Switzerland
Ponceau S	Sigma St. Louis USA
Protease inhibitor tablets	Roche Basel Switzerland
Skim milk powder	SERVA Electrophoresis Heidelberg Germany
Sodium chloride	Sigma St. Louis USA

Sodium deoxycholate	Euro Clone Pero Italy
Sodium dodecyl sulfate	AppliChem Darmstadt Germany
Tetramethylethylenediamine	Sigma St. Louis USA
Tris	AppliChem Darmstadt Germany
Trypsin-EDTA 0.25%	Thermo Fisher Scientific Waltham USA
Tween-20	Sigma St. Louis USA

8.1.2. Buffers and Solutions

- **Lower separating gel (10% pH 8.8):** 4.95 ml 30 % (w/v) acrylamide; 3.75 ml lower SDS-buffer pH 8.8; 6.3 ml H₂O; 150 µl 10 % APS; 15 µl TEMED;
- **Upper stacking gel (5% pH 6.8):** 0.8 ml 30 % (w/v) acrylamide; 1.2 ml upper SDS-buffer pH 6.8; 3 ml H₂O; 50 µl 10 % APS; 5 µl TEMED
- **Running buffer pH 8.3:** 25 mM Tris base; 190 mM glycine; 0.1 % SDS
- **TBS + Tween20 (pH 7.5):** 50 mM Tris-HCl; 150 mM NaCl; 0.1 % Tween-20
- **Lämmli buffer (1x):** 50 mM Tris-HCl pH 6.8; 2 % SDS; 10 % glycerol; 12.5 mM EDTA; 0.02 %, bromphenol blue; 1 % β-mercaptoethanol
- **Lower SDS-buffer pH 8.8:** 1.5 M Tris-HCl; 0.4 % (w/v) SDS
- **upper SDS-buffer pH 6.8:** 0.5 M Tris-HCl; 0.4 % (w/v) SDS
- **RIPA buffer:** 10 % NP-40; 10 % sodium deoxycholate; 5 M NaCl; 0.5 M EDTA; 1M Tris base, pH 7.5; protease inhibitor according to the manufacturer's instructions (Roche); phosphatase inhibitor according to the manufacturer's instructions (Roche)
- **Bjerrum Schafer-Nielsen Buffer:** 48 mM Tris base; 29mM glycine; 20 % methanol
- **Ponceau solution:** 0.2 % Ponceau S; 1 % acetic acid
- **EdU ClickIt cocktail:** 0.5 mM CuSO₄, 100 mM Tris pH 8.8, azide fluorophore 1 µM, 100 mM ascorbic acid.

8.1.3. Antibodies

Antibody (manufacture)	Size	Dilution	Organism	Solution	1st ab	Wash
a-Actin (Abcam)	100 kDa	1:100	Mouse	10% milk TBST 0.2%	0.5h	10 min

GAPDH (CellSignaling)	36 kDa	1:2000	Rabbit	10% milk TBST 0.2%	40min	10 min
Cyclin A (Abcam)	55 kDa	1:1000	Mouse	5% BSA TBST	ON 4°C	7 min
Cyclin E (CellSignaling)	48- 56 kDa	1:1000	Mouse	10% milk TBST 0.2%	ON 4°C	5 min
Cyclin D (CellSignaling)	36 kDa	1:1000	Rabbit	10% milk TBST	ON 4°C	5 min
H3 (Millipore)	220 kDa	1:2000	Mouse	10% milk TBST 0.2%	ON 4°C	5 min
ORC6 (3A4) (SantaCruz)	31 kDa	1:1000	Rat	10% milk TBST 0.2%	ON 4°C	5 min
MCM7 (141.2) (SantaCruz)	75 kDa	1:1000	Mouse	10% milk TBST	ON 4°C	5 min
Rb (CellSignaling)	110 kDa	1:2000	Mouse	10% milk TBST 0.2%	ON 4°C	5 min
Rb Ser795 (CellSignaling)	110 kDa	1:1000	Rabbit	10% milk TBST 0.2%	ON 4°C	5 min
Rb Ser780 (CellSignaling)	110 kDa	1:1000	Rabbit	10% milk TBST 0.2%	ON 4°C	5 min
Rb Ser 612 WA-AP3236a	110 kDa	1:1000	Rabbit	10% milk TBST 0.2%	ON 4°C	5 min
Rb Thr 821 MABE197	110 kDa	1:1000	Rabbit	10% milk TBST 0.2%	ON 4°C	5min
Rb Ser807/811 (CellSignaling)	110 kDa	1:1000	Rabbit	10% milk TBST 0.2%	ON 4°C	5min
CDKN2A/p16I NK4a (Abcam)	17 kDa	1:1000	Rabbit	5% BSA in TBST	ON 4°C	5min
p21 (CellSignaling)	20 kDa	1:1000	Rabbit	10% milk TBST 0.2%	ON 4°C	5 min
p27 (CellSignaling)	27 kDa	1:1000	Rabbit	5% BSA in TBST	ON 4°C	5 min

p18 (CellSignaling)	18 kDa	1:1000	Mouse	10% milk TBST 0.2%	ON 4°C	5 min
CDK2 (CellSignaling)	33 kDa	1:1000	Rabbit	5% BSA in TBST	ON 4°C	5 min
CDK6 (CellSignaling)	36 kDa	1:1000	Mouse	10% milk TBST 0.2%	ON 4°C	5 min
CDK4 (CellSignaling)	30 kDa	1:1000	Rabbit	5% BSA in TBST	ON 4°C	5 min
p53 phospho sc101762	~50 kDa	1:1000	Rabbit	10% milk TBST 0.2%	ON 4°C	5 min 1 st time with milk
RPA32 (Abcam)	~32 kDa	1:1000	Mouse	10% milk TBST 0.2%	ON 4°C	5 min 1 st time with milk
Active HSF1 ENZO ADI- SPA-902	85- 95 kDa	1:1000	Rabbit	10% milk TBST 0.2%	ON 4°C	5 min
HSF1 (Enzo)	75- 90 kDa	1:1000	Rabbit	10% milk TBST 0.2%	ON 4°C	5 min
CDC7 (SantaCruz)	64 kDa	1:1000	Mouse	10% milk TBST 0.2%	ON 4°C	6 min
MCM7 (CellSignaling)	80 kDa	1:1000	Rabbit	5% BSA in TBST	ON 4°C	5 min
CDC45 (CellSignaling)	65 kDa	1:1000	Rabbit	5% BSA in TBST	ON 4°C	5 min
MCM2 (Abcam)	110 KDa	1:2000 1:1000	Rabbit	10% milk TBST 0.2%	ON 4°C RT 1h	5 min
HSP90 (Enzo)	~90 kDa	1:1000	Rabbit	5%BSATBS T	ON 4°C	5 min
RPA32 S33 (bethyl)	32 kDa	1:1000	Rabbit	5% BSA in TBST	ON 4°C	6 min

RPA32 S4/S8 (BethylLab)	32 kDa	1:1000	Rabbit	5% BSA in TBST	ON 4°C	6 min
ORC2 (SantaCruz)	70 kDa	1:1000	Rat	10% milk TBST 0.2%	ON 4°C	6 min
MCM3 (CellSignaling)	100 kDa	1:1000	Rabbit	10% milk TBST 0.2%	ON 4°C	6 min
CDT1 (CellSignaling)	65 kDa	1:1000	Rabbit	10% milk TBST 0.2%	ON 4°C	6 min
E2F1 (SantaCruz)	60 kDa	1:1000	Rabbit	10% milk TBST 0.2%	ON 4°C	6 min
MCM10 (BethylLab)	110 kDa	1:1000	Rabbit	10% milk TBST 0.2%	ON 4°C	6 min
PCNA (SantaCruz)	36 kDa	1:1000	Mouse	10% milk TBST 0.2%	ON 4°C	6 min
PCNA (Chromotek)	36 kDa	1:1000	Rat	10% milk TBST 0.2%	ON 4°C	6 min

8.1.4. Cell lines

Wild-type cell line(s)	
HCT116	RPE1
HCT116 – H2B GFP	RPE1 – H2B GFP
HEK293T - GP	
Aneuploid cell line(s)	
HCT116 5/4	HCT116 5/4 – MCM2S13-27A
HCT116 5/4 – H2B GFP	HCT116 5/4 – MCM2S13-27D
HCT116 5/4 – MCM7	HCT116 5/3
HCT116 5/4 – MCM7S121A	RPE1 3/3
HCT116 5/4 – MCM7S121D	RPE1 7/3
HCT116 5/4 – MCM2	RPE1 21/3
HCT116 5/4 – MCM2S4-5-7A	RPE1 8/3
HCT116 5/4 – MCM2S4-5-7D	RPE1 5/3 12/3 11/3
HCT116 5/4 – MCM7CT	

Cell lines used for this projects; HCT116 and 5/3, 5/4 aneuploids; RPE1 and, 3/3, 7/3, 8/3, 21/3 . In addition, the cell lines expressing also MCM2, MCM7 and relative mutants. The human colorectal carcinoma cell line HCT116 and the tetrasomic cell line HCT116 5/4 were kindly donated by Minoru Koi (Baylor University Medical Centre, Dallas, Texas, USA).

8.1.5. Technical Equipment

Machine	Company
Eppendorf centrifuge 5415R	AH diagnostics, Tilst, Denmark
Trans-Blot Turbo	Bio-Rad, Hercules, USA
PowerPac™ HC High-Current Power Supply	Bio-Rad, Hercules, USA
WTE var 3185	Assistant, Paris, France
Rotina 420R	Hettich, Beverly, USA
Heat Block	Störk Tronic, Stuttgart, Germany
Incubator (Cell lines)	Hera cell, Thermo Fisher Scientific, Waltham USA
Trans-Blot Turbo	Bio-Rad, Hercules, USA
Clean bench (cell culture)	Heraeus Instruments, Hanau, Germany
Water bath	GFL, Burgwedel, Germany
Inverse-Mikroskop AE 2000-Trino	MOTIC, Wetzlar, Germany
Countess II	Thermo Fischer Scientific, Waltham, USA
Ultrospec 3100 pro	Amersham Biosciences, GE Healthcare Life Sciences, Sunnyvale, USA
c500	Azure biosystems, Dublin, USA
GloMay explorer	Promega, Madison, USA
Attune Nxt acoustic focussing cytometer	Life Technologies, Carlsbad, USA
C1000 touch thermal cycler + CFX95 realtime system	Bio-Rad, Hercules, USA
C1000 Thermal cycler	Bio-Rad, Hercules, USA
Epson perfection V370 Photo	Epson, Suwa, Japan
Rotator SB3	Stuart, Stone, UK
Clean bench (bacteria)	Antair, Coahuila, Mexico

Sorvall RC-58 Refrigerated Superspeed Centrifuge	DU Pont, Wilmington, USA
MAXQ 4000	Thermo Fisher Scientific, Waltham, USA
Nanodrop Lite	Thermo Fisher Scientific, Waltham, USA
UV-gel documentation	Intas, Ahmedabad, India
MACS Quant Analyzers	Miltenyi Biotec GmbH, Bergisch Gladbach, Germany
Mass Spectrometry	MPI for Biochemistry, Core Facility, Munich Germany
Confocal microscope observer D	Zeiss, Sweden
LightCycler® 480 System	Roche, Penzberg Germany
LAS-3000 Imaging System	FujiFilm Life Science, USA
Combing system	Genomic Vision, Paris

8.1.6. Software

The graphical analysis of data was carried out with GraphPad Prism 5 (GraphPad Software, La Jolla, USA). The relative densitometric units for quantitative immunoblotting were determined with the help of Image J software (Rasband, W.S., ImageJ, U. S. National Institutes of Health, Bethesda, Maryland, USA, <http://imagej.nih.gov/ij/>, 1997-2015). Data acquired by proteomics were analyzed using the Perseus as part of the MaxQuant Software Package (Cox and Mann 2008). ECDL Certified in Microsoft Office tools (Word™, Excel™ and PowerPoint™), Adobe PhotoShop, ImageJ, FlowJo, Cell Profiler, Slidebook, R software, BioRad PrimerPCR, Adobe Illustrator, Adobe Lightroom, AzureSpot analysis software, BioRad ProSort Software, Visual Basic, AttuneNXT software, Fiber Studio, Weka, ApE, Genome Compiler, Blast.

8.2. Methods

8.2.1. Cell culture

All human cell lines were cultivated in Dulbecco's Modified Eagle Medium GlutaMAX (DMEM) supplemented with 10 % Fetal Bovine Serum (FBS) and 1 % Penicillin/Streptomycin (Pen/Strep). The cells were grown and maintained in the incubator at 37 °C and

5 % CO₂. For passaging, the cells were incubated with 0.25 % Trypsin-EDTA for 5 min, and inactivated by dilution with cultivation media. Human tetrasomic HCT116 cells, called HCT116 5/4, with defined karyotypes derived from near-diploid and chromosomally stable parental HCT116 cell line. HCT116 cells divide approximately every 24 hours, while HCT116 5/4 cells divide slower. Therefore, the HCT116 cells were split one to five and the HCT116 5/4 one to three, every three days. Cells confluency was checked by microscopy

8.2.2. Microscopy

Confocal microscopy was performed using a fully automated Zeiss inverted microscope (AxioObserver Z1) equipped with a MS-2000 stage (Applied Scientific Instrumentation, Eugene, OR), the CSU-X1 spinning disk confocal head (Yokogawa) and LaserStack Launch with selectable laser lines (Intelligent Imaging Innovations, Denver, CO). Image acquisition was randomized and at least 12 non-overlapping fields were captured for each well using a CoolSnap HQ camera (Roper Scientific) and a $\times 40$ air objective (Plan Neofluar $\times 40/0.75$) under the control of the Slidebook software (version 5.0; Intelligent Imaging Innovations).

8.2.3. Cell synchronization by growth factors deprivation

Synchronization of cells was induced by serum starvation. Starvation reduces basal cellular activity, since cells resign from the cell cycle to enter the quiescent G₀/G₁ phase (Pontarin et al., 2011). Cells were grown to 80 % confluency, then the media was changed from full media to serum-free media (DMEM and 1 % (v/v) Pen/ Strep) and incubated for 48 h. To release the cells from G₀/G₁ phase, the serum-free media was replaced by cultivation media (time point 0 hours). Cells were pelleted in the centrifuge at 1400 rpm for 5 min and the culture medium was discarded with a vacuum pump. The cells for cDNA synthesis were washed in 1 ml of PBS and spun down. The buffer was discarded and cell pellets were stored at -20 °C. Cells for cell cycle analysis were proceeded according to section 4.3.2.

8.2.4. Cell synchronization in mitosis

I split cells in three different flasks for each cell line (one for each treatment), and I make grow cells for two days till confluence is around 60-70%. Then I treat cells differently:

- Starvation: I replace the media in the flasks containing HCT116 and HCT116 5/4 with DMEM without FBS, and I leave for 72h.

- Nocodazole: I replace medium with fresh complete DMEM containing Nocodazole [100 ng/mL] and I leave for 16h in incubator at 37 °C and 5% CO₂. Then I check at the microscope whether cells have the typical round shape of cells being in metaphase; I wash two times with fresh complete DMEM and then I shake off cells hitting flask.
- Hydroxyurea: I replace medium in flask with one containing HU [2 mM] and I leave for 24h in incubator at 37 °C and 5% CO₂.

After each of those treatment, I trypsinize cells, I count them and for time point 0h I collect 1×10^6 in two different Eppendorf 2 mL tubes (one for qPCR and the other for Western Blot), I collect also 500×10^3 cells for FACS analysis. I spin down cells in microcentrifuge for 5 min at 1600 rpm, and I wash once with PBS, and then I store cells at -20 °C (pellets for qPCR and WB); while I fix cells for FACS analysis with 1 mL of cold EtOH 70%, I rinse 2 times in PBS then I add 1mL of PBS supplemented with 1X PI and RNase enzyme 1:1000. I store it at 4 °C. For time point 4h I seed 2×10^6 cells in 10 cm dish and I leave in incubator at 37 °C and 5% CO₂. After I collect them like as described up.

8.2.5. Transfection

The reverse transfection of human cell lines with pcDNA3.1+ plasmids was carried out using an electroporation method. The transfection was done according to the Amaxa® Cell Line Nucleofector® Kit V (HCT116) (Lonza, Basel, Switzerland), using the same cell numbers for HCT116 and HCT116 5/4. DMEM supplemented with 10 % FBS and 1 % Penicillin/Streptomycin was removed after 24 hours and experiment dependent replaced by DMEM supplemented with 10 % FBS and 1 % Penicillin/Streptomycin plus 0.8 mg/ml G418 (InvivoGen, San Diego, USA). The transfected cells were harvested five days after electroporation and counted. Similar amounts of different transfected cells were collected for protein preparation (whole cell lysate and subcellular protein fractionation). In addition, equal numbers of cells were reseeded for later flow cytometry analyses. Cells for protein preparation were pelleted in the centrifuge at 1400 rpm for 5 min and the culture medium was discarded with a vacuum pump. The cells were washed in 1 ml of PBS and spun down. The buffer was discarded and cell pellets were stored at -20 °C.

8.2.6. Chromosome transfer

Donor cell line (A9 or K1-9, mouse background, carrying specific human chromosome) on four 150 mm cell culture plates, in growth medium (DMEM + 10% FCS and 400 U/mL Hygromycin B for A9 cells or Ham's F12 + 10% FCS and 500 U/mL Hygromycin B for K1-9 cells). Recipient cell line (fibroblasts (E7 and hTert) or myoblasts (E6/E7 and hTert) on one 100 mm plate in growth medium.

Bullets for enucleation: custom made by jigsaw from 150 mm TC plates to fit reusable centrifuge tubes in pairs. Centrifuge tubes: Nalgene 50 mL, round-bottom, polycarbonate (3117-0500). Filters: Whatman Cyclopure, 25 mm 5 μ M (70612513), Whatman Nuclepore 25 mm 8 μ M (110614). Filter holders and Gaskets: Millipore Swinnex 25 mm filter holder and gasket (SX0002500, SX0002501) Hygromycin B (Caibiochem 400051). Colchicine (Demecolcine, Sigma D1925). 10 μ g/mL sterile solution. Store 4 °C. Con A (Concanavalin A, Sigma C2631). Powder, store desiccated at 4 °C. WSC (1-cyclohexyl-3-(2-morpholinoethyl) carbodiimide metno-p-toluenesulfonate, Sigma C1011). Powder, store desiccated at -20 °C. Cytochalasin B (Sigma C6762). Powder, store protected from light at 4 °C. Resuspend at 10 mg/mL in DMSO. Store at -20 °C. Phytohemagglutinin P (PHA-P) (Difco 3110-56-4). Store powder at 4 °C. This powder is 50% PHA-P, i.e. 100 mg of powder contains 50 mg of PHA-P. Working solution of 4 mg/10mL serum-free medium, filter sterilize. Store aliquoted at -20 °C Polyethylene glycol (PEG) 1500

Method:

- i. Thaw the specific HCT116 or RPE1 recipient cell line, and culture to reach 80%-90% confluency of a 100 mm plate the day before the transfer.
- ii. Thaw A9 mouse donor cell line carrying the extra copy of human chromosome, 7-10 days before the transfer and culture as following: grow without selection in passage one, then add 800 U/ml hygromycin B for the next three passages, finally 400 U/mL hygromycin B. Three 150 mm plates are needed at 80%-90% confluency the day before the transfer.
- iii. Two days before transfer, micronucleation of donor cells is obtained by adding 150 μ L colchicine per 25 mL media per plate for 48 hours. Microenucleation can be monitored by observation under phase contrast.
- iv. Five bullets are needed per plate of donor cells. Bullets preparation is done as following:
 - a) Sterilization: Sterilize bullets in 70% EtOH overnight, and dry them in the hood by tilting on the edge of a 150 mm plate.

- b) Coat the bullets with ConA/WSC: prepare 20 mL solution for 15 bullets: 300 mg Con A add 20 mL 0.9% NaCl. Dissolve in 37°C water bath for 30 minutes. Filter using 0.45 µm filter, then 0.2 µm filter. Then, prepare WSC by dissolving 1500 mg WSC add 20 mL 0.9% NaCl. Sterilization by filtering as per the ConA preparation.
- v. Place bullets flat in plates. Pipette WSC solution over the surface of each bullet and ensure a complete coverage. Remove WSC, repeat with ConA and remove it. Leave bullets covered in hood for 1- 2 hours. Wash the bullets twice with 20mL sterile PBS, rocking dish back and forth to wash. Coated bullets can be stored in PBS overnight at 4°C or used right away.
- vi. Enucleation medium: In a sterile glass bottle, prepare 200 mL of DMEM medium supplemented with 10% FCS and 10 µg/mL cytochalasin B (stock is 10mg/mL so add 300 µL to 300 mL of serum-free medium). Enucleation medium can be reused four times, if filtered after every usage and stored in dark at 4 °C.
- vii. Material sterilization by autoclaving the Millipore Swinnex filters three 5µm and three 8µm filters, holders and gaskets and the Nalgene polycarbonate centrifuge tubes, 1 for every 2 bullets.
- viii. For the chromosome transfer: prewarm a centrifuge with Sorvall SS-34 rotor up to 34 °C (not more than 37 °C), by spinning at full speed for one hour. Warm the solutions PBS, Trypsin-EDTA 1x, DMEM + 10% FCS, DMEM to 37 °C in water bath.
- ix. The procedure: Trypsinize the donor cells and pool the three plates in 30 mL medium w/FCS. Pellet the cells in 50 mL Falcon tube by spinning down at 1100 rpm for 5-10 minutes. Resuspend the cells thoroughly in 15 mL medium w/FCS. Arrange the bullets on the plate preventing the contact. Aspirate the excess of PBS from a bullet and overlay it with 1 mL of resuspended cells. Let the cells attach for approximately 15 minutes in the hood. Monitor under microscope. After the cells were attached to the surface, bullets were centrifuged at 27,000g for 30 min at 30–34 °C in DMEM supplemented with 10 µg ml⁻¹ cytochalasin B. Cell pellets were resuspended in serum-free DMEM and filtered to clear suspension from mouse cells. Filtered microcells were mixed with phytohaemagglutinin (PHA-P) and added to the recipient cell lines: HCT116 or hTERT-RPE1 cell lines (Stingele, 2013). Fusion of microcells with the recipient cells was facilitated by polyethylene glycol 1500 treatment. All cells were passed every three days.
- x. Cells containing the additional human chromosome were selected in DMEM GlutaMax (Gibco) medium supplemented with 400 µg ml⁻¹ G418 or with hygromycin.

The cell lines were obtained because of a spontaneously occurring aberration. Cells were grown in supplemented with 10% fetal bovine serum and 5% penicillin–streptomycin under standard conditions.

- xi. Single colonies were collected by placing cotton disk embedded of trypsin per single colony. Then, clonal populations are expanded in series of cultures in 12 and 6 well plates and further in 100 mm dishes.

Chromosome transfer is checked by chromosome spreads combined with FISH.

Clonal populations that gained the expected extra chromosomes were further expanded for three passages and a minimum of 5 vials were stored in liquid nitrogen. Simultaneously, a sample was subjected to SNP-array analysis or array comparative genomic hybridization (aCGH). Only cells with fully analyzed karyotypes were used for the experiments.

8.2.7. Cell cycle analysis by flow cytometry

For analysis of cells by flow cytometry, each sample was incubated with 5-ethynyl-2'-deoxyuridine (EdU) for 30 min before harvesting, followed by fixation and permeabilization using Fix-Perm. Cell numbers were adjusted and the samples incubated with Click reaction for 30 min in the dark. After the last washing step prior to analysis using flow cytometry, the cells were resuspended in PBS with RNase (RNase Zap, Invitrogen, Carlsbad, USA) and 4',6-Diamidino-2-Phenylindole, Dihydrochloride (DAPI).

8.2.8. Isolation of RNA, cDNA synthesis and qRT-PCR

RNA from mammalian cells was purified using the “RNeasy Mini Kit” (Qiagen, Venlo, Netherlands) according to the manufacturer’s instructions to obtain high-purity RNA. Prior to cDNA synthesis, the RNA was treated with DNase (recombinant DNase, Roche, Basel, Switzerland) and stored at -80 °C. The synthesis of cDNA from RNA was carried out using the “Transcriptor First Strand cDNA Synthesis Kit” (Roche Diagnostics, Basel, Switzerland) with oligo18 primers. The synthesis was performed according to the manufacturer’s protocol, using 0.6 - 1 µg of RNA as template. In table 5 the primer sequences that have been used for qRT-PCR analysis of mRNA expression levels is shown. The specificity of the product amplification was confirmed in each run by analyzing the melting curve. Normalization was carried out using the constitutively expressed "housekeeping" gene of the ribosomal protein L27 (rp127), whose mRNA quantity is not influenced by the cell cycle (Jain et al., 2006).

Additionally, a spiked external standard was used (TataaBiocenter) for normalization. The evaluation of mRNA expression levels was carried out according to the mathematical model published by (Pfaffl, 2001). The PCR mix was pipetted according to the SYBR® Green Master Mix (Bio-Rad, Hercules, USA) protocol: qPCR programme (final volume 20 µl):

Process	Time	Cycle
Preincubation	98°C for 30 seconds	
Denaturation	95°C for 5 seconds and 57°C for 20 seconds	39x
Amplification	90°C for 30 seconds and 60°C for 30 seconds and 60°C for 31 sseconds	
Plate read		
Melting curve	60°C for 5 seconds (+0,5°C/cycle) Ramp rate: 0.5°C/seconds	70x

8.2.9. Cell lysis

To gain the whole cell lysate, the cell pellets were thawed on ice and re-suspended in 40 µl of RIPA buffer. Cell lysis was performed via sonication for 15 min. In order to remove the cell debris, the reaction tubes were centrifuged at 13600 rpm and 4 °C for 6 minutes. The supernatant (40 µl) was transferred into fresh reaction tubes and a volume of 1 µl taken from each sample was used to determine the protein concentration via Bradford protein assay. The protein lysates were denatured by the addition of 13.3 µl of 4 x Lämmli buffer and subsequent boiling at 95 °C for 5 min. The protein lysates were briefly centrifuged and stored at -20 °C.

To receive the different sub cellular fractions (cytoplasmic, nucleoplasmic and chromatin-bound), cells were prepared according to the “Subcellular Protein Fractionation Kit for Cultured Cells” (Thermo Fisher Scientific, Waltham, USA). The protein lysates were briefly centrifuged and stored at -20 °C.

8.2.10. SDS Page

The concentration of protein lysates was adjusted by ponceau staining intensities of a test run. Samples were equilibrated to even dilution with by adding appropriate volumes of Lämmli buffer (1x), and they were boiled at 95°C for 10 min. A volume of 15 µl/well per sample was used. The samples were loaded onto 12.5 % SDS gels. The proteins were first separated at 80 V and 40 mA for 15 min and then at 160 V and 93 mA for 50 minutes. The “Precision Plus Protein All Blue Standard” (BioRad, Hercules, USA) was loaded as a marker for size comparison of the molecular weight.

8.2.11. Towbin and Bjerrum Schafer-Nielsen Buffer (semidry transfer)

The most common transfers are from SDS-PAGE gels using the buffer systems originally described by Towbin (1979). Standard Towbin buffer contains 25 mM Tris, 192 mM glycine, pH 8.3, 20% methanol and, occasionally, 0.025–0.1% SDS. A buffer similar in composition to the standard Towbin buffer is the Bjerrum Schafer-Nielsen buffer (48 mM Tris, 39 mM glycine, pH 9.2, 20% methanol), which was developed for use in semi-dry applications. For experiments, SDS-Page was performed by using the callical Towbin and a modified version of Bjerrum Schafer-Nielsen with adjusted pH 10.0.

8.2.12. Cells Fractionation by Thermo Kit

Cell were fractionated by Subcellular Protein Fractionation Kit for Cultured Cells (Thermo Scientific). The protocol can be found by the link: https://assets.thermofisher.com/TFS-Assets/LSG/manuals/MAN0011667_Subcellular_Protein_Fraction_CulturedCells_UG.pdf. Additionally, I supplemented each buffer with 1X PhosphataseStop (Roche).

8.2.13. Cells Fractionation by CSK

CSK Buffer: 10 mM PIPES, 100 mM NaCl, 3 mM MgCl₂, 300 mM Sucrose, 1X Phosphatease inhibitors, 1X Protease Inhibitors, 0.2% Triton X.

Others: Cold 1X PBS, 20% TCA, ice cold Acetone, 1X Laemly buffer

- **In Eppendorf tube:**

Seed 1×10^6 cells/dish (10 cm^2); Working on ice, rinse in 2 mL PBS, scrape and collect half in 1.5 mL Eppendorf tube (now these will be the Whole Cellular Extract or WCE) and the rest in another 1.5 mL eppendorf tube (this will be triton soluble and chromatin bound fractions (Sur/Chr), Centrifuge at 1500 rpm for 5 min, throw the surnatant;

- I. **WCE:** lysate the pellet pipetting 100 μL of 1X lamely buffer, boil at 95 °C for 10 min.
- II. **Sur/Chr:**
 - a) add 1 mL CSK buffer, centrifuge at 13000 rpm for 10 min;
 - b) collect supernatant: this is Sur fraction, whereas the pellet is Chr fraction;
 - i. *Chr*: dissolve pellet pipetting 100 μL of 1X lamely buffer, boil at 95 °C for 10 min.
 - ii. *Sur*: add 1 mL 20% TCA centrifuge at 4 °C 13000 rpm for 10 min, throw supernatant, wash pipetting 1 mL of cold Acetone, spin at 4 °C 13000 rpm for 10 min, throw the supernatant and dry the pellet at vacuum centrifuge for 2 min, resuspend the pellet in 100 μL of 1X lamely buffer (it would become yellow due to acid pH, thus add 1-2 μL Tris base to restore it) and boil at 95 °C for 10 min.

- **In 6 cm dish:**

Seed 1×10^6 cells/dish (10 cm^2), 1 dish for each WCE and 1 for each Sur/Chr; Working on ice, rinse in 2 mL PBS,

- I. **WCE:** scrape and collect half in 1.5 mL Eppendorf tube (now these will be the Whole Cellular Extract or WCE), centrifuge at 1500 rpm for 5 min, throw the supernatant and lysate the pellet pipetting 100 μL of 1X lamely buffer, boil at 95 °C for 10 min.
- II. **Sur/Chr:**
 - a) add 1 mL CSK buffer directly in dish and shake on ice for 5 min;
 - b) collect supernatant: this is Sur fraction, whereas the pellet is Chr fraction;
 - i. **Chr:** dissolve pellet pipetting 100 μL of 1X lamely buffer, boil at 95 °C for 10 min.
 - ii. **Sur:** add 1 mL 20% TCA centrifuge at 4 °C 13000 rpm for 10 min, throw supernatant, wash pipetting 1 mL of cold Acetone, spin at 4 °C 13000 rpm for 10 min, throw the supernatant and dry the pellet at vacuum centrifuge for 2 min, resuspend the pellet in 100 μL of 1X lamely buffer (it would become yellow due to acid pH, thus add 1-2 μL Tris base to restore it) and boil at 95 °C for 10 min.

8.2.14. Cell fractionation for Mass spectrometry

Cells were lysed and fractionated into cytoplasm, soluble nuclear material, and chromatin after the procedure of Mendez and Stillman (28). Cells were resuspended (4×10^6 cells/ml) in buffer A (10 mM Hepes, pH 7.9/10 mM KCl/1.5 mM MgCl₂/0.34 M sucrose/10% glycerol/1 mM DTT/Roche protease inhibitors/0.1% Triton X-100) and incubated on ice for 5 min. Nuclei were collected (P1) by low-speed centrifugation ($1,300 \times g$ for 5 min at 4°C). P1 fraction was washed once again in buffer A and then lysed in buffer B (3 mM EDTA/0.2 mM EGTA/1 mM DTT/Roche protease inhibitors) and incubated on ice for 30 min. Nuclei were separated into soluble fraction (S3) and insoluble chromatin by centrifugation ($1,700 \times g$ for 5 min at 4°C). The final chromatin fraction (P3) was washed again in buffer B and centrifuged under the same conditions. P3 fraction was resuspended further in Laemmli buffer and sonicated for 10 sec.

- Buffer A (10 mM HEPES pH 7.9, 10 mM KCl, 1.5 mM MgCl₂, 340 mM sucrose, 10% (v/v) glycerol and 0.1% Triton X-100)
- Buffer B (10 mM HEPES pH 7.9, 3 mM EDTA and 0.2 mM EGTA)
- Buffer A* (10 mM HEPES pH 7.9, 10 mM KCl, 1.5 mM MgCl₂, 340 mM sucrose, 0.1 (v/v) Triton X-100 and benzonase (50 units/ml, Novagen).

8.2.15. Immunoblotting and quantification of band intensities

The SDS gels were equilibrated in Bjerrum Schafer-Nielsen transfer buffer for 5 minutes and protein transfer onto nitrocellulose membranes (Amersham Protran Premium 0.45 NC, GE Healthcare Life Sciences, Sunnyvale, USA) was carried out according to Trans-Blot® Turbo™ (semidry blotting) (BioRad, Hercules, USA) protocol for high molecular weight proteins. The nitrocellulose membranes were stained in ponceau solution for 5 minutes and washed with distilled water before scanning the membrane. This step serves as a quality control for successful protein transfer to the membranes and the estimation of loading. The membranes were incubated in blocking solution (TBS-T supplemented with 10 % skim milk) for 1 hour to prevent unspecific binding of antibodies before the primary antibody solution was applied overnight at 4 °C. The membranes were washed three times for 7 min with TBS-T before incubation with the secondary antibody conjugated to horseradish peroxidase (HRP) for one hour at room temperature. The membranes were washed to remove unbound secondary antibodies before detection of the enhanced chemiluminescence signal from HRP-catalyzed oxidation of luminol. The membranes were developed with the help of ECL

solution and imaging was performed using the Azure c500 system (Azure Biosystems, Dublin, USA). The intensities of protein bands were quantified using ImageJ software and obtained relative densitometric units were normalized to ponceau staining, serving as a loading control. In a further step of analysis, the normalized values were compared to the negative control, an empty plasmid transfection (pcDNA3.1+) in wild-type cells. The reference to a common negative control that values from individual experiments and different biological replicates can be used for comparison between independent experiments.

8.3. Bacteria work flow

For transformations and the preparation of glycerol-stocks the chemical competent *E. coli* strain XL1blue was used endA1 gyrA96(nalR) thi-1 recA1 relA1 lac glnV44 F'[:Tn10 proAB+ lacIq Δ(lacZ)M15] hsdR17(rK- mK+).

8.3.1. Culture medium and antibiotics

The used medium was Luria-Bertani medium (LB-medium) (Carl Roth) supplemented with ampicillin (Stock 100 mg/ml in 50 % EtOH/ 50 % MQ) end concentration 100 µg/ml. For preparation of agar plates 1.5% w/v of agar was added to the medium before autoclaving.

8.3.2. Heat shock transformation and glycerol-stocks

The *E. coli* XL1 blue strain was used. After cells were thawed, 1 µl of plasmid DNA, for retransformation, or 10 µl of ligation mixture, or the whole of QuickChange II reaction mix was added. Cells were then incubated for 30 min on ice, followed by a heat shock for 45 sec. at 42 °C. After cells were cooled down on ice, 600 µl LB-medium was added and cells were incubated for 45 min at 37 °C under agitation at 700 rpm. The cells were plated onto a LB plate containing the respective antibiotics (100 µg/ml Ampicillin).

The cells then grew over night at 37 °C. A single colony was transferred to 4 ml LB medium containing appropriate selective marker and incubated over night at 37 °C under continuous agitation of 700 rpm. Finally, 400 µl 60 % glycerol and 600 µl culture were added in a specific cryotube and stored at -80 °C.

8.3.3. Preparation of plasmid DNA

Plasmid	Manufature	Reference
pcDNA™ 3.1 (+) Mammalian Expression Vector	Invitrogen™	Référence: V79020
pcDNA™ 3.1 (-) Mammalian Expression Vector	Invitrogen™	Référence: V79520
pBABE-neo	Addgene	Plasmid #1767
pcDNA 3-MCM7	University ?	

Plasmid DNA for DNA work was isolated by using the AccuPrep® Plasmid Mini Extraction Kit (Bioneer, Smith Parish, Bermuda). Plasmid DNA for transfection of human cells was extracted by Plasmid Maxi Kit (Qiagen, Venlo, Netherlands). According to the instructions supplied by the manufacturer. All plasmid elations were done with nuclease-free water (Thermo Fisher Scientific, Waltham, USA).

8.4. Molecular biological methods

Polymerase chain reaction (PCR) to generate vector carrying *mcm2* gene (pcDNA3.1+_MCM2), end extending PCR was performed on the pBABE(neo)_MCM2 plasmid. Therefore, we designed primers that insert overhangs on 5' and 3'-end of the MCM2 gene. The PCR was carried out using 1x Phusion PCR buffer (NEB), [0.2 mM] dNTPs (NEB), 0.5 µM forward and reverse primers and 0.02 U/µl Phusion polymerase.

Initial denaturation:	98°C for 30 seconds	
Denaturation:	98°C for 10 seconds	
Primer annealing:	58°C for 30 seconds	30x
Elongation:	72°C for 2.5 minutes	
Final elongation:	72°C for 10 minutes	
Hold	4 °C for ∞	

The correct size of the PCR products was confirmed on a 2 % agarose gel, which was run at 100 V for about 1 h. The correct bands were cut out and gel extraction was performed using the QIAquick gel extraction kit (Qiagen, Venlo, Netherlands).

8.4.1. QuikChange mutagenesis

Site directed mutagenesis gave us the opportunity to directly create the MCM2-phospho mutant constructs. The QuikChange mutagenesis was carried out according to the instructions of QuikChange II Site-Directed Mutagenesis Kit. The primers were designed according to the script, Phusion® High-Fidelity DNA Polymerase was used (NEB). Followed up by PCR clean up with QIAquick gel extraction Kit (Qiagen, Venlo, Netherlands) and Dpn1 (NEB, Ipswich, USA) digestion. In the table are oligos used for the mutagenesis.

Name	Oligonucleotides
MCM2_S13_A_FWD	CCTTCACCATGGCATCCGCCCCGGCCCAGCGTCGG CG
MCM2_S13_A_REV	CGCCGACGCTGGGCCGGGGCGGATGCCATGGTGA AGG
MCM2_S13_D_FWD	CCTTCACCATGGCATCCGACCCGGCCCAGCGTCGG CG
MCM2_S13_D_REV	CGCCGACGCTGGGCCGGGTCGGATGCCATGGTGA AGG
MCM2_S27_A_FWD	GATCCTCTCACCTCCGCCCCTGGCCGAAGCTCC
MCM2_S27_A_REV	GGAGCTTCGGCCAGGGGCGGAGGTGAGAGGATC
MCM2_S27_D_FWD	GATCCTCTCACCTCCGACCCTGGCCGAAGCTCC
MCM2_S27_D_REV	GGAGCTTCGGCCAGGGTCGGAGGTGAGAGGATC
MCM2_Fwd	CGTGATGCTGGAGAGCTT
MCM2_Rev	CCATGCCATCTCCAATGA
pcDNA(+)_Frw	GGCTACTAGAGAACCCACTG
pcDNA(+)_Rev	GAAAAGTGCCACCTGACGTC
MCM2_1.2	GCTCCTGTATGACAGCGATG
MCM2_2.2	ACATCCATGTCCGCATCT CC
MCM2_2	AGGATGGAGAGGAGCTCAT
MCM2S53downstream_Rev	
v	TCATAGGCGTCCAGCTCTG
T7 promoter_Rev	CCTATAGTGAGTCGTATTA
T7 promoter_Fwd	TAATACGACTCACTA
CMV	CGCAAATGG GCG GTA GGC GTG

pcDNA3.1(+)	
_BamH1_Frw	TAAGCTTGGTACCGAGCTCG
vecMCM2_1	CCAAAATCAACGGGAC
MCM2_Fwd	CGTGATGCTGGAGAGCTT
MCM2_7	GAGTTGCGTATTCAGGCT
MCM2_1	CTATGGCGGAATCATCGG
MCM2_4	CAGAACCAGCATCCATAGGG
MCM2_3	GGCCAAGAAGGACAACAAGG
MCM2_6	AGCAGTTCTGAAGCCCTATG
MCM2_5	AATCTATGGCGACAGGCAGC
MCM2BamH1upstream_Fwd	TACATCTACGTATTAGTCATC
pcDNA3.1(+)_EcoRI-Rev	CTGTGCTGGATATCTGCAGAATT
MCM7 S121A FWD	GGACCCTGGGATGGTCCGAGCCCCCAGAAC-
MCM7 S121A REV	GTTCTGGGGGGCTCGGACCATCCCAGGGTCC
MCM7 S121D FWD	GACCCTGGGATGGTCCGAGACCCCCAGAAC
MCM7 S121D REV	GTTCTGGGGGTCTCGGACCATCCCAGGGTCC-
mcm7_1	TCACTCATTCTAGGCCCGCAC
mcm7_2	GATGCCGTACAAGAGCTGCTG
mcm7_3	CCGATCCAGTCTCCCACTTTC
mcm7_4	AACCTACCTGGAAGCCCATCG
mcm7_5	GGAGAACTGACCTTAGAGGGTGG
mcm7_6	GCAGCATACTGGAGATGAGG
mcm7_7	GTCTGATTCCAGCCTGCTTGC
HA Fwd	TAGTCAGGAACATCGTATGG

8.4.2. DNA extraction from agarose gels

Amplified DNA fragments of a specific size were cut off with a scalpel after separation via agarose gel electrophoresis. For extraction of the fragments the QUIAquick gel extraction Kit (Qiagen, Venlo, Netherlands) was used according to the instructions supplied by the manufacture.

8.4.3. Digestion and ligation of plasmid DNA

For the digestion of plasmid DNA, 500 ng of the plasmid DNA were incubated with the specific restriction enzyme (NEB, Ipswich, USA). Furthermore, the reaction mix contained 2 μ l of the appropriated buffer and was fill up with Milli-Q-water to a final volume of 20 μ l. The digestion mix was incubated for 1 h and 37 °C. Subsequently, the fragments were separated by agarose gel electrophoresis and correct fragment sizes were verified. The correct bands were cut out and gel extraction was performed using the QUIAquick gel extraction kit (Qiagen, Venlo, Netherlands). DNA fragments were ligated using the T4 ligase (NEB, Ipswich, USA) according to the protocol.

8.4.4. DNA sequencing

The DNA sequencing was performed by the GATC Biotech (Konstanz, Germany). The resulting sequences were analyzed using NCBI (BLAST).

8.5. Proteomics

8.5.1. Data pre-processing

In the first step the unnecessary or incorrect protein identifications were removed from four different main data sets, by filtering out protein identifications classified as “Only identified by site”, contaminants and reverse. Next the expression values were transformed into Log2. In the next step biological replicates were grouped for further analysis (the three biological replicates for one timepoint). To increase the confidence of the data the LFQ (label free quantification) data sets were filtered for a minimum 3 valid values per group. The STY data set was filtered for 3 valid values separately in every single time point. Overview of the whole workflow is shown in figure 5.

Parameters for clustering and statistical analysis are specified in chapter 6.2 under each figure.

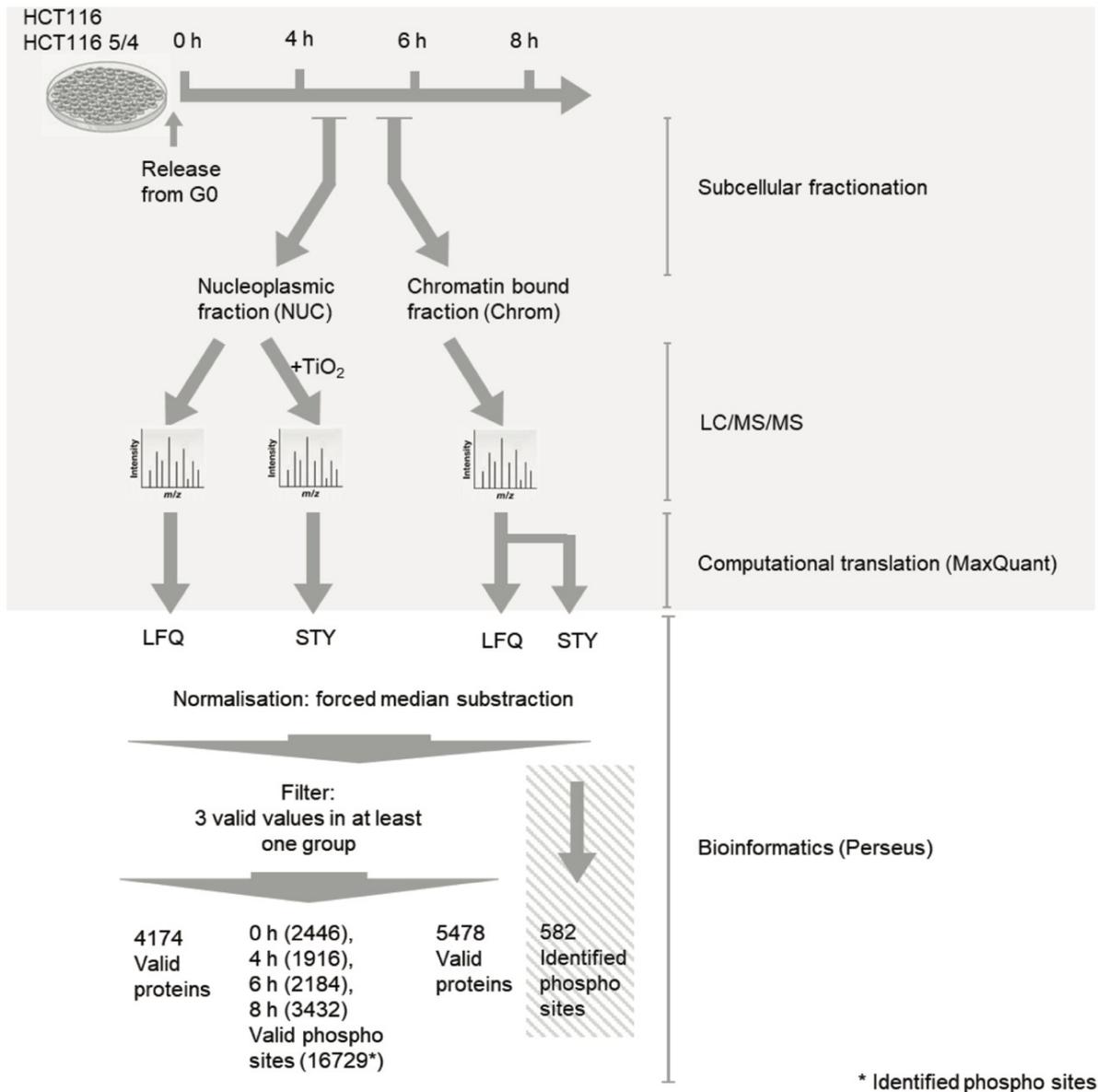


Figure 36: Proteomics workflow of serum starvation experiment, followed by subcellular fractioning.

Mass spectrometry run of nucleoplasmic fraction samples, nucleoplasmic phosphor-peptide enrichment samples and chromatin bound fraction of HCT116 and HCT116 5/4 cells was performed, followed by computational translation of MS-data by MaxQuant. First step of data analysis in Perseus was normalization by forced median subtraction. Second, data filtering was performed (Tyanova et al., 2016). In a next step the data was filtered for three valid values in at least one group. The missing values in the LFQ data were replaced by random numbers from the normal distribution.

9. Supplementary

S1: Cell cycle analyses by EdU staining. A) FACS analyses of HCT116 and derivative aneuploid cells. EdU is on the y axes: the blue boxes represent, while the EdU positive cells, red boxes the EdU negative. DNA is stained by DAPI on the x axes. B) Quantification by histogram of the FACS analyses of HCT116 and derivative aneuploid cells

S2: Differences of the pre-RC levels in time points in more cell lines: A-C) western blot of the different fractions in HCT116 and HCT116 3/3 synchronised cells by starvation and then released at different time points; D-F) western blot of the different fractions in RPE1, RPE1 3/3 and RPE1 21/3 synchronised cells by starvation and then released at different time points; G-H) western blot of the cytoplasmic and nucleoplasmic fraction of cells synchronised by nocodazole [100 ng/mL] for 16h and plated after shake-off and collected at different time points. I-J) western blot quantification for HCT116 and the 5/4 aneuploid derivative cells, n=3.

S3: Trends of the seven-cluster identified by mass spectrometry analyses: B) Nucleoplasmic fraction hierarchical clustering of 4174 proteins calculated by Euclidian distances. Missing values are substituted by imputation before z-scoring the data and normalised to the median value of the log₂ intensities of each protein profile (the green marked cluster contains the proteins of the MCM2-7 complex); D) Chromatin bound fraction hierarchical clustering of 5478 proteins calculated by Euclidian distances. Missing values are substituted by imputation before z-scoring the data and normalised to the median value of the log₂ intensities of each protein profile (the green marked cluster contains the proteins of the MCM2-7 complex); E) time dependent LFQ profile of the ORC1-6 cluster in the chromatin bound fraction.

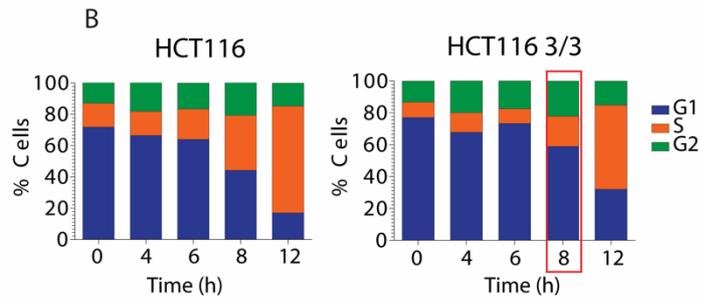
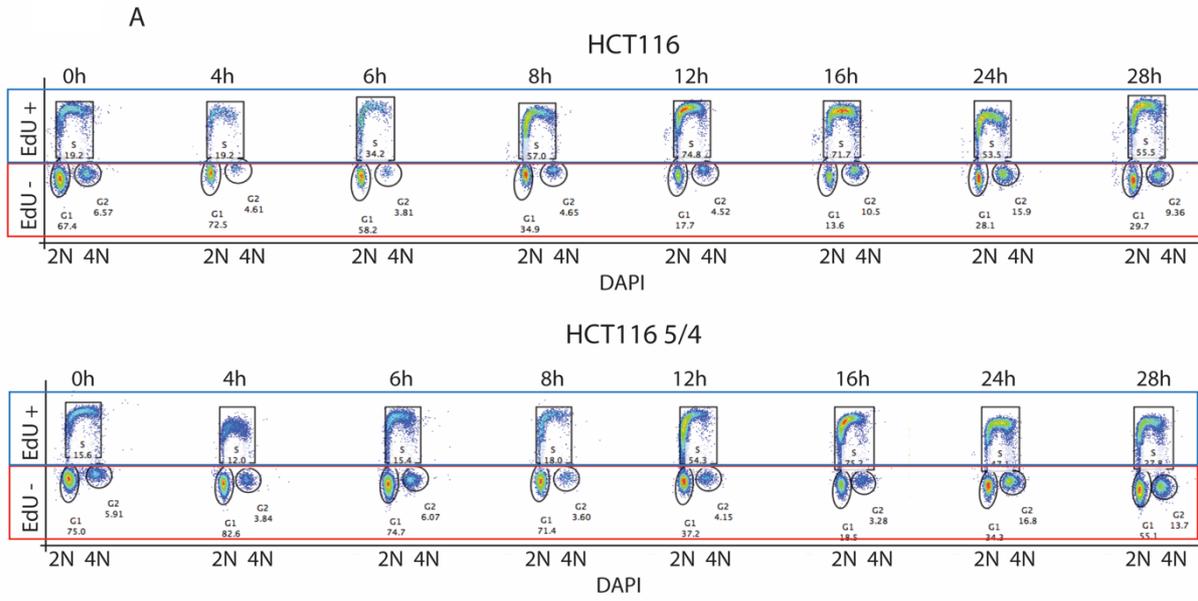
S4: pre-RC and MCMs are stable for all the G1: western blot of whole cell lysate collected at different time point after asynchronous cells have been treated by cyclohexamide and/or MG132; A) HCT116 stably expressing H2B-GFP and derivative 5/4 aneuploid cells; B) HCT116 stably expressing H2B-GFP and derivative 3/3 aneuploid cells; C) RPE1 derivative aneuploid cells. Western blots of the chromatin bound fraction of synchronized cell and treated by cyclohexamide and/or MG132 four after cells were released and quantification of the membrane HCT116 and HCT116 3/3 for D) time point four hours after and E) time point six hours after.

S5: MCM7 overexpression and MCM2 downregulation: A) quantification of the membrane for the WCE samples for MCM7 levels in cell overexpressing stably that subunit and the quantification of the blot; B) quantification of membrane of the chromatin bound fraction in order to discriminate the functional overexpression of MCM7; C) western blot of cells overexpressing MCM7.

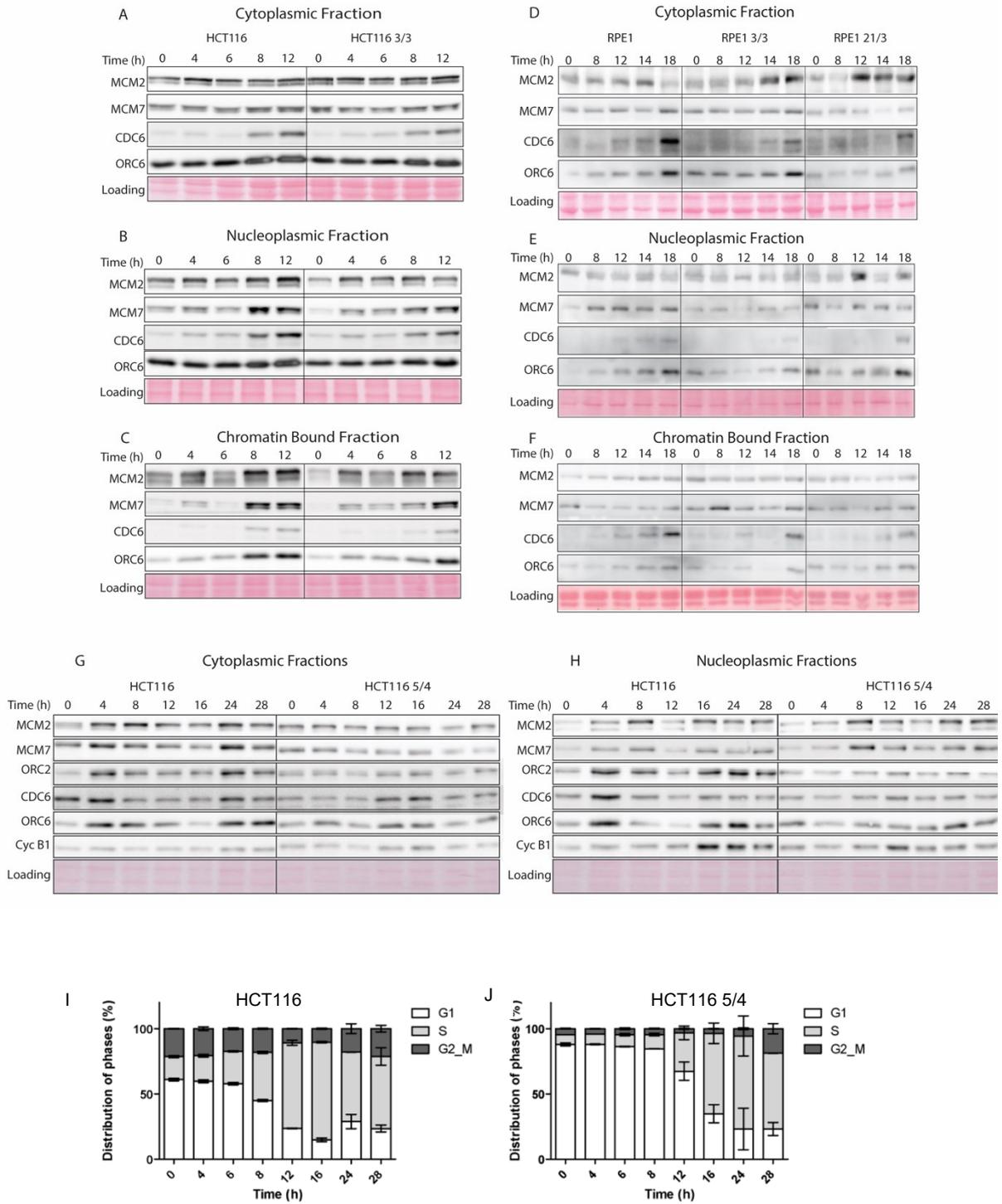
S6: Checkpoint regulators are affected in aneuploid cells: A) check point proteins levels in time point for various cell lines, with and without H2B-GFP expression; B) MCM2-7 and CDKs levels in nucleoplasmic fraction, quantified by LFQ mass spectrometry; C) clonogenic of cells treated with different kinase inhibitors, at various concentrations and for thirteen days.

S7: Phosphorylation sites are affected in aneuploid cells: A) table of the MCM2-7 phospho-sites; B) Maps of MCM2 and MCM7 mutants; C) Western blot of MCM2 mutants: upper left WCE, upper right Cytoplasmic fraction, lower left nucleoplasmic fraction and lower right chromatin bound fraction; D) WCE of the MCM7 mutants with and without aphidicolin [0.3 μ M].

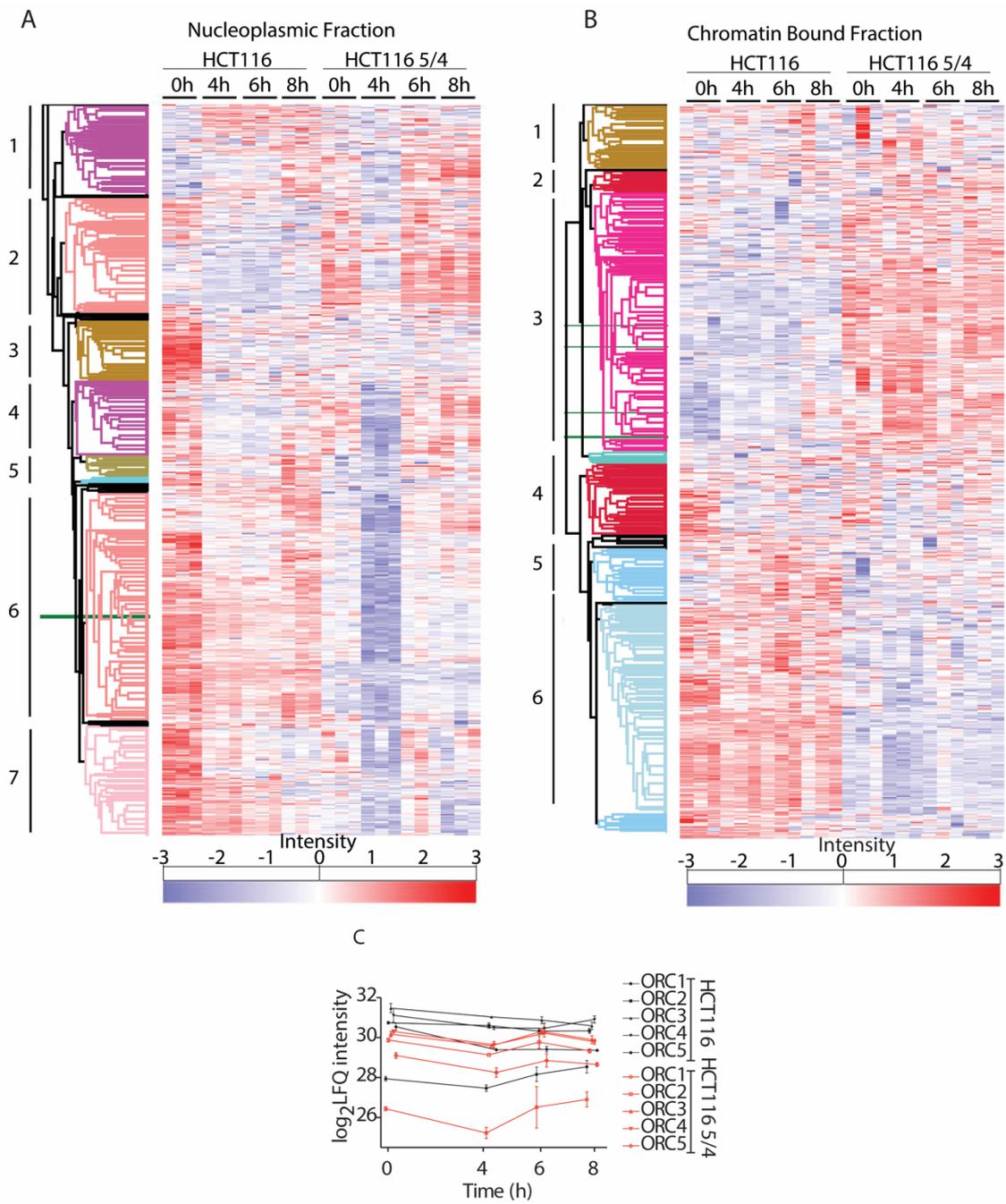
S1

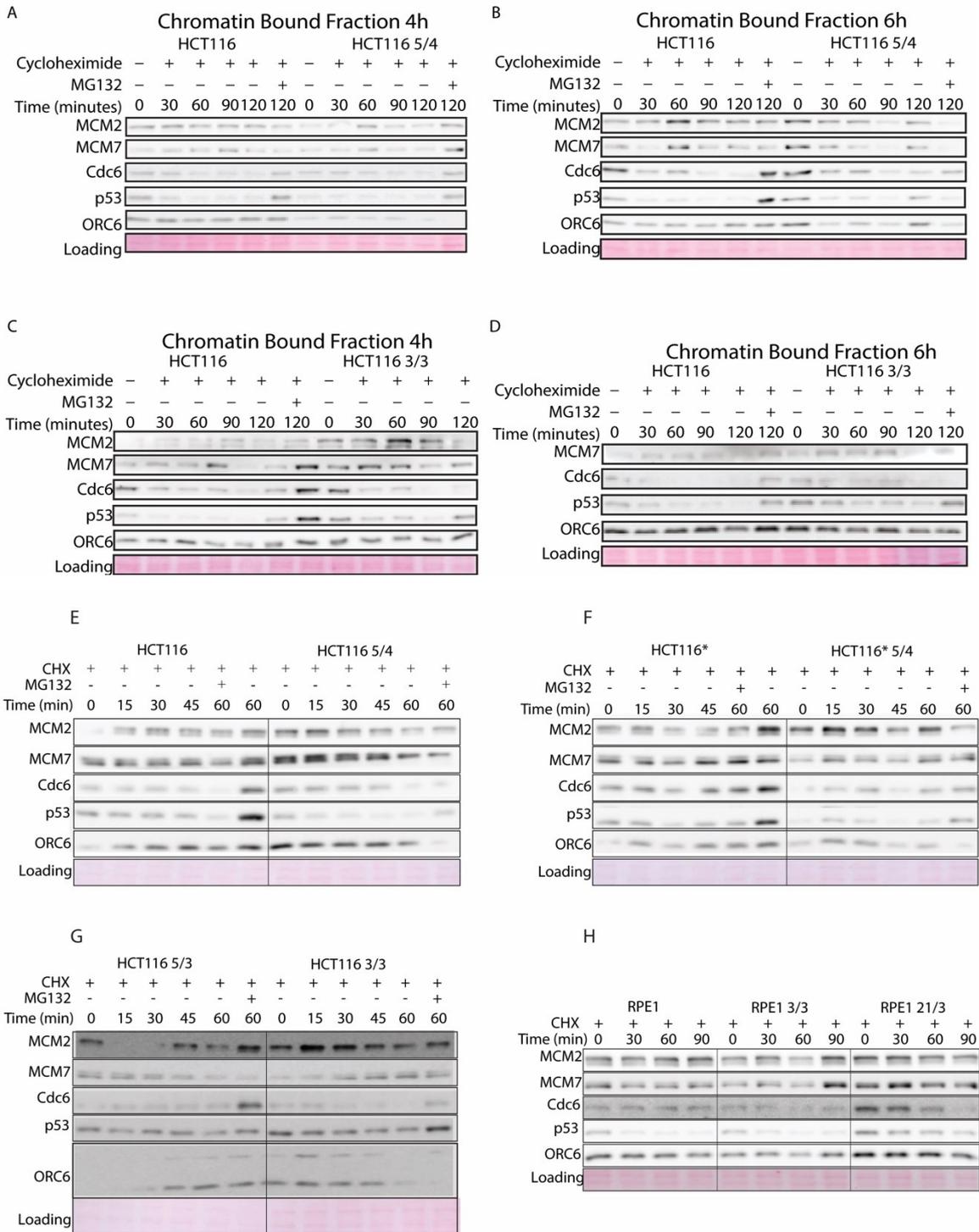


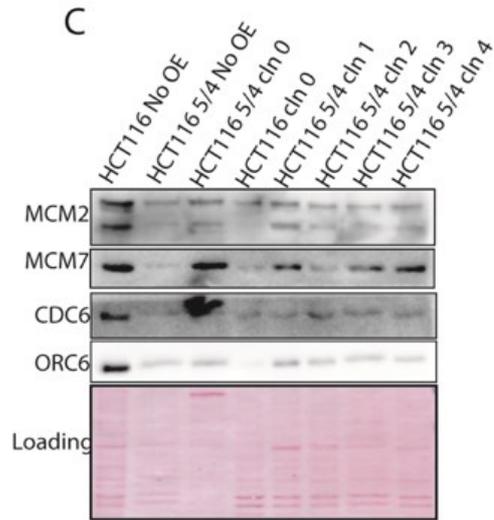
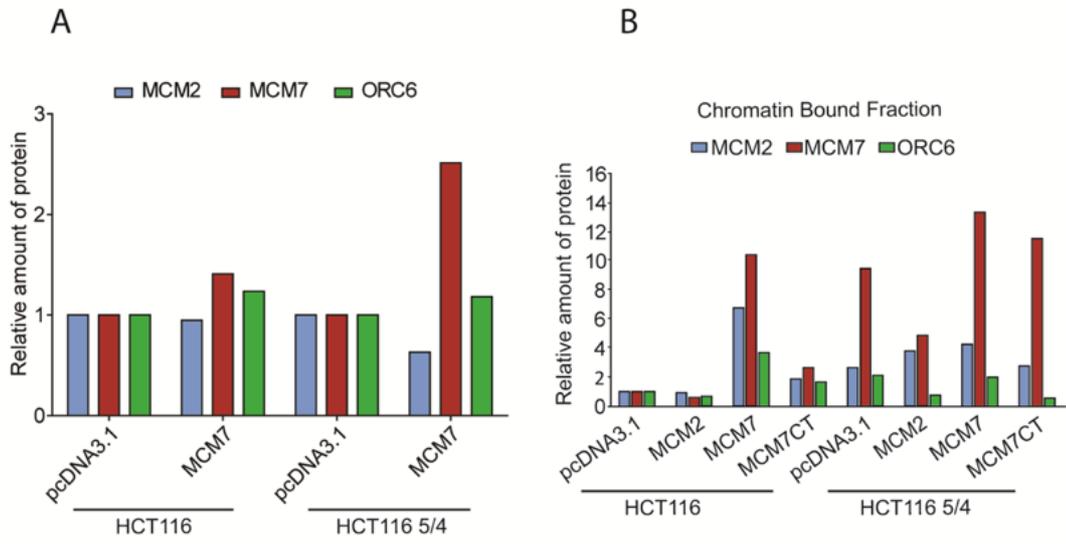
S2

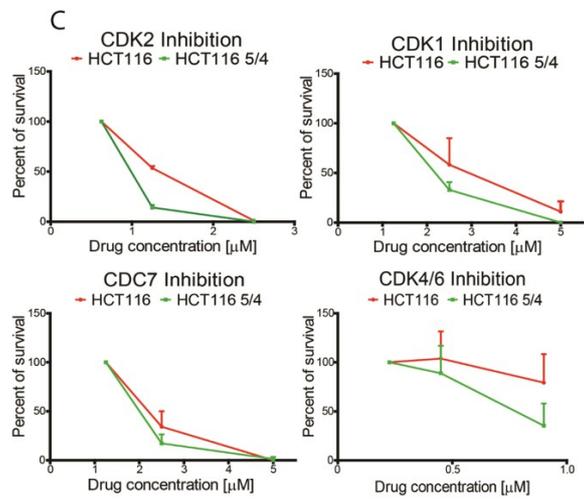
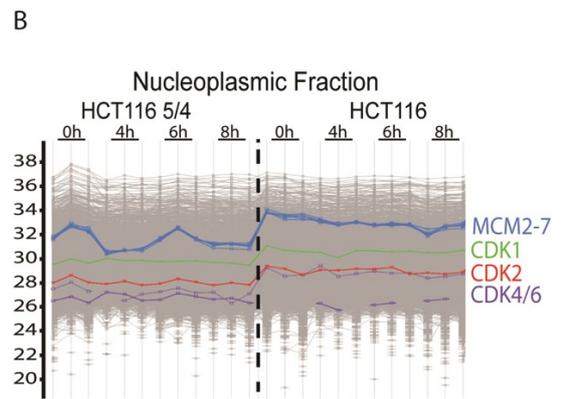
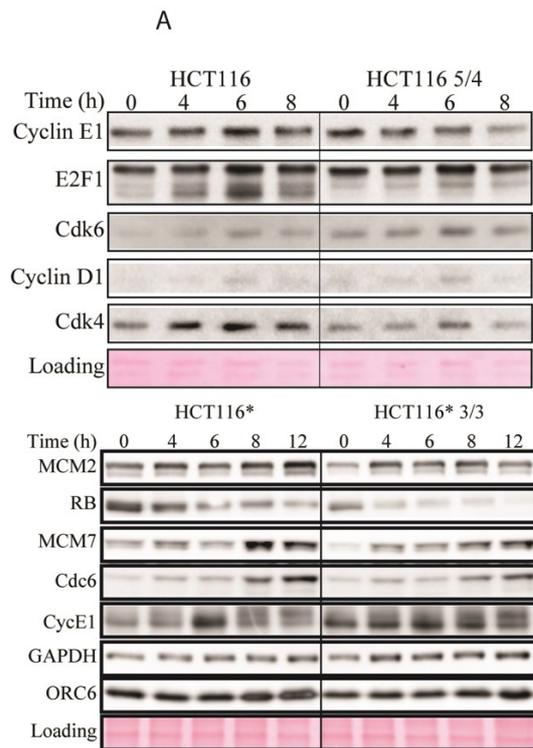


S3









10. References

- Abraham RT, Acquarone M, Andersen A, Asensi A, Belle R, Berger F, Bergounioux C, Brunn G, Buquet FC, Fagot D, Glab N, Goudeau H, Goudeau M, Guerrier P, Houghton P, Hendriks H, Kloareg B, Lippai M, Marie D, Maro B, Meijer L, Mester J, Mulner-Lorillon O, Poulet S, Schierenberg E, Schutte B, Vaultot D, Verlhac M (1995) Cellular effects of olomoucine, an inhibitor of cyclin-dependent kinases. *Biol. Cell* 83, 105.
- Agrawal A & Agrawal R (2011) Warkany syndrome: a rare case report. *Case Rep Pediatr* 2011: 437101
- Arellano M, Moreno S (1997) Regulation of CDK /cyclin complexes during the cell cycle. *Int. J. Biochem. Cell Biol.* 29, 559
- Asaithamby A, Hu B, Delgado O, Ding L-H, Story MD, Minna JD, Shay JW & Chen DJ (2011) Irreparable complex DNA double-strand breaks induce chromosome breakage in organotypic three-dimensional human lung epithelial cell culture. *Nucleic Acids Res.* 39: 5474–5488
- Awate, S., Dhar, S., Sommers, J. A. & Brosh, R. M. (2019) DNA Repair, Methods and Protocols. *Methods in molecular biology* (Clifton, N.J.) vol. 1999.
- Bai G, Smolka MB & Schimenti JC (2016) Chronic DNA Replication Stress Reduces Replicative Lifespan of Cells by TRP53-Dependent, microRNA-Assisted MCM2-7 Downregulation. *PLoS Genet.* 12: e1005787
- Baker DJ, Dawlaty MM, Wijshake T, Jeganathan KB, Malureanu L, van Ree JH, Crespo-Diaz R, Reyes S, Seaburg L, Shapiro V, Behfar A, Terzic A, van de Sluis B & van Deursen JM (2013) Increased expression of BubR1 protects against aneuploidy and cancer and extends healthy lifespan. *Nat. Cell Biol.* 15: 96–102
- Baker DJ, Jeganathan KB, Cameron JD, Thompson M, Juneja S, Kopecka A, Kumar R, Jenkins RB, de Groen PC, Roche P & van Deursen JM (2004) BubR1 insufficiency causes early onset of aging-associated phenotypes and infertility in mice. *Nat. Genet.* 36: 744–749
- Barlow, J.H., Faryabi, R.B., Calle' n, E., Wong, N., Malhowski, A., Chen, H.T., Gutierrez-Cruz, G., Sun, H.W., McKinnon, P., Wright, G., et al. (2013). Identification of early replicating fragile sites that contribute to genome instability. *Cell* 152, 620–632.
- Bartkova J, Horejsí Z, Koed K, Krämer A, Tort F, Zieger K, Guldberg P, Sehested M, Nesland JM, Lukas C, Ørntoft T, Lukas J & Bartek J (2005) DNA damage response as a candidate anti- cancer barrier in early human tumorigenesis. *Nature* 434: 864–870
- Bartkova J, Rezaei N, Lontos M, Karakaidos P, Kletsas D, Issaeva N, Vassiliou L-VF, Kolettas E, Niforou K, Zoumpourlis VC, Takaoka M, Nakagawa H, Tort F, Fugger K, Johansson F, Sehested M, Andersen CL, Dyrskjot L, Ørntoft T, Lukas J, et al (2006) Oncogene-induced senescence is part of the tumorigenesis barrier imposed by DNA damage checkpoints. *Nature* 444: 633–637
- Beckman RA & Loeb LA (2006) Efficiency of carcinogenesis with and without a mutator mutation. *Proc. Natl. Acad. Sci. U.S.A.* 103: 14140–14145
- Bell SD, Botchan MR. The minichromosome maintenance replicative helicase. *Cold Spring Harb Perspect Biol.* 2013 Nov 1;5(11):a012807. doi: 10.1101/cshperspect.a012807. PMID: 23881943; PMCID: PMC3809582.
- Beroukhim R, Mermel CH, Porter D, Wei G, Raychaudhuri S, Donovan J, Barretina J, Boehm JS, Dobson J, Urashima M, Mc Henry KT, Pinchback RM, Ligon AH, Cho Y-J, Haery L, Greulich H, Reich M, Winckler W, Lawrence MS, Weir BA, et al (2010) The landscape of somatic copy- number alteration across human cancers. *Nature* 463: 899–905
- Bilousova G, Marusyk A, Porter CC, Cardiff RD & DeGregori J (2005) Impaired DNA replication within progenitor cell pools promotes leukemogenesis. *PLoS Biol.* 3: e401

- Birkbak NJ, Eklund AC, Li Q, McClelland SE, Endesfelder D, Tan P, Tan IB, Richardson AL, Szallasi Z & Swanton C (2011) Paradoxical relationship between chromosomal instability and survival outcome in cancer. *Cancer Res.* 71: 3447–3452
- Birsoy K, Possemato R, Lorbeer FK, Bayraktar EC, Thiru P, Yucel B, Wang T, Chen WW, Clish CB & Sabatini DM (2014) Metabolic determinants of cancer cell sensitivity to glucose limitation and biguanides. *Nature* 508: 108–112
- Blank HM, Sheltzer JM, Meehl CM & Amon A (2015) Mitotic entry in the presence of DNA damage is a widespread property of aneuploidy in yeast. *Mol. Biol. Cell* 26: 1440–1451
- Blow JJ, Ge XQ, Jackson DA. How dormant origins promote complete genome replication. *Trends Biochem Sci.* 2011 Aug;36(8):405-14. doi: 10.1016/j.tibs.2011.05.002. Epub 2011 Jun 7. PMID: 21641805; PMCID: PMC3329722.
- Bolanos-Garcia VM. Assessment of the mitotic spindle assembly checkpoint (SAC) as the target of anticancer therapies. *Curr Cancer Drug Targets.* 2009 Mar;9(2):131-41. doi: 10.2174/156800909787580980. PMID: 19275754.
- Boveri T (2007) Concerning the Origin of Malignant Tumours by Theodor Boveri. Translated and annotated by Henry Harris. *J. Cell. Sci.* 121: 1–84
- Bruce A. Morgan, Donna M. (1996). Fekete, Chapter 10 Manipulating Gene Expression with Replication--Competent Retroviruses, *Methods in Cell Biology*, Volume 51, Pages 185-218,
- Carter SL, Eklund AC, Kohane IS, Harris LN & Szallasi Z (2006) A signature of chromosomal instability inferred from gene expression profiles predicts clinical outcome in multiple human cancers. *Nat. Genet.* 38: 1043–1048
- Chen, B., Retzlaff, M., Roos, T., & Frydman, J. (2011). Cellular strategies of protein quality control. *Cold Spring Harbor perspectives in biology*, 3(8), a004374. <https://doi.org/10.1101/cshperspect.a004374>
- Cho, W.-H., Y.-J. Lee, S.-I. Kong, J. Hurwitz, and J.-K. Lee. 2006. CDC7 kinase phosphorylates serine residues adjacent to acidic amino acids in the minichromosome maintenance 2 protein. *Proceedings of the National Academy of Sciences.* 103:11521-11526.
- Chuang, L.-C., L.K. Teixeira, J.A. Wohlschlegel, M. Henze, J.R. Yates, J. Méndez, and S.I. Reed. 2009. Phosphorylation of Mcm2 by Cdc7 promotes pre-replication complex assembly during cell-cycle re-entry. *Molecular Cell.* 35:206-216.
- Chunduri, N.K., Storchová, Z. The diverse consequences of aneuploidy. *Nat Cell Biol* 21, 54–62 (2019). <https://doi.org/10.1038/s41556-018-0243-8>
- Cimini D, Moree B, Canman JC & Salmon ED (2003) Merotelic kinetochore orientation occurs frequently during early mitosis in mammalian tissue cells and error correction is achieved by two different mechanisms. *J. Cell. Sci.* 116: 4213–4225
- Contestabile A, Fila T, Bartesaghi R & Ciani E (2009) Cell cycle elongation impairs proliferation of cerebellar granule cell precursors in the Ts65Dn mouse, an animal model for Down syndrome. *Brain Pathol.* 19: 224–237
- Conti C, Caburet S, Bensimon A. Targeting the molecular mechanism of DNA replication. *Drug Discov Today.* 2001 Aug 1;6(15):786-792. doi: 10.1016/s1359-6446(01)01854-2. PMID: 11470587.
- Cortez, D., G. Glick, and S.J. Elledge. 2004. Minichromosome maintenance proteins are direct targets of the ATM and ATR checkpoint kinases. *Proceedings of the National Academy of Sciences of the United States of America.* 101:10078-10083.
- Crasta K, Ganem NJ, Dagher R, Lantermann AB, Ivanova EV, Pan Y, Nezi L, Protopopov A, Chowdhury D & Pellman D (2012) DNA breaks and chromosome pulverization from errors in mitosis. *Nature* 482: 53–58
- Das, M., et al., MCM Paradox: Abundance of Eukaryotic Replicative Helicases and Genomic Integrity. *Mol Biol Int*, 2014. 2014: p. 574850.

- Davidsson, J., The epigenetic landscape of aneuploidy: constitutional mosaicism leading the way? *Epigenomics*, 2014. 6(1): p. 45-58.
- Davoli T, Uno H, Wooten EC, Elledge SJ. Tumor aneuploidy correlates with markers of immune evasion and with reduced response to immunotherapy. *Science*. 2017 Jan 20;355(6322):eaaf8399. doi: 10.1126/science.aaf8399. PMID: 28104840; PMCID: PMC5592794.
- Donnelly N, Passerini V, Durrbaum M, Stingele S and Storchova Z. HSF1 deficiency and impaired HSP90-dependent protein folding are hallmarks of aneuploid human cells. *The EMBO journal*. 2014 Oct 16; 33(20):2374-87
- Duncan AW, Hanlon Newell AE, Bi W, Finegold MJ, Olson SB, Beaudet AL & Grompe M (2012) Aneuploidy as a mechanism for stress-induced liver adaptation. *J. Clin. Invest.* 122: 3307– 3315
- Duncan AW, Taylor MH, Hickey RD, Hanlon Newell AE, Lenzi ML, Olson SB, Finegold MJ & Grompe M (2010) The ploidy conveyor of mature hepatocytes as a source of genetic variation. *Nature* 467: 707–710
- Dungrawala, H. et al. The Replication Checkpoint Prevents Two Types of Fork Collapse without Regulating Replisome The Replication Checkpoint Prevents Two Types of Fork Collapse without Regulating Replisome Stability. *Molecular Cell* 59, 998–1010 (2015).
- Dürbaum, M. & Storchová, Z. Effects of aneuploidy on gene expression: Implications for cancer. *FEBS J.* 283, 791–802 (2016).
- Dürbaum, M., Kuznetsova, A.Y., Passerini, V. et al. Unique features of the transcriptional response to model aneuploidy in human cells. *BMC Genomics* 15, 139 (2014). <https://doi.org/10.1186/1471-2164-15-139>
- Dyson N (1998) The regulation of E2F by pRB-family proteins. *Genes Dev.* 12: 2245–2262
- Edelmann W, Yang K, Umar A, Heyer J, Lau K, Fan K, Liedtke W, Cohen PE, Kane MF, Lipford JR, Yu N, Crouse GF, Pollard JW, Kunkel T, Lipkin M, Kolodner R & Kucherlapati R (1997) Mutation in the mismatch repair gene Msh6 causes cancer susceptibility. *Cell* 91: 467–477
- Ekholm-Reed S, Méndez J, Tedesco D, Zetterberg A, Stillman B & Reed SI (2004) Deregulation of cyclin E in human cells interferes with prereplication complex assembly. *J. Cell Biol.* 165: 789–800
- Ekholm, S. V & Reed, S. I. Regulation of G 1 cyclin-dependent kinases in the mammalian cell cycle. 676–684 (2000).
- el-Deiry WS, Tokino T, Velculescu VE, Levy DB, Parsons R, Trent JM, Lin D, Mercer WE, Kinzler KW, Vogelstein B: WAF1, a potential mediator of p53 tumor suppression. *Cell* 1993, 75:817-825.
- Fernandez-Cid, A., et al., An ORC/Cdc6/MCM2-7 complex is formed in a multistep reaction to serve as a platform for MCM double-hexamers assembly. *Mol Cell*, 2013. 50(4): p. 577-88.
- Fonseca, R. et al. Deletions of chromosome 13 in multiple myeloma identified by interphase FISH usually denote large deletions of the q arm or monosomy. *Leukemia* 15, 981–986 (2001).
- Galanos, P. et al. Chronic p53-independent p21 expression causes genomic instability by deregulating replication licensing. *Nat. Cell Biol.* 18, 777–789 (2016).
- Gan, H. et al. Short Article Checkpoint Kinase Rad53 Couples Leading- and Lagging-Strand DNA Synthesis under Replication Short Article Checkpoint Kinase Rad53 Couples DNA Synthesis under Replication Stress. *Mol. Cell* 1–10 (2017) doi:10.1016/j.molcel.2017.09.018.
- Ge XQ, Jackson DA & Blow JJ (2007) Dormant origins licensed by excess Mcm2-7 are required for human cells to survive replicative stress. *Genes Dev.* 21: 3331–3341

- Geng, Y., Lee, Y.-M., Welcker, M., Swanger, J., Zagozdzon, A., Winer, J.D., Roberts, J.M., Kaldis, P., Clurman, B.E., and Sicinski, P. (2007). Kinase-Independent Function of Cyclin E. *Molecular Cell*, 25(1), pp. 127–139.
- Gopinath RK, You S-T, Chien K-Y, Swamy KBS, Yu J-S, Schuyler SC & Leu J-Y (2014) The Hsp90-dependent proteome is conserved and enriched for hub proteins with high levels of protein-protein connectivity. *Genome Biol Evol* 6: 2851–2865
- Gordon, D., Resio, B. & Pellman, D. Causes and consequences of aneuploidy in cancer. *Nat Rev Genet* 13, 189–203 (2012). <https://doi.org/10.1038/nrg3123>
- Gorgoulis VG, Vassiliou L-VF, Karakaidos P, Zacharatos P, Kotsinas A, Liloglou T, Venere M, Ditullio RA, Kastriakis NG, Levy B, Kletsas D, Yoneta A, Herlyn M, Kittas C & Halazonetis TD (2005) Activation of the DNA damage checkpoint and genomic instability in human precancerous lesions. *Nature* 434: 907–913
- Gralewska, P., Gajek, A., Marczak, A. & Rogalska, A. Participation of the ATR/CHK1 pathway in replicative stress targeted therapy of high-grade ovarian cancer. *J. Hematol. Oncol.* 13, 1–16 (2020).
- Guacci V, Koshland D & Strunnikov A (1997) A direct link between sister chromatid cohesion and chromosome condensation revealed through the analysis of MCD1 in *S. cerevisiae*. *Cell* 91: 47–57
- Guilbaud G, Rappailles A, Baker A, Chen C-L, Arneodo A, Goldar A, d'Aubenton-Carafa Y, Thermes C, Audit B & Hyrien O (2011) Evidence for sequential and increasing activation of replication origins along replication timing gradients in the human genome. *PLoS Comput. Biol.* 7: e1002322
- Hakim O, Resch W, Yamane A, Klein I, Kieffer-Kwon K-R, Jankovic M, Oliveira T, Bothmer A, Voss TC, Ansarah-Sobrinho C, Mathe E, Liang G, Cobell J, Nakahashi H, Robbiani DF, Nussenzweig A, Hager GL, Nussenzweig MC & Casellas R (2012) DNA damage defines sites of recurrent chromosomal translocations in B lymphocytes. *Nature* 484: 69–74
- Hamperl, S., Saldivar, J., Bocek, M. & Cimprich, K. A. DNA Replication Modulates R-loop Levels to Maintain Genome Stability. *bioRxiv* 155978 (2017) doi:10.1101/155978.
- Han X, Aslanian A, Fu K, Tsuji T & Zhang Y (2014) The interaction between checkpoint kinase 1 (Chk1) and the minichromosome maintenance (MCM) complex is required for DNA damage- induced Chk1 phosphorylation. *J. Biol. Chem.* 289: 24716–24723
- Hanel, W., & Moll, U. M. (2012). Links between mutant p53 and genomic instability. *Journal of cellular biochemistry*, 113(2), 433–439. <https://doi.org/10.1002/jcb.23400>
- Henry IM, Dilkes BP, Miller ES, Burkart-Waco D & Comai L (2010) Phenotypic consequences of aneuploidy in *Arabidopsis thaliana*. *Genetics* 186: 1231–1245
- Hills, S. A. & Diffley, J. F. X. DNA replication and oncogene-induced replicative stress. *Curr. Biol.* 24, R435–R444 (2014).
- Hinchcliffe, E., Day, C., Karanjeet, K. et al. Chromosome missegregation during anaphase triggers p53 cell cycle arrest through histone H3.3 Ser31 phosphorylation. *Nat Cell Biol* 18, 668–675 (2016). <https://doi.org/10.1038/ncb3348>
- Hirayama A, Kami K, Sugimoto M, Sugawara M, Toki N, Onozuka H, Kinoshita T, Saito N, Ochiai A, Tomita M, Esumi H & Soga T (2009) Quantitative metabolome profiling of colon and stomach cancer microenvironment by capillary electrophoresis time-of-flight mass spectrometry. *Cancer Res.* 69: 4918–4925
- Holland, A., Cleveland, D. Boveri revisited: chromosomal instability, aneuploidy and tumorigenesis. *Nat Rev Mol Cell Biol* 10, 478–487 (2009). <https://doi.org/10.1038/nrm2718>
- Ibarra A, Schwob E & Méndez J (2008) Excess MCM proteins protect human cells from replicative stress by licensing backup origins of replication. *Proc. Natl. Acad. Sci. U.S.A.* 105: 8956–8961

- Imaimatsu, K., Fujii, W., Hiramatsu, R., Miura, K., Kurohmaru, M., & Kanai, Y. (2018). CRISPR/Cas9-mediated knock-in of the murine Y chromosomal Sry gene. *The Journal of reproduction and development*, 64(3), 283–287. <https://doi.org/10.1262/jrd.2017-161>
- Iourov, I. Y., Vorsanova, S. G., Zelenova, M. A., Korostelev, S. A. & Yurov, Y. B. Genomic Copy Number Variation Affecting Genes Involved in the Cell Cycle Pathway: Implications for Somatic Mosaicism. *Int. J. Genomics* 2015, 757680 (2015).
- Ishitsuka K, Utsunomiya A, Katsuya H, Takeuchi S, Takatsuka Y, Hidaka M, Sakai T, Yoshimitsu M, Ishida T & Tamura K (2015) A phase II study of bortezomib in patients with relapsed or refractory aggressive adult T-cell leukemia/lymphoma. *Cancer Sci.* 106: 1219–1223
- Jain M, Nilsson R, Sharma S, Madhusudhan N, Kitami T, Souza AL, Kafri R, Kirschner MW, Clish CB & Mootha VK (2012) Metabolite profiling identifies a key role for glycine in rapid cancer cell proliferation. *Science* 336: 1040–1044
- Janssen A, van der Burg M, Suzhai K, Kops GJPL & Medema RH (2011) Chromosome segregation errors as a cause of DNA damage and structural chromosome aberrations. *Science* 333: 1895–1898
- Jiang J, Jing Y, Cost GJ, Chiang J-C, Kolpa HJ, Cotton AM, Carone DM, Carone BR, Shivak DA, Guschin DY, Pearl JR, Rebar EJ, Byron M, Gregory PD, Brown CJ, Urnov FD, Hall LL & Lawrence JB (2013) Translating dosage compensation to trisomy 21. *Nature* 500: 296–300
- Jin Zhu, Hung-Ji Tsai, Molly R. Gordon, and Rong L (2018) Cellular Stress Associated with Aneuploid. *Developmental Cell* 44:420-431
- Johnson, D. G. & Walker, C. L. CYCLINS AND CELL CYCLE CHECKPOINTS. *Annu. Rev. Pharmacol. Toxicol.* **39**, 295–312 (1999).
- Joshua M. Nicholson, Daniela Cimini, (2015) Chapter Seven - Link between Aneuploidy and Chromosome Instability, *International Review of Cell and Molecular Biology*, Vol 315, Pages 299-317,
- Kahlem P, Sultan M, Herwig R, Steinfath M, Balzereit D, Eppens B, Saran NG, Pletcher MT, South ST, Stetten G, Lehrach H, Reeves RH & Yaspo M-L (2004) Transcript level alterations reflect gene dosage effects across multiple tissues in a mouse model of down syndrome. *Genome Res.* 14: 1258–1267
- Kang SH, Kang KW, Kim K-H, Kwon B, Kim S-K, Lee H-Y, Kong S-Y, Lee ES, Jang S-G & Yoo BC (2008) Upregulated HSP27 in human breast cancer cells reduces Herceptin susceptibility by increasing Her2 protein stability. *BMC Cancer* 8: 286
- Kara, N., et al., Orc1 Binding to Mitotic Chromosomes Precedes Spatial Patterning During G1 Phase and Assembly of the Origin Recognition Complex in Human Cells. *J Biol Chem*, 2015.
- Kastan, M., Bartek, J. Cell-cycle checkpoints and cancer. *Nature* 432, 316–323 (2004). <https://doi.org/10.1038/nature03097>
- Kaya, A., Mariotti, M., Tyshkovskiy, A. et al. Molecular signatures of aneuploidy-driven adaptive evolution. *Nat Commun* 11, 588 (2020). <https://doi.org/10.1038/s41467-019-13669-2>
- Killary A & Lott S (1996) Production of Microcell Hybrids. *Methods* 9: 3–11
- Klotz-Noack K & Blow JJ (2011) A role for dormant origins in tumor suppression. *Mol. Cell* 41:495–496
- Kneissig, M. et al. Micronuclei-based model system reveals functional consequences of chromothripsis in human cells. *Elife* 8, 1–20 (2019).
- Kon M, Kiffin R, Koga H, Chapochnick J, Macian F, Varticovski L & Cuervo AM (2011) Chaperone-Mediated Autophagy Is Required for Tumor Growth. *Science Translational Medicine* 3:109ra117–109ra117

- Kops, G., Weaver, B. & Cleveland, D. On the road to cancer: aneuploidy and the mitotic checkpoint. *Nat Rev Cancer* 5, 773–785 (2005). <https://doi.org/10.1038/nrc1714>
- Kraus J, Kraus M, Liu N, Besse L, Bader J, Geurink PP, de Bruin G, Kisselev AF, Overkleeft H & Driessen C (2015) The novel β 2-selective proteasome inhibitor LU-102 decreases phosphorylation of I kappa B and induces highly synergistic cytotoxicity in combination with ibrutinib in multiple myeloma cells. *Cancer Chemother. Pharmacol.* 76: 383–396
- Kunnev D, Rusiniak ME, Kudla A, Freeland A, Cady GK & Pruitt SC (2010) DNA damage response and tumorigenesis in Mcm2-deficient mice. *Oncogene* 29: 3630–3638
- Lazenby M, Hills R, Burnett AK & Zabkiewicz J (2015) The HSP90 inhibitor ganetespib: A potential effective agent for Acute Myeloid Leukemia in combination with cytarabine. *Leuk. Res.* 39: 617–624
- Lee AJX, Endesfelder D, Rowan AJ, Walther A, Birckbak NJ, Futreal PA, Downward J, Szallasi Z, Tomlinson IPM, Howell M, Kschischo M & Swanton C (2011) Chromosomal instability confers intrinsic multidrug resistance. *Cancer Res.* 71: 1858–1870
- Lew, D. J. & Kornbluth, S. Regulatory roles of cyclin dependent kinase phosphorylation in cell cycle control. *Curr. Opin. Cell Biol.* 8, 795–804 (1996).
- Li Z, Xu X. Post-Translational Modifications of the Mini-Chromosome Maintenance Proteins in DNA Replication. *Genes (Basel)*. 2019 Apr 30;10(5):331. doi: 10.3390/genes10050331. PMID: 31052337; PMCID: PMC6563057.
- Li T-S & Marbán E (2010) Physiological levels of reactive oxygen species are required to maintain genomic stability in stem cells. *Stem Cells* 28: 1178–1185
- Liang, J., Niu, Z., Zhang, B. et al. (2021) p53-dependent elimination of aneuploid mitotic offspring by entosis. *Cell Death Differ* 28, 799–813. <https://doi.org/10.1038/s41418-020-00645-3>
- Lindsley DL, Sandler L, Baker BS, Carpenter AT, Denell RE, Hall JC, Jacobs PA, Miklos GL, Davis BK, Gethmann RC, Hardy RW, Steven AH, Miller M, Nozawa H, Parry DM, Gould-Somero M & Gould-Somero M (1972) Segmental aneuploidy and the genetic gross structure of the Drosophila genome. *Genetics* 71: 157–184
- Liu P, Slater DM, Lenburg M, Nevis K, Cook JG & Vaziri C (2009) Replication licensing promotes cyclin D1 expression and G1 progression in untransformed human cells. *Cell Cycle* 8: 125–136
- Loane M, Morris JK, Addor M-C, Arriola L, Budd J, Doray B, Garne E, Gatt M, Haeusler M, Khoshnood B, Klungsoyr Melve K, Latos-Bielenska A, McDonnell B, Mullaney C, O'Mahony M, Queisser-Wahrendorf A, Rankin J, Rissmann A, Rounding C, Salvador J, et al (2013) Twenty- year trends in the prevalence of Down syndrome and other trisomies in Europe: impact of maternal age and prenatal screening. *Eur. J. Hum. Genet.* 21: 27–33
- Lygeros J, Koutroumpas K, Dimopoulos S, Legouras I, Kouretas P, Heichinger C, Nurse P, Lygerou Z. Stochastic hybrid modeling of DNA replication across a complete genome. *Proc Natl Acad Sci U S A.* 2008 Aug 26;105(34):12295-300. doi: 10.1073/pnas.0805549105.
- Macheret, M. & Halazonetis, T. D. Intragenic origins due to short G1 phases underlie oncogene-induced DNA replication stress. *Nature* 555, 112–116 (2018).
- MacIntyre DJ, Blackwood DHR, Porteous DJ, Pickard BS & Muir WJ (2003) Chromosomal abnormalities and mental illness. *Mol. Psychiatry* 8: 275–287
- Magnuson T, Smith S & Epstein CJ (1982) The development of monosomy 19 mouse embryos. *J Embryol Exp Morphol* 69: 223–236
- Mailand N, Gibbs-Seymour I, Bekker-Jensen S. Regulation of PCNA-protein interactions for genome stability. *Nat Rev Mol Cell Biol.* 2013 May;14(5):269-82. doi: 10.1038/nrm3562. Epub 2013 Apr 18. PMID: 23594953.
- Mailand, N. & Diffley, J. F. X. CDKs promote DNA replication origin licensing in human cells by protecting Cdc6 from APC/C-dependent proteolysis. *Cell* 122, 915–926 (2005).

- Makhnevych T & Houry WA (2012) The role of Hsp90 in protein complex assembly. *Biochim. Biophys. Acta* 1823: 674–682
- Malumbres M, Carnero A (2003) Cell cycle deregulation: a common motif in cancer. *Prog Cell Cycle Res* 5:5–18
- Mao R, Zielke CL, Zielke HR & Pevsner J (2003) Global up-regulation of chromosome 21 gene expression in the developing Down syndrome brain. *Genomics* 81: 457–467
- Maréchal A, Zou L. DNA damage sensing by the ATM and ATR kinases. *Cold Spring Harb Perspect Biol.* 2013 Sep 1;5(9):a012716. doi: 10.1101/cshperspect.a012716. PMID: 24003211; PMCID: PMC3753707.
- Marnef Aline, Cohen Sarah, Legube Gaëlle, (2017). Transcription-Coupled DNA Double-Strand Break Repair: Active Genes Need Special Care. *Journal of Molecular Biology*, Volume 429, Issue 9, Pages 1277-1288
- Mary Kay McCormick, Albert Schinzel, Michael B. Petersen, Gail Stetten, Daniel J. Driscoll, Eduardo S. Cantu, Lisbeth Tranebjaerg, Margareta Mikkelsen, Paul C. Watkins, Stylianos E. Antonarakis, (1989) Molecular genetic approach to the characterization of the “Down syndrome region” of chromosome 21. *Genomics*, Vol 5, Issue 2, Pages 325-331. [https://doi.org/10.1016/0888-7543\(89\)90065-7](https://doi.org/10.1016/0888-7543(89)90065-7).
- Masai, H., You, Z. & Arai, K. I. Control of DNA replication: Regulation and activation of eukaryotic replicative helicase, MCM. *IUBMB Life* 57, 323–335 (2005).
- McClellan AJ, Xia Y, Deutschbauer AM, Davis RW, Gerstein M & Frydman J (2007) Diverse cellular functions of the Hsp90 molecular chaperone uncovered using systems approaches. *Cell* 131: 121–135
- McGarry TJ & Kirschner MW (1998) Geminin, an inhibitor of DNA replication, is degraded during mitosis. *Cell* 93: 1043–1053
- Méndez J & Stillman B (2000) Chromatin association of human origin recognition complex, cdc6, and minichromosome maintenance proteins during the cell cycle: assembly of prereplication complexes in late mitosis. *Mol. Cell. Biol.* 20: 8602–8612
- Mieczkowski PA, Resnick MA & Gordenin DA (2012) Clustered mutations in yeast and in human cancers can arise from damaged long single-strand DNA regions. *Mol. Cell* 46: 424–435
- Miyabara, S., Gropp, A. & Winking, H. (1982) Trisomy 16 in the Mouse Fetus Associated With Generalized Edema and Cardiovascular and Urinary Tract Anomalies. 380.
- Montagnoli, A., B. Valsasina, D. Brotherton, S. Troiani, S. Rainoldi, P. Tenca, A. Molinari, and C. Santocanale. 2006. Identification of Mcm2 phosphorylation sites by S-phase-regulating kinases. *Journal of Biological Chemistry.* 281:10281-10290.
- Morimoto RI (2008) Proteotoxic stress and inducible chaperone networks in neurodegenerative disease and aging. *Genes Dev.* 22: 1427–1438
- Mukherjee, P., Winter, S. L. & Alexandrow, M. G. Cell cycle arrest by transforming growth factor beta1 near G1/S is mediated by acute abrogation of prereplication complex activation involving an Rb-MCM interaction. *Mol. Cell. Biol.* 30, 845–56 (2010).
- Mukherjee, P., Winter, S. L. & Alexandrow, M. G. Cell cycle arrest by transforming growth factor beta1 near G1/S is mediated by acute abrogation of prereplication complex activation involving an Rb-MCM interaction. *Mol. Cell. Biol.* 30, 845–56 (2010).
- Natarajan AT (2015) Radiosensitivity of Cells Derived from Down Syndrome Patients. *Springer Link:* 1–6
- Nawata H, Kashino G, Tano K, Daino K, Shimada Y, Kugoh H, Oshimura M & Watanabe M (2011) Dysregulation of gene expression in the artificial human trisomy cells of chromosome 8 associated with transformed cell phenotypes. *PLoS ONE* 6: e25319
- Necchi D, Pinto A, Tillhon M, Dutto I, Serafini MM, Lanni C, Govoni S, Racchi M & Prospero E (2015) Defective DNA repair and increased chromatin binding of DNA repair factors in Down syndrome fibroblasts. *Mutat. Res.* 780: 15–23

- Nevis, K.R., M. Cordeiro-Stone, and J.G. Cook. 2009. Origin licensing and p53 status regulate Cdk2 activity during G1. *Cell cycle*. 8:1952-1963.
- Ninomiya, H., Nomura, K., Satoh, Y. et al. Genetic instability in lung cancer: concurrent analysis of chromosomal, mini- and microsatellite instability and loss of heterozygosity. *Br J Cancer* 94, 1485–1491 (2006). <https://doi.org/10.1038/sj.bjc.6603121>
- Norbury C, Nurse P: Animal cell cycles and their control. *Annu Rev Biochem* 1992, 61:441-470.
- Ohashi A, Ohori M, Iwai K, Nakayama Y, Nambu T, Morishita D, Kawamoto T, Miyamoto M, Hirayama T, Okaniwa M, Banno H, Ishikawa T, Kandori H & Iwata K (2015) Aneuploidy generates proteotoxic stress and DNA damage concurrently with p53-mediated post-mitotic apoptosis in SAC-impaired cells. *Nat Commun* 6: 7668
- Ohashi A, Ohori M, Iwai K, Nakayama Y, Nambu T, Morishita D, Kawamoto T, Miyamoto M, Hirayama T, Okaniwa M, Banno H, Ishikawa T, Kandori H & Iwata K (2015) Aneuploidy generates proteotoxic stress and DNA damage concurrently with p53-mediated post-mitotic apoptosis in SAC-impaired cells. *Nat Commun* 6: 7668
- Ohtsuka, T., Jensen, M. R., Kim, H. G., Kim, K. & Lee, S. W. The negative role of cyclin G in ATM-dependent p53 activation. *Oncogene* 23, 5405–5408 (2004).
- Oromendia AB, Dodgson SE & Amon A (2012) Aneuploidy causes proteotoxic stress in yeast. *Genes Dev.* 26: 2696–2708
- Oromendia, A.B. and A. Amon, Aneuploidy: implications for protein homeostasis and disease. *Dis Model Mech*, 2014. 7(1): p. 15-20.
- Pacek M & Walter JC (2004) A requirement for MCM7 and Cdc45 in chromosome unwinding during eukaryotic DNA replication. *EMBO J.* 23: 3667–3676
- Park I-H, Arora N, Huo H, Maherali N, Ahfeldt T, Shimamura A, Lensch MW, Cowan C, Hochedlinger K & Daley GQ (2008) Disease-specific induced pluripotent stem cells. *Cell* 134: 877–886
- Park, H. Y. et al. Induction of p53-Independent Apoptosis and G1 Cell Cycle Arrest by Fucoidan in HCT116 Human Colorectal Carcinoma Cells. 1–14 (2017) doi:10.3390/md15060154.
- Passerini, V, Ozeri-Galai E, de Pagter MS, Donnelly N, Schmalbrock S, Kloosterman WP, Kerem B, Storchová Z The presence of extra chromosomes leads to genomic instability. *Nat. Commun.* 7:10754 doi: 10.1038/ncomms10754 (2016).
- Patel AP, Tirosch I, Trombetta JJ, Shalek AK, Gillespie SM, Wakimoto H, Cahill DP, Nahed BV, Curry WT, Martuza RL, Louis DN, Rozenblatt-Rosen O, Suvà ML, Regev A & Bernstein BE (2014) Single-cell RNA-seq highlights intratumoral heterogeneity in primary glioblastoma. *Science* 344: 1396–1401
- Pei, XH., Xiong, Y. Biochemical and cellular mechanisms of mammalian CDK inhibitors: a few unresolved issues. *Oncogene* 24, 2787–2795 (2005). <https://doi.org/10.1038/sj.onc.1208611>
- Piunti, A., Rossi, A., Cerutti, A. et al. Polycomb proteins control proliferation and transformation independently of cell cycle checkpoints by regulating DNA replication. *Nat Commun* 5, 3649 (2014). <https://doi.org/10.1038/ncomms4649>
- Pomerantz, R. T., & O'Donnell, M. (2010). What happens when replication and transcription complexes collide?. *Cell cycle (Georgetown, Tex.)*, 9(13), 2537–2543. <https://doi.org/10.4161/cc.9.13.12122>
- Potapova, T. A., Zhu, J., & Li, R. (2013). Aneuploidy and chromosomal instability: a vicious cycle driving cellular evolution and cancer genome chaos. *Cancer metastasis reviews*, 32(3-4), 377–389. <https://doi.org/10.1007/s10555-013-9436-6>
- Prolla TA, Baker SM, Harris AC, Tsao JL, Yao X, Bronner CE, Zheng B, Gordon M, Reneker J, Arnheim N, Shibata D, Bradley A & Liskay RM (1998) Tumour susceptibility

- and spontaneous mutation in mice deficient in Mlh1, Pms1 and Pms2 DNA mismatch repair. *Nat. Genet.* 18: 276–279
- Quintyne NJ, Reing JE, Hoffelder DR, Gollin SM & Saunders WS (2005) Spindle multipolarity is prevented by centrosomal clustering. *Science* 307: 127–129
- Rangwala R, Chang YC, Hu J, Algazy KM, Evans TL, Fecher LA, Schuchter LM, Torigian DA, Panosian JT, Troxel AB, Tan K-S, Heitjan DF, DeMichele AM, Vaughn DJ, Redlinger M, Alavi A, Kaiser J, Pontiggia L, Davis LE, O'Dwyer PJ, et al (2014) Combined MTOR and autophagy inhibition: phase I trial of hydroxychloroquine and temsirolimus in patients with advanced solid tumors and melanoma. *Autophagy* 10: 1391–1402
- Regenberg B, Grotkjaer T, Winther O, Fausbøll A, Akesson M, Bro C, Hansen LK, Brunak S & Nielsen J (2006) Growth-rate regulated genes have profound impact on interpretation of transcriptome profiling in *Saccharomyces cerevisiae*. *Genome Biol.* 7: R107
- Remus D, Beuron F, Tolun G, Griffith JD, Morris EP & Diffley JFX (2009) Concerted loading of Mcm2-7 double hexamers around DNA during DNA replication origin licensing. *Cell* 139: 719–730
- Rieder CL, Cole RW, Khodjakov A & Sluder G (1995) The checkpoint delaying anaphase in response to chromosome monoorientation is mediated by an inhibitory signal produced by unattached kinetochores. *J. Cell Biol.* 130: 941–948
- Rinaldi, C., Pizzul, P., Longhese, M. P. & Bonetti, D. Sensing R-Loop-Associated DNA Damage to Safeguard Genome Stability. *Front. Cell Dev. Biol.* 8, 1657 (2021).
- Roberts SA, Sterling J, Thompson C, Harris S, Mav D, Shah R, Klimeczak LJ, Kryukov GV, Malc E,
- Roper RJ, Reeves RH (2006) Understanding the Basis for Down Syndrome Phenotypes. *PLoS Genet* 2(3): e50. <https://doi.org/10.1371/journal.pgen.0020050>
- Rouschop KMA, Ramaekers CHMA, Schaaf MBE, Keulers TGH, Savelkoul KGM, Lambin P, Koritzinsky M & Wouters BG (2009) Autophagy is required during cycling hypoxia to lower production of reactive oxygen species. *Radiother Oncol* 92: 411–416
- Santaguida et al., 2017, *Developmental Cell* 41, 638–651 June 19, 2017 Elsevier Inc. <http://dx.doi.org/10.1016/j.devcel.2017.05.022>
- Santaguida S, Vasile E, White E & Amon A (2015) Aneuploidy-induced cellular stresses limit autophagic degradation. *Genes Dev.* 29: 2010–2021
- Santaguida Stefano, Musacchio Andrea (2009). The life and miracles of kinetochores. *EMBO J.* Sep 2; 28(17): 2511–2531. doi: 10.1038/emboj.2009.173
- Santaguida, S., Amon, A. Short- and long-term effects of chromosome mis-segregation and aneuploidy. *Nat Rev Mol Cell Biol* 16, 473–485 (2015). <https://doi.org/10.1038/nrm4025>
- Segal DJ & McCoy EE (1974) Studies on Down's syndrome in tissue culture. I. Growth rates and protein contents of fibroblast cultures. *J. Cell. Physiol.* 83: 85–90
- Selmecki, A., Forche, A. & Berman, J. Aneuploidy and Isochromosome Formation in Drug-Resistant *Candida albicans*; *Science* (80-.). 313, 367 LP – 370 (2006).
- Sharma K, Vabulas RM, Macek B, Pinkert S, Cox J, Mann M & Hartl FU (2012) Quantitative proteomics reveals that Hsp90 inhibition preferentially targets kinases and the DNA damage response. *Mol. Cell Proteomics* 11: M111.014654
- Sharma, K., et al., Quantitative proteomics reveals that Hsp90 inhibition preferentially targets kinases and the DNA damage response. *Mol Cell Proteomics*, 2012. 11(3): p. M111 014654.
- Sheltzer JM (2013) A transcriptional and metabolic signature of primary aneuploidy is present in chromosomally unstable cancer cells and informs clinical prognosis. *Cancer Res.* 73: 6401–6412

- Sheltzer JM, Blank HM, Pfau SJ, Tange Y, George BM, Humpton TJ, Brito IL, Hiraoka Y, Niwa O & Amon A (2011) Aneuploidy drives genomic instability in yeast. *Science* 333: 1026–1030
- Sheltzer JM, Ko JH, Habibe Burgos NC, Chung ES, Meehl CM, Passerini V, Storchova Z & Amon A (2016) Single-chromosome aneuploidy commonly functions as a tumor suppressor. *bioRxiv*: 040162
- Sheltzer JM, Torres EM, Dunham MJ & Amon A (2012) Transcriptional consequences of aneuploidy. *Proc. Natl. Acad. Sci. U.S.A.* 109: 12644–12649
- Sherr, C.J., and Roberts, J.M. (1999). CDK inhibitors: positive and negative regulators of G1-phase progression. *Genes Dev.* 13, 1501–1512.
- Sherr, C.J., Beach, D., and Shapiro, G.I. (2016). Targeting CDK4 and CDK6: From Discovery to Therapy. *Cancer Discov.* 6, 353–367. Smith,
- Shima N, Alcaraz A, Liachko I, Buske TR, Andrews CA, Munroe RJ, Hartford SA, Tye BK & Schimenti JC (2007) A viable allele of Mcm4 causes chromosome instability and mammary adenocarcinomas in mice. *Nat. Genet.* 39: 93–98
- Shlien A, Campbell BB, de Borja R, Alexandrov LB, Merico D, Wedge D, Van Loo P, Tarpey PS, Coupland P, Behjati S, Pollett A, Lipman T, Heidari A, Deshmukh S, Avitzur N, Meier B, Gerstung M, Hong Y, Merino DM, Ramakrishna M, et al (2015) Combined hereditary and somatic mutations of replication error repair genes result in rapid onset of ultra-hypermutated cancers. *Nat. Genet.* 47: 257–262
- Siegel, J. J., & Amon, A. (2012). New insights into the troubles of aneuploidy. *Annual review of cell and developmental biology*, 28, 189–214. <https://doi.org/10.1146/annurev-cellbio-101011-155807>
- Siliciano JD, Canman CE, Taya Y, Sakaguchi K, Appella E and Kastan MB . (1997). *Genes Dev.*, 11, 3471–3481.
- Sin, O., Nollen, E.A.A. Regulation of protein homeostasis in neurodegenerative diseases: the role of coding and non-coding genes. *Cell. Mol. Life Sci.* 72, 4027–4047 (2015). <https://doi.org/10.1007/s00018-015-1985-0>
- Sionov E, Lee H, Chang YC & Kwon-Chung KJ (2010) *Cryptococcus neoformans* overcomes stress of azole drugs by formation of disomy in specific multiple chromosomes. *PLoS Pathog.* 6: e1000848
- Skourti-Stathaki, K., & Proudfoot, N. J. (2014). A double-edged sword: R loops as threats to genome integrity and powerful regulators of gene expression. *Genes & development*, 28(13), 1384–1396. <https://doi.org/10.1101/gad.242990.114>
- Slonim DK, Koide K, Johnson KL, Tantravahi U, Cowan JM, Jarrah Z & Bianchi DW (2009). Functional genomic analysis of amniotic fluid cell-free mRNA suggests that oxidative stress is significant in Down syndrome fetuses. *Proc. Natl. Acad. Sci. U.S.A.* 106: 9425–9429
- Solomon DA, Kim T, Diaz-Martinez LA, Fair J, Elkahloun AG, Harris BT, Toretsky JA, Rosenberg SA, Shukla N, Ladanyi M, Samuels Y, James CD, Yu H, Kim J-S & Waldman T (2011) Mutational inactivation of STAG2 causes aneuploidy in human cancer. *Science* 333: 1039–1043
- Spreatico A, Delord J-P, De Mattos-Arruda L, Berge Y, Rodon J, Cottura E, Bedard PL, Akimov M, Lu H, Pain S, Kaag A, Siu LL & Cortes J (2015) A first-in-human phase I, dose-escalation, multicentre study of HSP990 administered orally in adult patients with advanced solid malignancies. *Br. J. Cancer* 112: 650–659
- Stingele S, Stoehr G, Peplowska K, Cox J, Mann M & Storchova Z (2012) Global analysis of genome, transcriptome and proteome reveals the response to aneuploidy in human cells. *Mol. Syst. Biol.* 8: 608
- Storchova, Z., Pellman, D. (2004) From polyploidy to aneuploidy, genome instability and cancer. *Nat Rev Mol Cell Biol* 5, 45–54. <https://doi.org/10.1038/nrm1276>

- Taipale M, Tucker G, Peng J, Krykbaeva I, Lin Z-Y, Larsen B, Choi H, Berger B, Gingras A-C & Lindquist S (2014) A quantitative chaperone interaction network reveals the architecture of cellular protein homeostasis pathways. *Cell* 158: 434–448
- Taipale, M., Tucker, G., Peng, J., Krykbaeva, I., Lin, Z.-Y., Larsen, B. et al. (2014) A quantitative chaperone interaction network reveals the architecture of cellular protein homeostasis pathways. *Cell* 158, 434–448 <https://doi.org/10.1016/j.cell.2014.05.039>
- Tamara A. Potapova & Jin Zhu & Rong Li (2013) Aneuploidy and chromosomal instability: a vicious cycle driving cellular evolution and cancer genome chaos. *Cancer Metastasis Rev* 32:377–389 DOI 10.1007/s10555-013-9436-6
- Tanaka T, Fuchs J, Loidl J & Nasmyth K (2000) Cohesin ensures bipolar attachment of microtubules to sister centromeres and resists their precocious separation. *Nat. Cell Biol.* 2: 492–499
- Tang Y-C, Williams BR, Siegel JJ & Amon A (2011) Identification of aneuploidy-selective antiproliferation compounds. *Cell* 144: 499–512
- Tang, Y. C., & Amon, A. (2013). Gene copy-number alterations: a cost-benefit analysis. *Cell*, 152(3), 394–405. <https://doi.org/10.1016/j.cell.2012.11.043>
- Thomer M, May NR, Aggarwal BD, Kwok G & Calvi BR (2004) *Drosophila* double-parked is sufficient to induce re-replication during development and is regulated by cyclin E/CDK2. *Development* 131: 4807–4818
- Thompson SL & Compton DA (2008) Examining the link between chromosomal instability and aneuploidy in human cells. *J. Cell Biol.* 180: 665–672
- Thompson, S. L. & Compton, D. A. Examining the link between chromosomal instability and aneuploidy in human cells. *J. Cell Biol.* 180, 665–672 (2008).
- Todaro GJ & Green H (1963) Quantitative studies of the growth of mouse embryo cells in culture and their development into established lines. *J. Cell Biol.* 17: 299–313
- Tomasini R, Mak TW, Melino G. The impact of p53 and p73 on aneuploidy and cancer. *Trends Cell Biol.* 2008 May;18(5):244-52. doi: 10.1016/j.tcb.2008.03.003. Epub 2008 Apr 10. PMID: 18406616.
- Torres EM, Dephoure N, Panneerselvam A, Tucker CM, Whittaker CA, Gygi SP, Dunham MJ & Amon A (2010) Identification of aneuploidy-tolerating mutations. *Cell* 143: 71–83
- Torres EM, Sokolsky T, Tucker CM, Chan LY, Boselli M, Dunham MJ & Amon A (2007) Effects of aneuploidy on cellular physiology and cell division in haploid yeast. *Science* 317: 916–924
- Torres EM, Williams BR & Amon A (2008) Aneuploidy: cells losing their balance. *Genetics* 179:737–746
- Tuduri, S., Crabb?e, L., Conti, C., Tourrière, H., Holtgreve-Grez, H., Jauch, A., et al. (2009). Topoisomerase I suppresses genomic instability by preventing interference between replication and transcription. *Nature Cell Biology*, 11(11), 1315–1324. <http://doi.org/10.1038/ncb1984>
- Uppender MB, Habermann JK, McShane LM, Korn EL, Barrett JC, Difilippantonio MJ & Ried T (2004) Chromosome transfer induced aneuploidy results in complex dysregulation of the cellular transcriptome in immortalized and cancer cells. *Cancer Res.* 64: 6941–6949
- Valind A, Jin Y, Baldetorp B & Gisselsson D (2013) Whole chromosome gain does not in itself confer cancer-like chromosomal instability. *Proc. Natl. Acad. Sci. U.S.A.* 110: 21119–21123
- Varley JM (2003) Germline TP53 mutations and Li-Fraumeni syndrome. *Hum. Mutat.* 21: 313–320
- Vermeulen Katrien, Bockstaele Dirk R. Van, Berneman Zwi N. (2003). The cell cycle: a review of regulation, deregulation and therapeutic targets in cancer. *Cell Proliferation*, Volume36, Issue3, Pages 131-149

- Waddell N, Pajic M, Patch A-M, Chang DK, Kassahn KS, Bailey P, Johns AL, Miller D, Nones K, Quek K, Quinn MCJ, Robertson AJ, Fadlullah MZH, Bruxner TJC, Christ AN, Harliwong I, Idrisoglu S, Manning S, Nourse C, Nourbakhsh E, et al (2015) Whole genomes redefine the mutational landscape of pancreatic cancer. *Nature* 518: 495–501
- Wang, G., & Vasquez, K. M. (2017). Effects of Replication and Transcription on DNA Structure-Related Genetic Instability. *Genes*, 8(1), 17.
<https://doi.org/10.3390/genes8010017>
- Weaver BAA & Cleveland DW (2007) Aneuploidy: instigator and inhibitor of tumorigenesis. *Cancer Res.* 67: 10103–10105
- Weaver BAA, Silk AD, Montagna C, Verdier-Pinard P & Cleveland DW (2007) Aneuploidy acts both oncogenically and as a tumor suppressor. *Cancer Cell* 11: 25–36
- Wei Q, Li J, Liu T, Tong X, Ye X. Phosphorylation of minichromosome maintenance protein 7 (MCM7) by cyclin/cyclin-dependent kinase affects its function in cell cycle regulation. *J Biol Chem.* 2013 Jul 5;288(27):19715-25. doi: 10.1074/jbc.M112.449652. Epub 2013 May 17. PMID: 23720738; PMCID: PMC3707676
- Wilhelm, T., Ragu, S., Magdalou, I. & Machon, C. Slow Replication Fork Velocity of Homologous Recombination-Defective Cells Results from Endogenous Oxidative Stress. 1–20 (2016) doi:10.1371/journal.pgen.1006007.
- Williams BR, Prabhu VR, Hunter KE, Glazier CM, Whittaker CA, Housman DE & Amon A (2008) Aneuploidy affects proliferation and spontaneous immortalization in mammalian cells. *Science* 322: 703–709
- Wimalasundera R. C., Gardiner H. M. (2004) Congenital heart disease and aneuploidy. *Prenat Diagn* 2004; 24: 1116–1122. DOI: 10.1002/pd.1068
- Wong C & Stearns T (2003) Centrosome number is controlled by a centrosome-intrinsic block to reduplication. *Nat. Cell Biol.* 5: 539–544
- Wong, R. P., García-Rodríguez, N., Zilio, N., Hanulová, M. & Ulrich, H. D. Processing of DNA Polymerase-Blocking Lesions during (2020) Genome Replication Is Spatially and Temporally Segregated from Replication Forks. *Mol. Cell* 77, 3-16.e4.
- Woodward AM, Göhler T, Luciani MG, Oehlmann M, Ge X, Gartner A, Jackson DA & Blow JJ (2006) Excess Mcm2-7 license dormant origins of replication that can be used under conditions of replicative stress. *J. Cell Biol.* 173: 673–683
- Wu L, Timmers C, Maiti B, Saavedra HI, Sang L, Chong GT, Nuckolls F, Giangrande P, Wright FA, Field SJ, Greenberg ME, Orkin S, Nevins JR, Robinson ML & Leone G (2001) The E2F1-3 transcription factors are essential for cellular proliferation. *Nature* 414: 457–462
- Xu, H. et al. (2017) Replication dynamics: Biases and robustness of DNA fiber analysis. *J. Mol. Biol.* 8, 4845–4855.
- Yeeles JTP, Deegan TD, Janska A, Early A & Diffley JFX (2015) Regulated eukaryotic DNA replication origin firing with purified proteins. *Nature* 519: 431–435
- Yona AH, Manor YS, Herbst RH, Romano GH, Mitchell A, Kupiec M, Pilpel Y & Dahan O (2012) Chromosomal duplication is a transient evolutionary solution to stress. *Proc. Natl. Acad. Sci. U.S.A.* 109: 21010–21015
- Yüce, O., West, S.C. (2013). Senataxin, defective in the neurodegenerative disorder ataxia with oculomotor apraxia 2, lies at the interface of transcription and the DNA damage response. *Molecular and Cellular Biology*, Volume 33, Issue 2, Pages 406-417
- Yurov YB, Iourov IY, Vorsanova SG, Liehr T, Kolotii AD, Kutsev SI, Pellestor F, Beresheva AK, Demidova IA, Kravets VS, Monakhov VV & Soloviev IV (2007) Aneuploidy and confined chromosomal mosaicism in the developing human brain. *PLoS ONE* 2: e558
- Yurov YB, Vorsanova SG, Liehr T, Kolotii AD & Iourov IY (2014) X chromosome aneuploidy in the Alzheimer's disease brain. *Mol Cytogenet* 7: 20

- Zeman, M.K., and Cimprich, K.A. (2014). Causes and consequences of replication stress. *Nat. Cell Biol.* 16, 2–9.
- Zhang C-Z, Spektor A, Cornils H, Francis JM, Jackson EK, Liu S, Meyerson M & Pellman D (2015) Chromothripsis from DNA damage in micronuclei. *Nature* 522: 179–184
- Zhang S, Matsunaga S, Lin Y-F, Sishc B, Shang Z, Sui J, Shih H-Y, Zhao Y, Foreman O, Story MD, Chen DJ & Chen BPC (2015b) Spontaneous tumor development in bone marrow-rescued DNA-PKcs(3A/3A) mice due to dysfunction of telomere leading strand deprotection. *Oncogene*
- Zhong W, Feng H, Santiago FE & Kipreos ET (2003) CUL-4 ubiquitin ligase maintains genome stability by restraining DNA-replication licensing. *Nature* 423: 885–889
- Zhu J, Pavelka N, Bradford WD, Rancati G & Li R (2012) Karyotypic determinants of chromosome instability in aneuploid budding yeast. *PLoS Genet.* 8: e1002719
- Zhu JW, Field SJ, Gore L, Thompson M, Yang H, Fujiwara Y, Cardiff RD, Greenberg M, Orkin SH & DeGregori J (2001) E2F1 and E2F2 determine thresholds for antigen-induced T-cell proliferation and suppress tumorigenesis. *Mol. Cell. Biol.* 21: 8547–8564
- Zhu, J., Tsai, H.-J., Gordon, M. R. & Li, R. Cellular Stress Associated with Aneuploidy. *Dev. Cell* 44, 420–431 (2018).
- Zirkle RE (March 1970). "Ultraviolet-microbeam irradiation of newt-cell cytoplasm: spindle destruction, false anaphase, and delay of true anaphase". *Radiation Research.* 41 (3): 516–37

11. Curriculum Vitae

Mario Davide Maria Avarello

Personal data

Date of Birth: 06/04/1985

City of Birth: Caltanissetta, Caltanissetta, Italy

Citizenship: Italian

Research Experience

**University of
Kaiserslautern
(Germany)**

PhD at Molecular Genetics Dep. of Prof Storchova

Aug 2016 to Sep 2018

Lead the development of the projects
Design experimental procedures by setup of new protocols and using the existing technologies (NGS, Mass spectrometry, FACS, RT-PCR, PCR, SDS-PAGE, Electrophoresis, Microscopy, Gene Editing, Cell generation)

Manage undergraduate students for their experimental thesis

Make presentations, papers and thesis

Give lectures to undergraduate students

**Max Planck Institute
for Biochemistry
(Germany)**

PhD at Molecular Cell Biology Dep. of Prof Jentsch

Oct 2014 to Aug 2016

Lead the development of the projects
Design experimental procedures by setup of new protocols and using the existing technologies (NGS, Mass spectrometry, FACS, RT-PCR, PCR, SDS-PAGE, Electrophoresis, Microscopy, Gene Editing, Cell generation)

Manage undergraduate students for their experimental thesis

Make presentations, papers and thesis

Give lectures to undergraduate students.

**Italian National
Research Council
(Italy)**

Intern for MSc Thesis, Institute of Molecular Genetics

Dec2012 to Aug 2014

I worked for two years in DNA Damage lab of Dr. Sabbioneda at the National Council of Research – Institute of Molecular Genetics (CNR-IGM) where I could step deep into the specific molecular processes of how cancer can be able to escape at the normal checkpoint and the damage repair system. In particular I worked on the characterization of new putative phosphorylated residues on DNA Polymerase ϵ , a TLS polymerase capable of bypassing UV adducts, and their role in the molecular mechanism driving TLS.

**University of Palermo
(Italy)**

Intern for BSc Thesis, STEM BIO department

Mar 2012 to Nov 2012

I worked in the epigenetic lab of Prof. Di Leonardo where I gained confidence in working with cancerous cells and exploit genetics technique. There I studied aneuploidy related to Spindle Assembly Checkpoint dysfunctions in M Phase of the cell cycle in human cells and characterization of aneuploid cells by FISH technique.

Education

Doctor of Philosophy	2015 – 2021: Ludwig Maximilian University (Germany):
Master of Science	2012 – 2014: University of Pavia (Italy)
Bachelor of Science	2008 – 2012: University of Palermo (Italy)
Highschool	1999 – 2005: Lyceum for classic studies “U. Foscolo” (Italy):

Education Curricula

Doctor of Philosophy	Cancer research applied at Molecular Genetics, Biology and Cellular Biology department
Molecular Biology and Genetics	Methods in biochemistry, Bioinformatics, Advanced molecular biology, Structural biology and pharmacology, Molecular pharmacology, Microbial genetics, Human genetics, Developmental biology, Advanced microscopy, Plant molecular biology and biotechnology, Cellular biochemistry, Molecular microbiology.
Biology Science - Applied Molecular Biology	Mathematic, Physic, Inorganic Chemistry, Organic Chemistry, Botanic, Cytology and Histology, Informatics, English language, Molecular Biology, Biochemistry, Biostatistics, Chemistry-Physics, Physiology, Genetic, Cytogenetic, Immunology, Environmental and Food Healthy, Microbial, Molecular, Genetics, Methods in biochemistry and in Molecular Biology, Applied Microbial, Didactics Laboratories, Methodology Laboratory in Genetic, Molecular Biology, Microbial and Biochemistry

Publications

Papers	2021 - Cytogenomics, Chapter 5 - Molecular combing solutions, Liher et al Elsevier 2019 - Nature Communications, https://doi.org/10.1038/s41467-019-12763-9 2017 - Nucleic Acids Res., 45(16):9441-9454. doi: 10.1093/nar/gkx619
Patent	2021 – Physical Characterization of Telomere, USPTO and WIPO

Conference participations and posters

2020 Poster	PARP and DDR Inhibitors Summit (USA) January 28 - 30
2019 Posters	AEK, Heidelberg (Germany) February 27 - Mar 1 AACR2019 Atlanta (USA), March 29 - April 3 3R Presqu'île de Giens (France), May 21 - 24 FASEB Genetic Recombination & Genome Rearrangements, Steam Boat Colorado (USA); July 14 - 19 CSH Eukaryotic DNA Replication & Genome Maintenance, Cold Spring Harbor (USA) September 3 – 7 EMBO: The DNA damage response in physiology and disease; Sounio (Greece), October 7-11
2018 Poster:	DNA replication: From Basic to Disease, May 07-10, Heidelberg, Germany
2017 Posters	2nd DNA Replication as a Source of DNA Damage Conference, July 03-06, Rome, Italy
2016	DGZ International Meeting, March 14 – 16, Munich Germany.

2015 DNA Repair & Genome Stability in a Chromatin Environment, 4
-7 June, Institute of Molecular

Supervision and teaching activities

Supervision May 2018 – October 2018 - Maria Berruezo (MSc student)

Undergraduates Jan-Dec 2017 - Simon Braun (MSc student)

Practical Molecular Genetic Courses 2016 – 2018 - Lectures for the practical courses of genetics methodologies at university of Kaiserslautern:

Acquired skills and achievements

Certifications FSHD CE-IVD diagnostic test

Confocal, ApoE and inverted microscopes by Zeiss

Workshops and Trainings

DNA combing by Genomic Vision company; Advanced uses of ImaJ and Fiji; Scientific writing; Advanced course of Adobe packet; Basic course of R software; Course of FACS operating by Thermo Fisher; Immunofluorescence Imaging by Zeiss; Mass spectrometry